AFWAL-TR-87-2091

Nb_3Sn SUPERCONDUCTOR LOSS STUDY

W. J. Carr Jr. and G. R. Wagner
Westinghouse Electric Corporation
Pittsburgh, Pennsylvania 15235

8 January 1988

Final Report for Period 1 March 1982 - 1 July 1985

Approved for public release; distributed unlimited.

AERO PROPULSION LABORATORY
AIR FORCE WRIGHT AERONAUTICAL LABORATORIES
AIR FORCE SYSTEMS COMMAND
WRIGHT-PATTERSON AIR FORCE BASE, OHIO 45433-6563

NOTICE

WHEN GOVERNMENT DRAWINGS, SPECIFICATIONS, OR OTHER DATA ARE USED FOR ANY PURPOSE OTHER THAN IN CONNECTION WITH A DEFINITELY GOVERNMENT-RELATED PROCUREMENT, THE UNITED STATES GOVERNMENT INCURS NO RESPONSIBILITY OR ANY OBLIGATION WHATSOEVER. THE FACT THAT THE GOVERNMENT MAY HAVE FORMULATED OR IN ANY WAY SUPPLIED THE SAID DRAWINGS, SPECIFICATIONS, OR OTHER DATA, IS NOT TO BE REGARDED BY IMPLICATION, OR OTHERWISE IN ANY MANNER CONSTRUED, AS LICENSING THE HOLDER, OR ANY OTHER PERSON OR CORPORATION; OR AS CONVEYING ANY RIGHTS OR PERMISSION TO MANUFACTURE, USE, OR SELL ANY PATENTED INVENTION THAT MAY IN ANY WAY BE RELATED THERETO.

THIS REPORT HAS BEEN REVIEWED BY THE OFFICE OF PUBLIC AFFAIRS (ASD/PA) AND IS RELEASABLE TO THE NATIONAL TECHNICAL INFORMATION SERVICE (NTIS). AT NTIS IT WILL BE AVAILABLE TO THE GENERAL PUBLIC INCLUDING FOREIGN NATIONS.

THIS TECHNICAL REPORT HAS BEEN REVIEWED AND IS APPROVED FOR PUBLICATION.

CHARLES E. OBERLY, Proj Engineer
Advanced Power Systems Branch

RICHARD E. QUIGLEY, JR.
Chief, Advanced Power Systems Branch
Aerospace Power Division
Aero Propulsion & Power Laboratory

FOR THE COMMANDER

MICHAEL D. BRAYDICH, Maj, USAF
Deputy Director
Aerospace Power Division
Aero Propulsion & Power Laboratory

IF YOUR ADDRESS HAS CHANGED, IF YOU WISH TO BE REMOVED FROM OUR MAILING LIST, OR IF THE ADDRESSEE IS NO LONGER EMPLOYED BY YOUR ORGANIZATION PLEASE NOTIFY WRDC/POOX, WRIGHT-PATTERSON AFB, OH 45433-6563 TO HELP MAINTAIN A CURRENT MAILING LIST.

COPIES OF THIS REPORT SHOULD NOT BE RETURNED UNLESS RETURN IS REQUIRED BY SECURITY CONSIDERATIONS, CONTRACTUAL OBLIGATIONS, OR NOTICE ON A SPECIFIC DOCUMENT.

SECURITY CLASSIFICATION OF THIS PAGE

REPORT DOCUMENTATION PAGE

Form Approved OMB No 0704-0188

1a REPORT SECURITY CLASSIFICATION Unclassified	1b RESTRICTIVE MARKINGS None
2a SECURITY CLASSIFICATION AUTHORITY 2b DECLASSIFICATION / DOWNGRADING SCHEDULE	3 DISTRIBUTION / AVAILABILITY OF REPORT Approved for Public Release Distribution Unlimited
4 PERFORMING ORGANIZATION REPORT NUMBER(S) 85-9C9-INSIT-R1	5 MONITORING ORGANIZATION REPORT NUMBER(S) AFWAL-TR-87-2091
6a NAME OF PERFORMING ORGANIZATION Westinghouse Research and Development Center 6b OFFICE SYMBOL (If applicable)	7a NAME OF MONITORING ORGANIZATION Department of the Air Force Air Force Wright Aeronautical Labs
6c ADDRESS (City, State, and ZIP Code) 1310 Beulah Road Pittsburgh, PA 15235	7b ADDRESS (City, State, and ZIP Code) Wright-Patterson Air Force Base Ohio 45433-6563
8a NAME OF FUNDING / SPONSORING ORGANIZATION Air Force 8b OFFICE SYMBOL (If applicable)	9 PROCUREMENT INSTRUMENT IDENTIFICATION NUMBER F33615-81-C-2040
8c ADDRESS (City, State, and ZIP Code) U. S. Air Force WPAFB, OH 45433-6563	10 SOURCE OF FUNDING NUMBERS PROGRAM ELEMENT NO 61102F; PROJECT NO 2301; TASK NO S3; WORK UNIT ACCESSION NO 06

11 TITLE (Include Security Classification)

Nb_3Sn SUPERCONDUCTOR LOSS STUDY

12 PERSONAL AUTHOR(S)

W. J. Carr Jr. and G. R. Wagner

13a TYPE OF REPORT	13b TIME COVERED	14 DATE OF REPORT (Year, Month, Day)	15 PAGE COUNT
Final	FROM 820301 TO 850701	1988 January 08	141

16 SUPPLEMENTARY NOTATION

17 COSATI CODES			18 SUBJECT TERMS (Continue on reverse if necessary and identify by block number)
FIELD	GROUP	SUB-GROUP	Superconductors, filaments, hysteresis, magnets, wire, magnetization, A-C, losses, niobium-tin.

19 ABSTRACT (Continue on reverse if necessary and identify by block number)

Theoretical and experimental studies of the ac losses in continuous fine filament superconductors and in situ Nb_3Sn superconductors are reported. The results indicate that surface currents may play a major role in determining the loss and critical current characteristics of fine filament superconductors. In situ superconductors hold promise for high critical current density, but will exhibit large ac losses unless a means for separating the filaments transverse to the conductor axis is developed.

20 DISTRIBUTION / AVAILABILITY OF ABSTRACT ☒ UNCLASSIFIED/UNLIMITED ☐ SAME AS RPT ☐ DTIC USERS	21 ABSTRACT SECURITY CLASSIFICATION Unclassified	
22a NAME OF RESPONSIBLE INDIVIDUAL CHARLES E. OBERLY	22b TELEPHONE (Include Area Code) (513) 255-9185	22c OFFICE SYMBOL WRDC/POOX

DD Form 1473, JUN 86 — Previous editions are obsolete — SECURITY CLASSIFICATION OF THIS PAGE

Unclassified

FOREWORD

This final technical report covers the work performed by Westinghouse Electric Corporation, Research and Development Center, Pittsburgh, PA 15235 under Contract No. F33615-81-C-2040. The effort was sponsored by the Aero Propulsion Laboratory, Air Force Wright Aeronautical Laboratories, Air Force Systems Command, Wright-Patterson AFB, OH 45433.

The work reported here was performed during the period March 1, 1982 to July 1, 1985 under the direction of Dr. George R. Wagner, Project Manager. Dr. Charles Oberly, AFWAL/POOS was the Air Force Program Manager.

The authors are grateful to Dr. G. M. Ozeryanski and Dr. B. A. Zeitlin of Intermagnetics General Corp. and Dr. E. Adam and Dr. E. Gregory both formerly with Airco Superconductors for supplying samples to be studied in this program, to J. H. Uphoff, H. C. Pohl, and J. Buttyan for experimental assistance, and to Mrs. M. B. Cross for typing the manuscript.

TABLE OF CONTENTS

TABLE OF CONTENTS (Continued)

SUMMARY

This program was initiated to investigate the possibility of developing radically improved superconductors through the use either of in situ material or very fine continuous filament material, in the submicron range of filament diameters. The properties studied were the hysteresis and critical current density. The behavior of continuous filament material in the submicron range of filament diameter seems to be dominated by surface current. In general very fine filaments offer the possibility of increasing current density with decreasing diameter, and therefore the in situ materials hold promise for increased critical current density, but such conductors are expected to exhibit a large transverse field hysteresis loss. The loss can be reduced about a factor of ten by twisting, but the means to further reduce the loss are not apparent, except by reducing the diameter of the conductor itself. In principle, we can imagine an in situ material where the filaments are sufficiently separated transverse to the filament axis so that, for practical purposes, the material is superconducting only in one direction, as in a continuous filament material. This construction should lower the loss, but as yet no in situ material approaching the desired characteristics has been observed.

Continuous filament superconductors show more promise for high current density, low-loss material. This follows from the fact that since the filaments are continuous, a superconducting matrix is unnecessary, and the proximity effect can be poisoned by the addition of ferromagnetic ion in the matrix. Thus, very fine filaments with low hysteresis loss can be relatively closely packed. As is well-known, eddy current losses then appear in alternating fields, and to lower the latter, small diameter wires must be used.

II. INTRODUCTION

The general purpose of this program was to investigate the possibility of developing radially improved low-loss high-current-density superconductors through the use of very fine continuous-filament material, on in situ material with disconnected fine filaments. Since all the work performed under this contract has either been published or is submitted for publication, only a summary will be presented here. All publications have been attached as an Appendix.

III. IN SITU MATERIAL

In regard to in situ material, a macroscopic theory was developed whereby three critical current densities were assumed: one parallel to the average filament direction, the other two transverse. The latter were much smaller than the former. The parallel critical current density for long filaments is determined by the critical current of the filaments themselves, and for moderately dense packing it was assumed that pairs of disconnected filaments are connected by a bridge through another filament, or filaments, whereby the super current reaches the third filament by flowing across a large area of matrix transverse to the filaments. The matrix is rendered slightly superconducting by the proximity effect. This model predicts that the transverse field loss in in situ superconductors is essentially the same as that for a "solid" superconductor, which is in substantial agreement with observations. It also correctly predicts the effect of twist on the loss, where in essence the twist lowers the effective critical current density along the axis of the conductor, since current flowing along the conductor axis must pass through the matrix. For heavily twisted material the longitudinal current density in the conductor is determined by the critical current density of the matrix. Analysis of published data consistently indicates that the matrix has a critical current density between one and two orders of magnitude smaller that of the filaments.

IV. CONTINUOUS FILAMENT MATERIAL

We found that in continuous filament NbTi below 1 μm in filament diameter, the dominate component of current which flows in the filaments is surface current. The evidence for this is, firstly, a high degree of asymmetry of the m-H hysteresis loop about the horizontal axis (zero magnetic moment). This hysteresis loop for submicron filaments is much closer to reversibility than that for larger filaments, and the loops for 0.8 μm and 0.4 μm material are nearly the same. Secondly, when the material was cooled through the transition temperature in a constant transverse magnetic field, a spontaneous magnetic moment appeared, indicating a partial Meissner effect up to the highest magnetic fields investigated, which was several teslas. The magnitude of the spontaneous magnetic moment was comparable with that observed on the hysteresis loop. The final evidence is that the measured critical current density for the 0.4 μm filaments was considerably greater than that for the 0.8 μm filaments.

V. CONCLUSIONS

Since fine filaments have the possibility of having a higher critical current density than larger filaments, the <u>in situ</u> materials hold promise for increased critical current density, but such conductors are expected to exhibit a large transverse field hysteresis loss. The loss can be reduced about a factor of ten by twisting, but the means to further reduce the loss are not apparent, except by reducing the diameter of the conductor itself. In principle, we can imagine an <u>in situ</u> material where the filaments are sufficiently separated transverse to the filament axis so that, for practical purposes, the material is superconducting only in one direction, as in a continuous filament material. This construction should lower the loss, but as yet no *in situ* material approaching the desired characteristics has been observed.

Continuous filament superconductors show more promise for high current density, low-loss material. The essential difference between continuous and *in situ* type material is that when the filaments are continuous, a superconducting matrix is unnecessary, and the proximity effect can be poisoned by the addition of ferromagnetic ions in the matrix. Thus, the hysteresis loss can be kept small while a reasonable density of filaments is maintained. As is well-known, eddy current losses then appear in alternating fields, and to lower the latter, small diameter wires must be used.

The greatest promise for a radically improved conductor is in the development of continuous fine filament material having a CuNi matrix and a filament diameter the order of twice the London penetration depth, or less. Limitations on the theory prevent a quantitative estimate of the ultimate limits on loss and critical current which can be expected.

VI. SUGGESTION FOR FUTURE WORK

Experimental progress in the development of fine filament superconductors has reached the point where theoretical guidelines are quite uncertain. It is suggested that future work should include basic programs, at a more fundamental level, to better understand the reversible and irreversible behavior of fine filaments.

Published in J. Appl. Phys. *54*, *5911 (1983).*

APPENDIX A

MACROSCOPIC AND MICROSCOPIC MODELS OF IN SITU SUPERCONDUCTORS*

W. J. Carr, Jr.

Westinghouse R&D Center
Pittsburgh, Pennsylvania 15235

ABSTRACT

It is argued that a macroscopic formalism similar to that for continuous filament material can be applied to in situ superconductors, providing an elongated volume element is used for averaging over the microscopic fields and currents. Microscopic dimensions in this context are "anisotropic" since the volume element must contain entire filaments. The difference between in situ and continuous filament materials is found in the constitutive equations. For an in situ tape these consist of a specification of three critical current densities for the macroscopic superconducting state, together with three conductivities for the non-superconducting state, and, under some conditions, three magnetization components. The interesting region of the non-superconducting state occurs when the material is macroscopically non-superconducting, but superconducting microscopically. A microscopic model based on the proximity effect is developed for computing the constitutive equations. For

---

*Supported by the Air Force Aero Propulsion Laboratory Contract No. F33615-81-C-2040.

calculating the axial current density, the model assumes that chains of filaments run through the conductor. When the superconducting proximity layers surrounding a pair of chains overlap, the chains can carry macroscopic supercurrent. In general, a conductor can be superconducting in one, two or three directions. The critical current densities are expected to be highly anisotropic.

INTRODUCTION

The electromagnetic behavior of any system that is sufficiently large can be described by a macroscopic set of Maxwell equations. Such equations arise from a volume average of the Maxwell-Lorentz equations describing the microscopic details.[1,2] In this way quantities such as the electromagnetic loss can be calculated in a relatively simple fashion even for a very complex system. The size of the volume element over which the average is made depends upon the scale of the microscopic detail, and if more than one microscopic scale can be assumed, a hierarchy of Maxwell equations exist, with the simplest description being that for the largest scale. In the case of a continuous filament superconductor the filament diameter may be considered to be the largest microscopic dimension, and a volume element may be selected, as in Fig. 1(b), to give an average over the cross-section of filaments and matrix.[3,4] An in situ filamentary superconductor,[5] characterized by discontinuous filaments, can be expected to yield to the same approach, providing an elongated volume element is chosen as shown in Fig. 1(a). The volume element must now enclose entire filaments. It will be noted that a length which is considered to be microscopic in one direction may be macroscopic in a different direction. The difference between continuous filament and in situ material will be found in the constitutive relations required to solve the Maxwell equations, and it is only at this point that microscopic details play a role. In essence, the use of large scale macroscopic theory divides the problem

Dwg. 7770A55

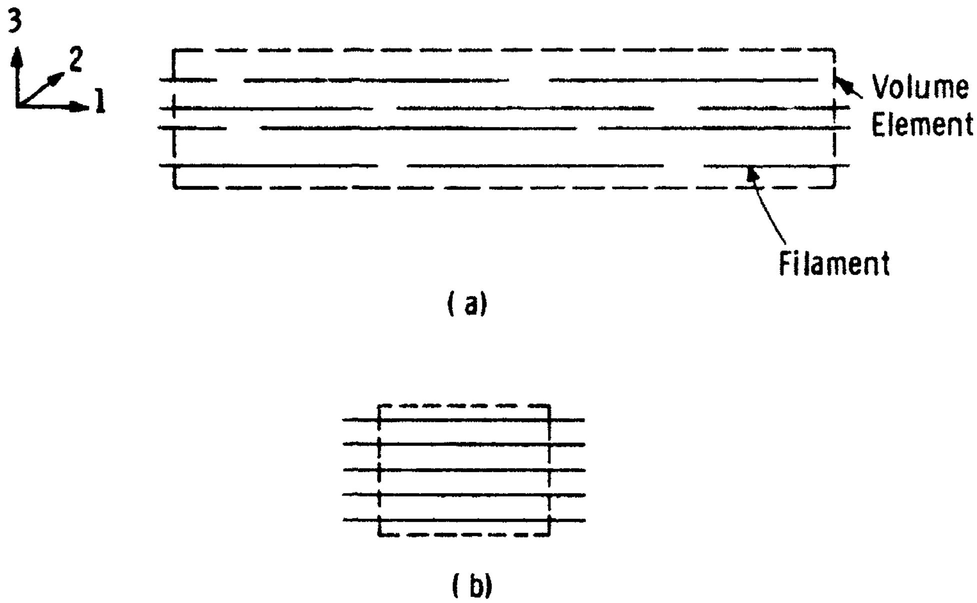

Fig. 1 — Cross-section of volume element for making averages for (a) in situ material and (b) continuous filament material. The number of filaments enclosed in (a) , for a strip, is limited by the condition that in the 1, 2, 3 directions the volume element must be small compared with the conductor length, width and thickness respectively.

into two parts: (1) a solution satisfying all the boundary conditions is obtained in terms of certain constants describing the constitutive relations, and (2) the constants are then either obtained empirically or from a microscopic model.

The purpose of the present analysis is to specify the macroscopic constants needed to describe the electromagnetic response of an in situ material, and to estimate these constants from a rough microscopic model.

CONSTITUTIVE RELATIONS

In most in situ materials which have been drawn out into the shape of a tape, the individual filaments deform into the shape of ribbon segments.[6,7] Let 1, 2, 3 denote the average principal axes of the filaments, as in Fig. 1, where the 1 axis gives the average direction of the filament length near any macroscopic point, and the 2 and 3 axes correspond to those for the width and thickness respectively. For a tape the principal filament axes correspond to the principal axes x, y, z of the conductor, but in order to generalize later, a distinction will be maintained between filament and conductor coordinates.

In the presence of a small static electric field along a principal direction, an expansion of the current density, for an idealized material, gives as the first two terms a current density independent of the magnitude of the electric field plus a term linear in the field:

$$j_i = j_{ci} \operatorname{sgn} E_i + \sigma_i E_i \qquad (i = 1, 2, 3) \tag{1}$$

where $j_{ci} = j_{ci}(\underset{\sim}{H}, T)$ is a critical current density for the supercurrent, σ is a conductivity, $\underset{\sim}{H}$ is the magnetic field and T is temperature. The question of how the critical current densities behave when the electric field has an appreciable component in more than one principal direction is an important question which must be resolved by experiment. If the material is in a macroscopic superconducting state, then for most purposes one may use the approximation

$$j_i \approx j_{ci} \operatorname{sgn} E_i \ . \tag{2}$$

(When $E_i = 0$, j_i depends on the history of the material.[8]) In the simplest macroscopic resistive or non-superconducting state

$$j_i \approx \sigma_i E_i \ , \tag{3}$$

but in cases where non-uniformity in filament spacing becomes important it will be found that the full expression given by (1) is needed, because only part of the observed current has resistance. Calculation of σ is trivial for the case of a normal state, but the case of particular interest here is the absence of macroscopic superconductivity while microscopic superconductivity still exists. σ in this case can be very large compared with a normal conductivity, as indicated in Fig. 2. If σ becomes too large, ordinary electric fields encountered when the magnetic field is changed will tend to saturate the current density, leading to an apparent critical current.

The remaining constitutive equations of interest are those which give $\underset{\sim}{B}$ or $\underset{\sim}{M}$ as a function of $\underset{\sim}{H}$ and T. In addition to atomic sources, a true magnetization can arise from current circulating within a filament, or from currents circulating within local closed paths due to interconnections among filaments, with the latter expected to dominate for most

Curve 740045-A

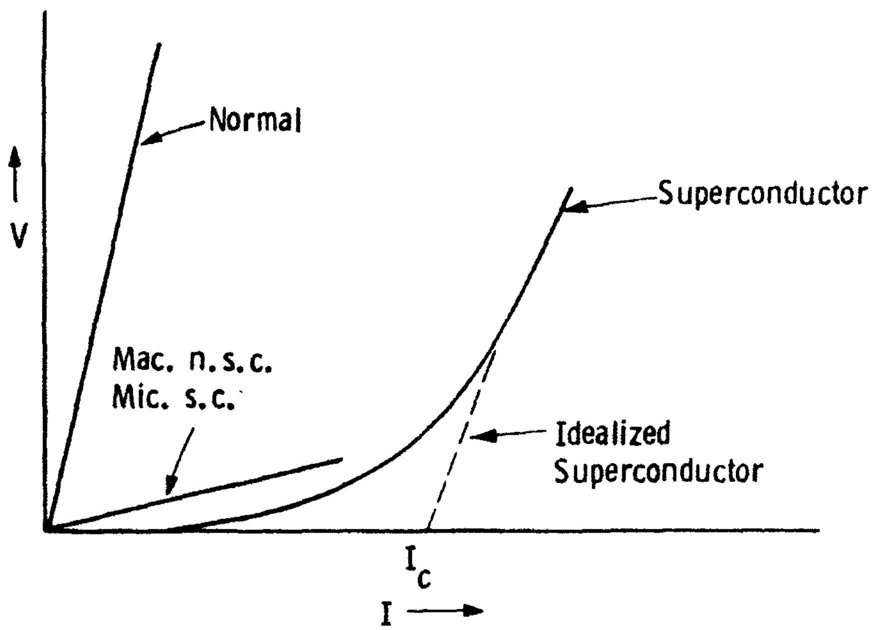

Fig. 2 — The voltage-current relationship for various conditions

in situ materials. In a macroscopic superconducting state the true magnetization $\underset{\sim}{M}$ will tend to be overshadowed by the magnetic moment of the conduction current $\underset{\sim}{j}$, and, in general, this magnetization can become a dominant factor only for weak macroscopic superconductivity, or when relatively large diameter paths exist for the magnetization current.

It follows in summary that three critical current densities and three conductivities are required, and, under some conditions, three components of magnetization. The macroscopic non-superconducting state can be subclassified according to whether the filaments are normal or superconducting. Subclassification of the macroscopic superconducting state can be made based on whether it is superconducting in one, two or three directions.

MICROSCOPIC MODEL

The microscopic picture of in situ materials has been examined previously by Tinkham[6,9,10] and his colleagues, and various concepts were explored which are retained in the present formulation. However, no distinction will be made between conduction by percolation and conduction by proximity effect. In the present analysis conduction is assumed to be a percolation process, with the percolation occurring between regions enlarged by the proximity effect. (This is true even when filaments touch, inasmuch as physical contact tends to occur at a point.) Two approaches have been previously used to study the conductivity, one involving the use of probability theory for continuous paths or infinite clusters,[10] the other making use of a physical model for connections between neighboring filaments.[9] The latter type approach will be used here. Supercurrents which flow between filaments of an in situ material are of two types: the magnetization currents which find local closed paths in which to circulate, and conduction current which proceeds along continuous paths through the conductor. For a uniform distribution of filaments the problem of finding continuous paths becomes trivial, since, in this case, translational symmetry exists and all filaments tend to behave the same. Microscopic examination indicates that in the early stages of deformation filaments are not uniformly spaced, because they tend to bunch together, but, clearly, the bunching does not prevent approximate uniformity along the axis of a conductor. (Uniformity can be further increased by imagining a slight rearrangement of filaments which makes zigzag percolation paths into straight paths.) For this reason the model suggested for computing the axial current density is that of straight chains of filaments, where the spacing between chains is random or arbitrary. Attention can now be focussed on individual filaments, and axial supercurrents can flow when individual filaments have a superconducting connection with their neighbors. (The same does not necessarily follow for current flow in a transverse direction.)

Figure 3 shows a gap between two filaments bridged by a third filament, which is the filament in closest vertical proximity. The vertical separation denoted by s will be associated with the filament n, and, more precisely, c can represent multiple neighboring filaments, depending on the environment. The microscopic current density $\underset{\sim}{i}$ is indicated for the case where a macroscopic current density $\underset{\sim}{j}$ is established along an axis parallel to the filaments. The thickness of the filaments is denoted by d, while the thickness including the proximity region, of thickness s', is d' = d + 2s'. Resistance goes to zero when the regions denoted by d' overlap. In a given material the value of d' - d, or 2s', is controlled by the magnetic field and the temperature. When the proximity regions do not overlap, a normal layer s" is assumed to exist, which can vary between zero and the vertical separations between filaments.

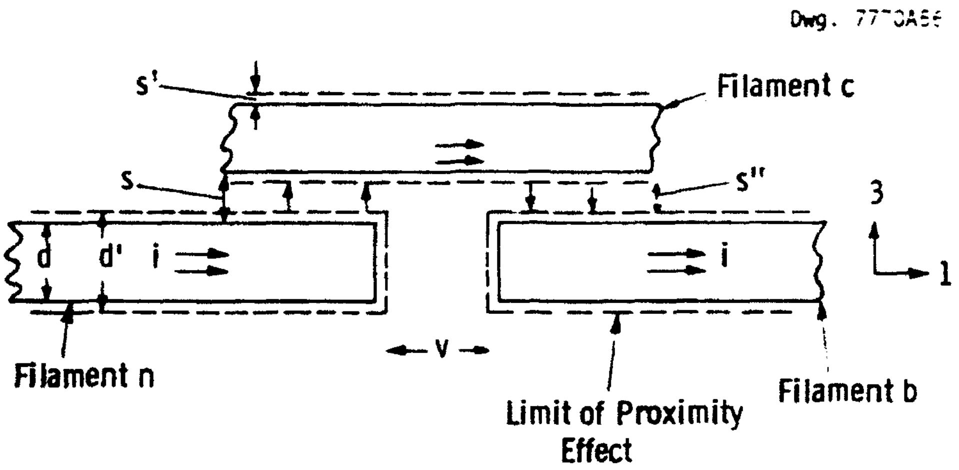

Fig. 3 — Model for the pattern of microscopic current flow in response to an applied electric field along the 1 axis. Filament c is the closest filament to the pair nb. The figure shows the cross-section of the ribbon-like filaments where d is the thickness. d' is a thickness which includes the proximity effect, s is the separation between filaments, s' is the thickness of the proximity layer, and s'' is the thickness of the normal region between filaments.

CALCULATION OF THE AXIAL MACROSCOPIC CURRENT DENSITY AND ELECTRIC FIELD

Consider, first, the case where the current density in a filament is at or below its critical value, so that no electric field exists in the filaments. In the average of the microscopic electric field $\tilde{e}$ over filaments and matrix, only the region between the ends of filaments n and b in Fig. 3 makes a contribution, and the average of this field is in the 1 direction. If each filament is assumed to have a length ℓ and a width w, where $\ell >> w >> d$, the volume (filament plus matrix) associated with the n^{th} filament is $\ell wd/\lambda_n$ where λ_n (not to be confused with the London penetration depth) is the fraction of superconductor in a cell determined by bisecting the distance between neighboring filaments. The integral of the electric field over this volume is the order of $v_n d'w$ for closely spaced filaments, and the average electric field of th n^{th} cell is

$$< e_1 >_n \sim \frac{v_n \lambda_n}{\ell} \frac{d'}{d} . \tag{4}$$

where v_n is the voltage between filaments n and b. The average current density is also in the 1 direction and given by

$$< i_1 >_n \sim \frac{1}{2} j_{1fn} \lambda_n \tag{5}$$

where j_{1fn} is the average current density near the middle of the n^{th} filament. The voltage v_n is twice the voltage between filaments n and c, which is given roughly by $v_n \approx (j_{1fn}\, dw)(\frac{2}{\ell w})\, 2s_n''\, \rho_m$, where ρ_m is the resistivity of the matrix, and s_n'' is the thickness of the normal layer for the n^{th} filament. From (4) and (5).

$$\langle e_1 \rangle_n \sim 8 \langle i_1 \rangle_n \rho_m \frac{d' s_n''}{\ell^2} . \tag{6}$$

The macroscopic variables are obtained by averaging over all cells in the volume element ΔV used to define a macroscopic average, i.e.

$$j_1 = \frac{1}{\Delta V} \sum_n \Delta V_n \langle i_1 \rangle_n$$

$$\sim \frac{1}{2\Delta V} \sum_n \Delta V_n \lambda_n j_{1fn} \tag{7}$$

$$E_1 \sim \frac{4\rho_m}{\Delta V} \frac{d'}{\ell^2} \sum_n \Delta V_n \lambda_n j_{1fn} s_n'' . \tag{8}$$

When no field is applied to the conductor, the left-hand side of (8) is zero and $j_{1fn} s_n'' = 0$ for all n. If macroscopic supercurrents are flowing, then for some chains of filaments $s_n'' = 0$ and $j_{1fn} \neq 0$.

Because the thickness of the normal layer s_n'' depends on s' through the relation $s_n'' = s_n - 2s'$, it follows that $s_n'' = s_n''(s_n; \underset{\sim}{H}, T)$, with a minimum value $s_n''(s_n; 0, 0)$ that can vanish only for closely spaced filaments where the separation s_n is less than the maximum thickness of twice the proximity layer. The latter is estimated to be in the range of a fraction of a micron by Bevk et al.,[6] but obviously, the actual value depends upon the matrix material. The average value of s_n depends upon the amount of mechanical reduction Re performed in forming the tapes.[6,11] For small values of Re the average s_n can be very much larger than $2s'$, but nevertheless, through non-uniformity in distribution one can expect some filaments with $s_n'' = 0$. In this way superconductivity, characterized by a very small critical current density, can be explained even for small values of Re and small amounts of superconductor in the composite.

In deriving Eq. (8) it was assumed that no electric field exists in the filaments, but as s" in any filament becomes so small that the current in the filament slightly exceeds its critical value this will not be the case when $E_1 \neq 0$. Therefore, the equation does not apply under these conditions. To generalize one can assume that $\langle e_1 \rangle_n$ is essentially the same, and approximately equal to E_1, in all cells near a macroscopic point. Thus, the average given by (8) is of no interest, and j_1 is given by the first line of (7) where $\langle i_1 \rangle_n$ is the smaller of the value given by (6) or the value given by (5) with j_{1fn} replaced by its critical value.

THE CASE OF A TAPE WITH LARGE MECHANICAL REDUCTION

In the remaining analysis a large mechanical reduction will be assumed, such that the average separation between chains of filaments is the order of or less than twice the maximum proximity layer thickness. In this case non-uniformity in the filament spacing becomes less important, and the subscript n will be dropped on λ, i, s and s". Equations (7) and (8) reduce to

$$j_1 \sim \frac{\lambda}{2} j_{1f} \tag{9}$$

$$E_1 \sim 4\rho_m \frac{d' \, s''}{\ell^2} \lambda \, j_{1f} \, . \tag{10}$$

The sole requirement for superconductivity in the 1 direction is now that $s''(s; \underset{\sim}{H}, T) = 0$. But if a proximity bridge exists across the filaments in connection with longitudinal current flow, the same bridge can carry current resulting from the application of an electric field in a transverse direction; and if sufficient uniformity exists in the distribution of filaments the in situ material can become superconducting in all three directions like a normal bulk superconductor.

CRITICAL CURRENT DENSITIES FOR CLOSELY SPACED FILAMENTS

In an ordinary superconducting tape or wire the longitudinal critical current density is usually the order of, or smaller than, the transverse for moderate, or large, applied transverse magnetic fields.[12] On the contrary , for some in situ materials in large fields the anisotropy of the current density is such that the longitudinal j_c is largest.[13]

The value of j_1 given by (9) for $E_1 = 0$ when macroscopic superconductivity exists defines the critical current density j_{c1}. The value of j_{1f} under this condition is determined either by the longitudinal critical current density of an isolated filament, or by a critical current density for the proximity region. Since the current density in the filament is larger by a factor the order of $\ell/2d$, j_{c1} is the smaller of $\lambda j_{c1f}/2$ and $\lambda j_{cp}\ell/4d$. A rough approximation which incorporates this condition into a single equation is given by

$$\frac{1}{j_{c1}} \sim \frac{2}{\lambda j_{c1f}} + \frac{1}{\lambda j_{cp}} \frac{4d}{\ell} \qquad (11)$$

where $j_{c1f} = f(\underset{\sim}{H},T)$ is the longitudinal critical current density for an isolated filament, and j_{cp}, also a function of $\underset{\sim}{H}$ and T, is the effective critical current density for the proximity region, in a direction perpendicular to the filament. One may define j_{cp} to be zero when the proximity regions do not overlap. If the direction along the width of the filament is also superconducting, one can expect for closely spaced filaments that the critical current density is obtained by replacing ℓ with w, i.e.

$$\frac{1}{j_{c2}} \sim \frac{2}{\lambda j_{c2f}} + \frac{1}{\lambda j_{cp}} \frac{4d}{w} , \tag{12}$$

and for a direction through the tape thickness

$$\frac{1}{j_{c3}} \sim \frac{1}{j_{c3f}} + \frac{1}{j_{cp}} . \tag{13}$$

$$\sim \frac{1}{j_{cp}}$$

assuming j_{cp} is small compared with j_{c3f}. At present no theory exists for j_{cp} but one may hope to obtain experimental values.

In a tape the principal axes of the filaments tend to align themselves with the principal axes x, y, z of the tape, and the measured longitudinal and transverse critical current densities j_{cz} and j_{cx}, respectively, are given by (11) and (12). If one assumes that $j_{c2f} \gtrsim j_{c1f}$, the low anisotropy ratio found by Braginski and Wagner[13] in some samples suggests that in these cases j_{cz} is determined by the filament, and j_{cx} by the proximity region.

RESISTIVITY IN THE NON-SUPERCONDUCTING STATE

In a macroscopic non-superconducting state the conductivity $\sigma = 1/\rho$ is given, according to (9) and (10) for the case of a closely-spaced nearly uniform distribution of filaments, by a resistivity of order

$$\rho_1 \sim 8\rho_m \frac{d' \; s''}{\ell^2} \; . \tag{14}$$

The dimension ℓ can be written in terms of the mechanical reduction[6,9,11] but widely different results are obtained from different assumptions. It will be assumed here that one may examine the reduction by considering the deformation of a unit cell placed around an initial superconducting particle, and that the number of unit cells cut by a cross-section of the conductor is conserved. The initial volume of the unit cell is $\ell_{uco}{}^3$ and the initial volume of the particle is $\ell_o{}^3$ where $\ell_o{}^3 = \lambda \ell_{uco}{}^3$. The final volume of the filament is ℓwd, and the final unit cell volume is taken to be approximately $\ell w(d+s)$. Thus $\lambda = d/(d+s)$. The reduction is defined to be the ratio of the initial to the final area of the unit cell, or alternatively, since the volume is unchanged $Re = \ell/\ell_{uco}$. Therefore $Re^3 = \lambda \ell^3/\ell_o{}^3$. The factor sd/ℓ^2 can be written as $(\frac{d}{w})(\frac{s}{d})\, wd\ell/\ell^3$ where $wd\ell$ is the filament volume, equal to $\ell_o{}^3$, and $s/d = (1-\lambda)/\lambda$. Then sd/ℓ^2 is equal to $(\frac{d}{w})(1-\lambda)\; Re^{-3}$ and

$$\rho_1 \sim 8\rho_m \frac{d}{w} \frac{(1 - \lambda)}{Re^3} \frac{d'}{d} \frac{s''}{s} . \qquad (15)$$

The result differs from the original calculation of Davidson et al.[9] mainly by a factor d/w and also a factor of λ. Nevertheless, if d/w is regarded as only a weak function of Re, the dependence of ρ_1 on Re in this model is roughly Re^{-3} as previously calculated.[6,9,11] In the case where $d' \approx d$ one observes that the dependence of ρ_1 on temperature or magnetic field is given by s"/s, which for closely-spaced filaments goes from zero to unity as the temperature or field is increased from zero.

In analogy with (14) one can expect in the transverse direction, for similar conditions,

$$\rho_2 \sim 8\rho_m \frac{d' \, s''}{w^2} \qquad (16)$$

and through the thickness

$$\rho_3 \sim \frac{\rho_m \, s''}{s + d} \qquad (17)$$

Although ρ_2 and ρ_3 are large enough to be measurable, ρ_1 for very elongated filaments may not be, and in this case the resistive current in a non-superconducting state will appear to be a macroscopic supercurrent. Furthermore, the application of a very small electric field will cause it to saturate. Thus over a certain range of temperature and magnetic field one would expect the conductor to act like a superconductor along the length and a non-superconductor in the transverse directions.

EVIDENCE FOR A TRUE MAGNETIZATION

A true magnetization may be defined by

$$\mathbf{M}(\mathbf{r}t)\ \langle \Sigma_n\ \mathbf{m}_n(t)\ \delta(\mathbf{r} - \mathbf{r}_n)\rangle \tag{18}$$

where $\mathbf{m}_n$ is a local dipole moment at $\mathbf{M}_n$, δ is a Dirac delta function, the angular brackets indicate a volume average, and $\mathbf{r}$ and t represent position and time.

For filaments arranged on a uniform lattice only conduction currents can flow since the environment for each filament is the same. Magnetization currents leading to $\mathbf{m}_n$, therefore, depend upon non-uniformity in the filament distribution. In a conductor with non-uniform filament distribution the model for in situ material can be completed by introducing closed rings of a given area, or diameter, which are superimposed on the filament chains. In a sample measured by Braginski and Wagner[13] the observed magnetic moment was found to be not proportional to the measured j_c, and this behavior is taken as evidence that an appreciable part of the magnetic moment of this sample comes from true magnetization. In increasing magnetic fields the magnetic moment decreased more rapidly than j_c, as would be anticipated if the magnetic moment is due to M, since magnetization supercurrents can circulate around paths having a range of values, and the large diameter paths are destroyed first. The hysteresis in this case is determined by the sum of $\oint \mathbf{H} \cdot d\mathbf{M}$ and $\oint \mathbf{E} \cdot \mathbf{j}dt$.

THE CASE OF A WIRE

The microstructure of a wire differs from that for a tape, but insofar as the difference is simply in the orientation of the filaments relative to the conductor axes, the previous results may be used to compute the properties of the wire. For example, in an untwisted wire let it be assumed that the filaments are oriented so that the 2 direction (width) corresponds to the radial direction R, the 3 direction (thickness) is the θ or circumferential direction and the 1 axis corresponds to the z axis in cylindrical coordinates R, θ, z for the wire. One can then investigate the effect of twist on the hysteresis of a superconducting wire, since twisting of the wire reorders the orientation of filaments in a predictable way.

In a transverse applied field, the current induced in the wire is a shielding current which must flow down the axis on one side of the wire, and back along the axis of the wire on the other side. In contrast, a bulk transport current can simply flow along the filaments. It follows that in a twisted wire the critical current density measured from the transport current may be larger than that measured from the hysteresis. Depending on the twist, the latter has a component along the 3 direction, which according (13) will be small if j_{cp} is small compared with the intrinsic filament critical current density. This fact offers a possible explanation for the decrease in full penetration hysteresis with increasing twist which has been observed by Braginski and Wagner,[13] and Shen and Verhoeven.[14]

SUMMARY AND DISCUSSION

In order to understand electromagnetic properties such as the loss behavior of in situ superconductors it is necessary to know various macroscopic "constitutive constants." The most important of these for a full superconducting state are three critical current densities referred to a set of principal axes; while for a macroscopic state that is not superconducting the resistivity is of interest. A simple microscopic model involving the proximity effect has been used to estimate these values. The model consists of longitudinal chains of filaments distributed through the cross-section of the conductor. Any pair of chains closer together than twice the thickness of the superconducting proximity layer around each filament can carry an axial supercurrent. Macroscopic transverse supercurrent can flow only when nearly all neighboring chains are separated by less than twice the proximity layer thickness. In general, macroscopic superconductivity can exist in one, two or three directions. The macroscopic critical current densities are given in terms of the filament dimensions and a critical current density for the proximity layer, in addition to the critical current densities of the filaments.

Some qualitative consequences which immediately fall out of the model are the following. (a) In an in situ conductor that has not been severely stretched (average filament spacing large compared with twice the approximity layer thickness) only a weak critical current density in the axial direction should be observed since the current is carried by the relatively small number of filament chains which are close neighbors. The conductor should be superconducting in only one direction. (b) For a severely reduced conductor, where the average filament spacing is small compared with twice the proximity layer thickness, superconductivity should be observed in all three directions, as in an ordinary superconductor. However, the critical current densities are expected to be highly anisotropic, and this anisotropy should be evident in the effect of twist on the hysteresis loss, and in the difference in hysteresis loss for longitudinal and transverse magnetic fields. (c) For conductors which are intermediate between the above limiting cases and where a given transverse direction is nearly superconducting, one would expect to find a relatively large true magnetization, due to currents circulating in closed paths among the filaments, in the case of a longitudinal applied magnetic field. Some quantitative investigations of these predictions are planned for a later paper.

REFERENCES

1. J. H. Van Vleck, Theory of Electric and Magnetic Susceptibilities, Oxford Univ. Press, Oxford (1932).
2. W. J. Carr, Jr., AC Loss and Macroscopic Theory of Superconductors, Gordon and Breach, London (in press).
3. W. J. Carr, Jr., J. Appl. Phys. 45, 929 (1974).
4. W. J. Carr, Jr., Phys. Rev. B 11, 1547 (1975).
5. C. C. Tsuei, Science 180, 57 (1973).
6. J. Bevk, M. Tinkham, F. Habbal, C. J. Lobb and J. P. Harbison, IEEE Trans. MAG 17, 235 (1981).
7. J. D. Verhoeven, D. K. Finnemore, E. D. Gibson, J. E. Ostenson and L. F. Goodrich, Appl. Phys. Lett. 33, 101 (1978).
8. C. P. Bean, Rev. Mod. Phys. 36, 31 (1964).
9. A. Davidson, M. R. Beasley and M. Tinkham, IEEE Trans. MAG 11, 276 (1975).
10. C. J. Lobb, M. Tinkham and W. J. Skocpol, Solid State Comm. 27, 1273 (1978).
11. T. J. Callaghan and L. E. Toth, J. Appl. Phys. 46, 4013 (1975).
12. M. P. Mathur, M. S. Walker, D. W. Deis and C. K. Jones, J. Appl. Phys. 43, 3831 (1972).
13. A. I. Braginski and G. R. Wagner, IEEE Trans. MAG 17, 243 (1981).
14. S. S. Shen and J. D. Verhoeven, IEEE Trans. MAG 17, 248 (1981).

Published in J. Appl. Phys. 54, 5917 (1983).

APPENDIX B

THE ELECTRICAL BEHAVIOR OF IN SITU SUPERCONDUCTORS WITH LARGE FILAMENT SEPARATION*

W. J. Carr, Jr.

Westinghouse R&D Center
Pittsburgh, Pennsylvania 15235

ABSTRACT

The electrical properties of in situ superconductors are calculated for the case where the average filament separation is large compared with the range of the proximity effect. The calculations are based on a model recently described by the author, where chains of filaments run through the length of the conductor. The distribution of the chains is assumed to be non-uniform and described by a distribution function f(s), where s is the separation between neighboring chains. The critical temperature T_c for superconductivity in a filament is also assumed to be a function of s. At any given temperature some filaments, as a result of the proximity effect, have a superconducting connection with their neighboring filaments, others are superconducting but with a resistive connection, while others are normal. The first category of filaments determines the critical current I_c, while the first two categories determine another critical current I_c^*. Both I_c and I_c^* are functions of the magnetic field and temperature. For a fixed current I the equations $I = I_c$ and $I = I_c^*$

*Supported by the Air Force Aero Propulsion Laboratory Contract No. F33615-81-C-2040.

define two critical temperatures T_1 and T_2, which together with the highest value of T_c describe the features of the electrical behavior. The results compare favorably with some published measurements. The value of the proximity length obtained from the model with the aid of the measurements is in good agreement with previous estimates.

INTRODUCTION

In situ superconductors are characterized by discontinuous filaments embedded in a normal metal matrix. In the following analysis the electrical behavior is calculated in the case where the average filament separation is large compared with the range of the proximity effect. The results are compared with some previous measurements for this case reported by Lobb et al.[1] The calculations are based on a simple model recently proposed by the author for an in situ material.[2] In this model chains of filaments run along the length of the conductor, with arbitrary spacing between the chains. Attention is focussed on the electrical connection of a given filament with its surroundings. For a transport current along the conductor axis the microscopic picture of current flow is that shown in Fig. 1, where the filaments n and b in a chain are bridged by c, the filament in closest proximity. More generally c can represent multiple filaments, depending on the surroundings. Except for detail the pattern is that proposed by Davidson et al.[3] for computing remanent resistance, with a modification made to include the proximity effect. The region separating filament c and n or b is not entirely normal, since superconductivity extends into the matrix material in proximity to the superconducting filaments,[4,5] thereby shortening the thickness of the normal layer. An outline of the theory is as follows: (a) Only one mechanism for conduction is assumed: proximity aided percolation between

Dwg. 7770A56

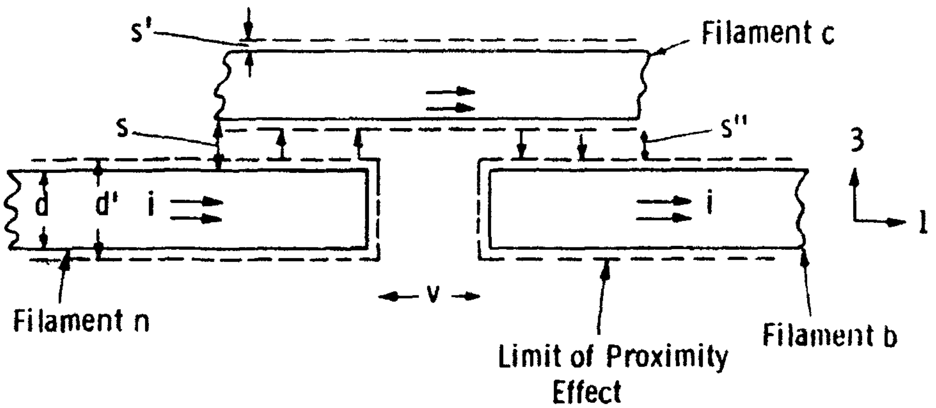

Fig. 1 — Model for the pattern of microscopic current flow in response to an applied electric field along the 1 axis. Filament c is the closest filament to the pair nb. The figure shows the cross-section of the ribbon-like filaments where d is the thickness. d' is a thickness which includes the proximity effect, s is the separation between filaments, s' is the thickness of the proximity layer, and s'' is the thickness of the normal region between filaments.

neighboring filaments. (b) When the proximity layer surrounding filament c overlaps those surrounding a and b a superconducting connection exists. Otherwise the connection is resistive. (c) When the average value of the spacing s (see Fig. 1) is large compared with the thickness of the proximity layer the distribution of values for s is important. (d) The thickness s' of the proximity layer in a given material depends only upon temperature and the magnetic field. (e) An additional assumption which is made in connection with the present calculation is that the transition temperature for microscopic superconductivity in a filament depends upon the local density of filaments.

For a high current density superconductor the filaments, obviously, must be closely packed, and this case was considered in some detail in Ref. 2. The loosely packed case considered here may have less promise for a practical superconductor, but it offers a critical test of the theory.

THE CRITICAL CURRENT

The average separation between filaments depends upon the fraction of superconductor in the composite and the amount of mechanical reduction Re performed upon the conductor.[4,6] For small fractions of superconductor and relatively small values of Re the average separation is large compared with the extent of the proximity layer, and it is important to consider the distribution of values of s. Only the relatively few filaments bridged by a third filament with a small value of s contribute to the critical current.

The separation s in Fig. 1 is associated with the n^{th} filament, and in Fig. 2 a schematic curve is shown for the distribution of values of s, where s is considered as a continuous variable. For filaments aligned along the conductor axis, the current carried by the conductor in weak electric fields is approximately

$$I = \int_0^{\infty} I_f \; f(s) \; ds \tag{1}$$

where $I_f(s)$ is the average axial current in a filament having a separation s from its nearest neighbor in another chain, and f(s) ds is the number of filaments in the range between s and s+ds which intersect a given cross section. Filaments with s less than 2s', which is twice the thickness of

Curve 740611-A

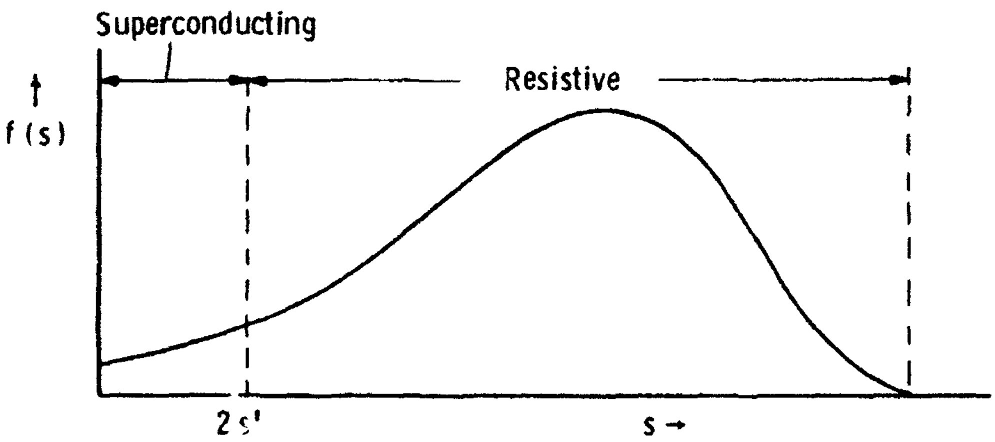

Fig. 2 — Distribution function f (s) for the perpendicular separation of a filament from its closest neighbors (schematic). 2s' is twice the thickness of the proximity layer. For s <2s' the proximity layers overlap and the connection between a filament and its surroundings is superconducting

the proximity layer, have a superconducting connection with their

bors, and the critical current for a superconducting state is

$$I_c = \frac{1}{2} \int_0^{2s'} I_{cf}\, f(s)\, ds$$

where $I_{cf}(s;\underset{\sim}{H},T)$ is the critical current for a filament. The factor arises because the current varies along the length of the filam[illegible] I_{cf} at the middle to zero at the end. Since s' is also a func[illegible] magnetic field $\underset{\sim}{H}$ (regarded here as the applied field) and tempe[illegible] with a maximum value s'(0,0) and a minimum value equal to zer[illegible] tical current density has a stronger dependence on $\underset{\sim}{H}$ and T than [illegible] superconductor, due to the upper limit on the integral. If I_{c}[illegible] filaments in the integral of Eq. (2) is approximately the same [illegible] will be found to be the case only at temperatures not too close [illegible] since T_c is different in different filaments. For small s' the I_{cf} for small s should be used.)

$$I_c \approx \frac{1}{2} I_{cf}(0;\underset{\sim}{H},T) \int_0^{2s'} f(s)\, ds\ .$$

Then I_{cf} is determined by the filament rather than the proximity [illegible] at a given field and temperature is a function that depends [illegible] [illegible] forces in the filaments, while the integral depends on the [illegible]ment distribution. The additional temperature and field dependen[illegible] is now isolated in the integral factor. If N is the total number of filaments intersecting any conductor cross section

$$\int_0^\infty f(s)\, ds = N \ , \tag{4}$$

and if each filament has the area a, and the conductor has the area A, then

$$N = \frac{\lambda A}{a} \tag{5}$$

where λ is the fraction of superconductor in the composite. It follows from these results and (3) that

$$I_c \approx \frac{A\lambda j_{cf}}{2} \frac{\int_0^{2s'} f(s)\, ds}{\int_0^\infty f(s)\, ds} \tag{6}$$

where j_{cf} is the filamentary critical current density. The ratio of the two integrals in (6) is the fraction of filaments with values of s less than 2s', which will be denoted as $N_{2s'}/N$. If j_c is defined to be the average current density I_c/A, Eq. (6) can be written as

$$j_c \approx \frac{\lambda}{2}\, j_{cf}(0;H,T)\, \frac{N_{2s'}}{N} \ , \tag{7}$$

and when 2s' is small compared with the average value of s, j_c will be quite small compared with λj_{cf}. The equation holds within the approximation (3).

TRANSITION TEMPERATURE FOR MACROSCOPIC SUPERCONDUCTIVITY

In the theory for ordinary superconductors the temperature which results in the loss of superconductivity depends only on H. For an in situ material the temperature for transition between a macroscopic superconducting and non-superconducting state will depend on the current, or average current density $j = \frac{I}{A}$, in addition to the magnetic field. The transition at a fixed current is caused by the appearance of a normal layer s'' for some of the filaments carrying the supercurrent. Since only a small part of the total volume is changed from superconducting to normal the current is easily held constant at the transition by the application of a small electric field. The resistive state will occur whenever I_c becomes smaller than the fixed current I, forcing filaments with resistive connections to carry the excess current. Thus the temperature producing the transition is defined by the equation $I_c = I$, or

$$\frac{1}{2} \int_{o}^{2s'(\underset{\sim}{H},T)} I_{cf}(s;\underset{\sim}{H},T)\ f(s)\ ds = I \qquad (8)$$

with a solution

$$T = T_1(j,H) \qquad (9)$$

which decreases with increasing j and H. T_1 will be called the transition temperature for macroscopic superconductivity, or the first critical temperature. For $j = I = 0$, T_1 is the temperature which makes the proximity layer thickness approach zero, assuming $f(0) \neq 0$. [For $f(0) = 0$, T_1 is the temperature which makes $s' = s_{min}/2$ where s_{min} is the smallest separation between filaments.)

RESISTANCE FOR $I > I_c$

Above the first critical temperature, I is greater than I_c and an electric field E exists. For small electric fields one may write

$$I = I_c^{+} + \int_{2s'+\gamma}^{\infty} I_f \, f(s) \, ds \qquad (10)$$

where

$$I_c^{+} = \frac{1}{2} \int_{o}^{2s'+\gamma} I_{cf} \, f(s) \, ds \qquad (11)$$

and

$$I_f = \frac{E\ell}{R_f} \qquad (12)$$

with R_f the resistance of a filament and ℓ its length. γ is a small parameter which insures that the value of I_f given by (12) is less than I_{cf}. For values of s between 2s' and 2s'+γ the filaments carry a critical current even though they are resistive. However, for very small electric fields γ approaches zero, and I_c^{+} approaches I_c.

Substituting (12) into (10), solving for E and calculating the conductor resistance $\dot{R} = EL/I$ where L is the conductor length, one obtains

$$R = R_o \left(1 - \frac{I_c^{\dagger}}{I}\right) \qquad (13)$$

$$\approx R_o \left(1 - \frac{I_c}{I}\right)$$

where

$$R_o^{-1} = \frac{\ell}{L} \int_{2s'+\gamma}^{\infty} \frac{f(s)\,ds}{R_f} \;. \qquad (14)$$

From previous results [Eq. (8) of Ref. 2], the resistance for superconducting filaments is found to be

$$R_f \sim \frac{8\rho_m\, d'\, \lambda_\ell\, s''}{\ell a} \;, \qquad (15)$$

where ρ_m is the resistivity of the normal layer of thickness s", and λ_ℓ is the local value of λ. It is shown in the following section that filaments having a value of s greater than a critical value s_c are normal, and since R_f given by (15) is small compared with a normal resistance, one may write

$$R_o^{-1} \sim \frac{\ell^2 a}{8\rho_m L d'} \int_{2s'+\gamma}^{s_c} \frac{f(s)\, ds}{\lambda_\ell (s - 2s')} \tag{16}$$

$$= R_m^{-1} \frac{\ell^2}{8d'} \frac{1}{N} \int_{2s'+\gamma}^{s_c} \frac{\lambda}{\lambda_\ell} \frac{f(s)\, ds}{(s - 2s')}$$

where R_m is the resistance of a conductor with resistivity ρ_m (which for thin layers may differ somewhat from bulk material). For the special case where the lower limit is small and the upper limit is large compared with the average value s_{av}, R_o is relatively insensitive to the limits of the integral, and a very rough estimate for (16) in this case gives

$$R_o \sim \frac{R_m \, 8d' \, s_{av}}{\ell^2} \tag{17}$$

$$\sim \frac{R_m \, 8\lambda^{1/2}}{Re^3} ,$$

which is sufficient to show that even for moderately elongated filaments, R_o is small compared with R_m.

The behavior described by (13) will terminate at a second transition temperature T_2 which results from a critical number of filaments becoming normal.

THE SECOND TRANSITION TEMPERATURE

It has been shown by Luhman and Suenaga[7] that the critical temperature T_c for superconductivity in a continuous multifilament wire depends upon the fraction of superconductor in the wire. The effect is attributed to stresses established during cool-down, as a result of the difference in thermal expansion between the filament and matrix. For reasons noted by the authors the stresses are very difficult to calculate, but they may be inferred from the measurements. The lower the filament concentration the lower the observed T_c.

For filaments of a few thousand angstroms or less, a similar behavior is expected due to the proximity effect.[5] Whatever the cause may be, the assumption is made that for a non-uniform filament distribution the T_c for microscopic superconductivity depends upon the local concentration of filaments. It follows from this assumption that

$$T_c = T_c(s) \tag{18}$$

with the maximum value $T_c(0)$ and minimum value $T_c(s_{max})$. Thus the temperature at which a filament becomes normal is a function of H and s. For temperatures within the range where some filaments are normal, a critical value

$$s_c = s_c(H,T) \tag{19}$$

exists such that for $s > s_c$ the filaments are normal, and for $s < s_c$ they are superconducting.

Consider the maximum current which can be carried by superconducting filaments in a strong electric field. This is given by $I_c^* + \Delta I$ where

$$I_c^* = \int_o^{s_c} I_{cf}\, f(s)\, ds \tag{20}$$

represents the maximum current that can be carried without exceeding the critical current density in the filaments, and ΔI is due to the increase of filament current beyond its critical value. Thus the total current in a strong electric field is

$$I = I_c^* + \Delta I + I_{nor.} \tag{21}$$

where I_{nor} is the normal current flowing in the matrix and the normal filaments, given by

$$I_{nor} = \frac{LE}{R_{nor.}}$$

$$= \frac{IR}{R_{nor.}}\ , \tag{22}$$

with $R_{nor.}$ the resistance of the normal part at any temperature. ΔI is given by

$$\Delta I = \int_0^{s_c} \Delta I_f \, f(s) \, ds$$

where ΔI_f can be approximated by the empirical expression[8]

$$\Delta I_f = \frac{1}{\Lambda} \ln\left(\frac{E}{E_o} + 1\right) . \tag{23}$$

Λ and E_o are constants for the filament.

Both ΔI and $I_{nor.}$ require relatively large electric fields for appreciable values. The current I_c^* corresponds to the current resulting when a critical current exists in all superconducting filaments over their entire length. The value $I_c^*/2$ is achieved in very small electric fields, but for currents I approaching I_c^* and beyond the electric field must rise rapidly. It follows that the temperature $T = T_2(j,H)$ obtained from the equation

$$I_c^*(H,T) = I \tag{24}$$

defines, approximately, a second macroscopic critical temperature.

The resistance for I above I_c^* is determined by solving Eq. (21) for the electric field. At temperatures approaching the highest value of

$T_c(s)$, where all the filaments become normal, s_c and I_c^* approach zero, and (21) reduces to

$$I \approx I_{nor.} \quad , \tag{25}$$

and

$$R \approx R_{o\,nor.} \quad , \tag{26}$$

where $R_{o\,nor.}$ is the resistance of a fully normal conductor.

COMPARISON WITH MEASUREMENTS

A schematic curve showing the features of the calculated results as a function of temperature is given in Fig. 3, which may be compared with the measurements of Lobb et al.[1] reproduced in Fig. 4. For smaller values of current T_1 and T_2 will shift to the right, and, therefore, the calculated curve is in good qualitative agreement with the measurements. A plot of the critical current density as obtained from a point on each of the four measured curves is shown in Fig. 5, along with a curve for j_c^* obtained in a similar way. The dashed curve in the figure corresponds to j_c divided by $\lambda j_{cf}(T)/2j_{cf}(0)$. To obtain the latter, the approximation was made that for no applied magnetic field, $j_{cf}(T)$ is a linear function[9] of T which goes to zero near 7°K, since j_{cf} in Eq. (7) refers to the critical current density of a filament with small s and high T_c. It is immediately observed, as predicted, that the in situ critical current density has a much different temperature dependence than the filament current density. With the use of Eq. (7) the dashed curve in Fig. 5 is a measure of $j_{cf}(0)\ N_{2s'}/N$. For an assumed value of 5×10^5 amps/cm^2 for $j_{cf}(0)$ it follows that at T = 0, $N_{2s'}/N = 0.04$. To obtain a rough calculated estimate of $N_{2s'}/N$, let f(s) be treated as constant with a cut-off at $s = 2s_{av}$. Thus $N_{2s'}/N \sim s'/s_{av}$. Equating this result with the measured value, and noting that for circular filaments $s_{av} \sim d/\sqrt{\lambda} \sim 5\ \mu m$ for the measured material, one obtains a value of $s'(0,0) \sim 0.2\ \mu m$ derived from the

Curve 740612-A

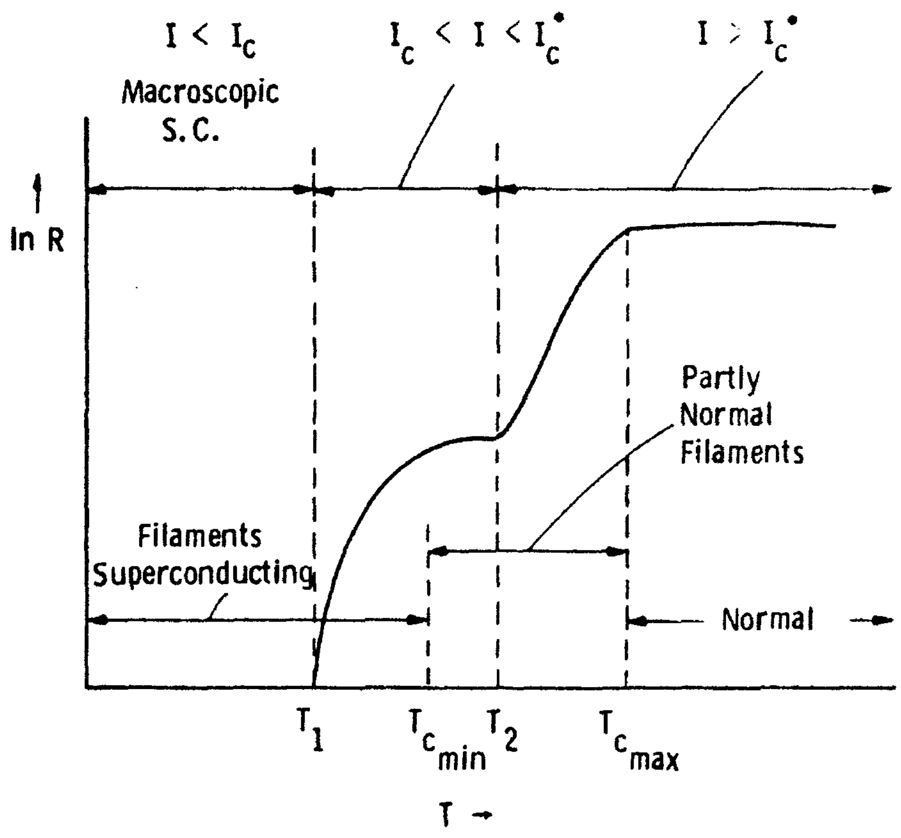

Fig. 3 — Plot of logarithm of the resistance vs temperature for a fixed value of current I and magnetic field. $T_{c_{min}}$ and $T_{c_{max}}$ are the minimum and maximum T_c for filaments. T_1 and T_2 are the macroscopic critical temperatures

Curve 740613-A

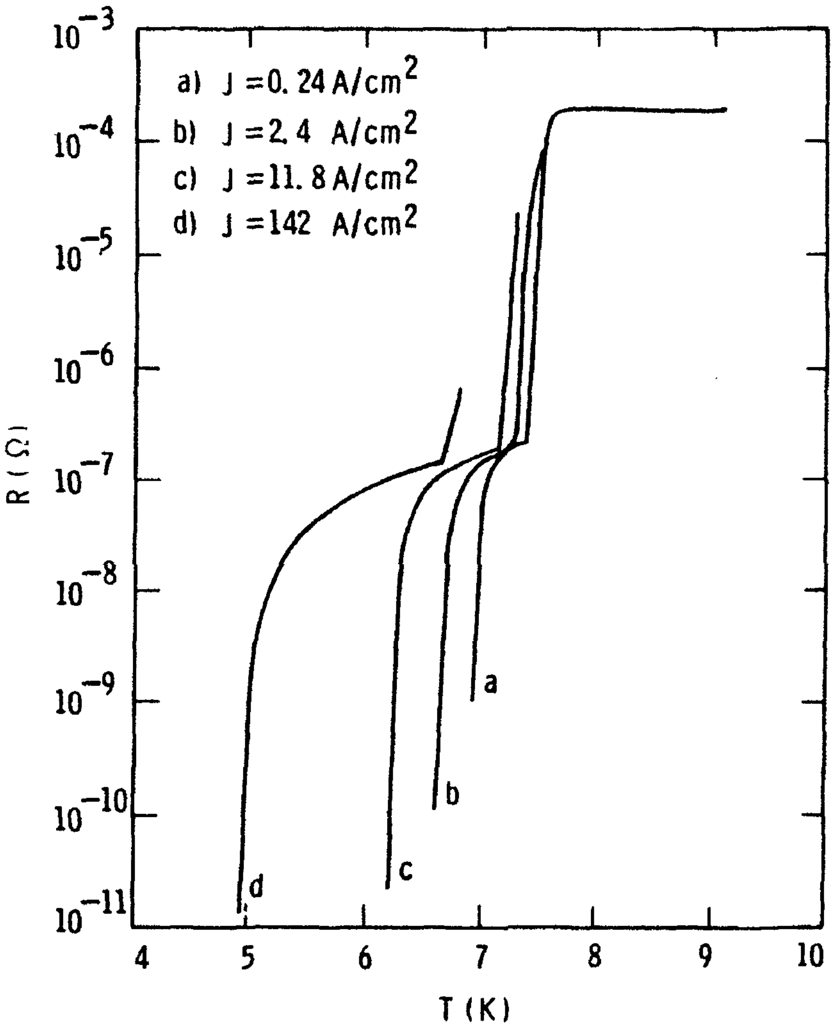

Fig. 4 — The measurements of C. J. Lobb, M. Tinkham and W. J. Skocpol for 7 vol % Nb in a Cu - 3 at. % Ni matrix. Re = 16 (Taken from Ref. 1)

measurements. This is just the order of magnitude one would expect for the proximity length.[4,5]

With the use of the critical current density curve of Fig. 5 and the measured values of T_1 and T_2 one can calculate R/R_o in the range between T_1 and T_2 with the aid of Eq. (13). The result is shown in Fig. 6 which again compares favorably with Fig. 4, if R_o is assumed to be only a weak function of temperature.

The plateau in the curve of Fig. 3 will disappear under any set of conditions where $T_1 \rightarrow T_2$. While these conditions have not been investigated in general, it is clear that T_1 tends to approach T_2 when (a) the filaments are more uniformly spaced, (b) when the current I is relatively small, and (c) when the temperature dependence of I_c is weak.

Curve 740615-A

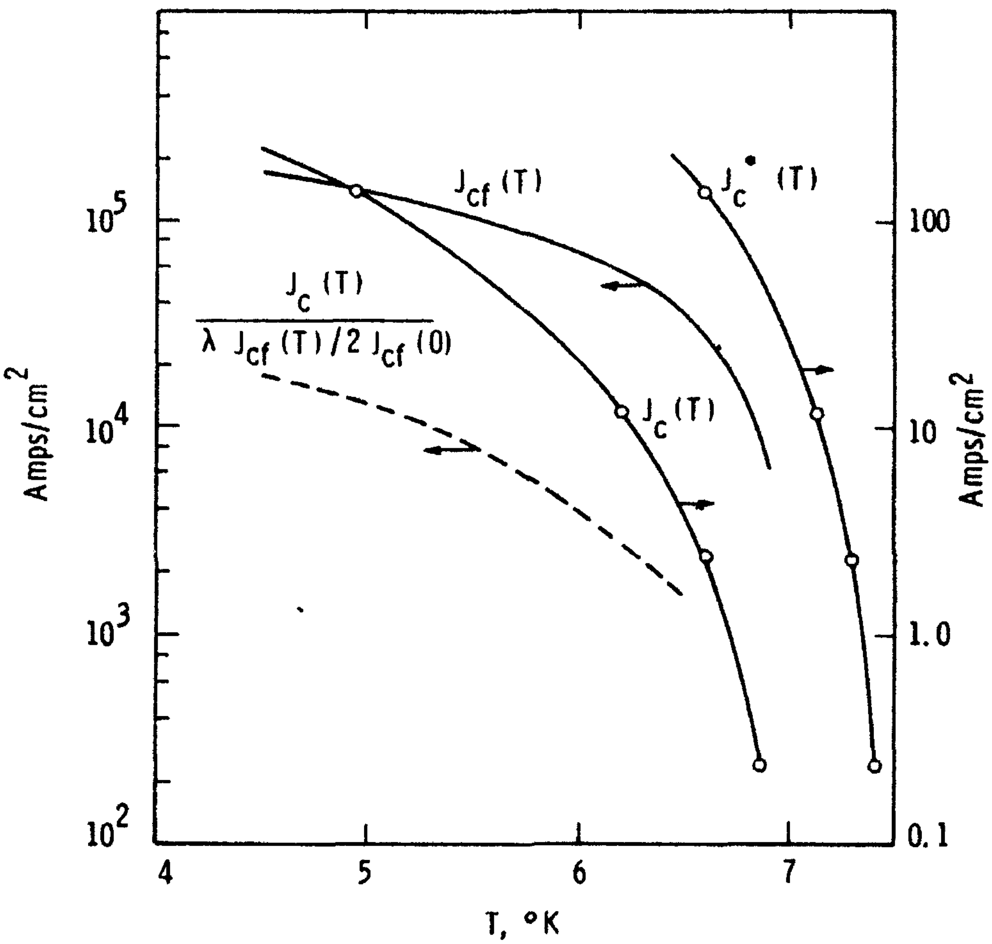

Fig. 5 — J_c and J_c^* as deduced from the data in Fig. 4. J_{cf} for no applied field is estimated by assuming the relation $J_{cf}(T) \approx J_{cf}(0)\,[1 - T/7]$ where 5×10^5 amps/cm^2 is assumed for J_{cf} (0)

Curve 740614-A

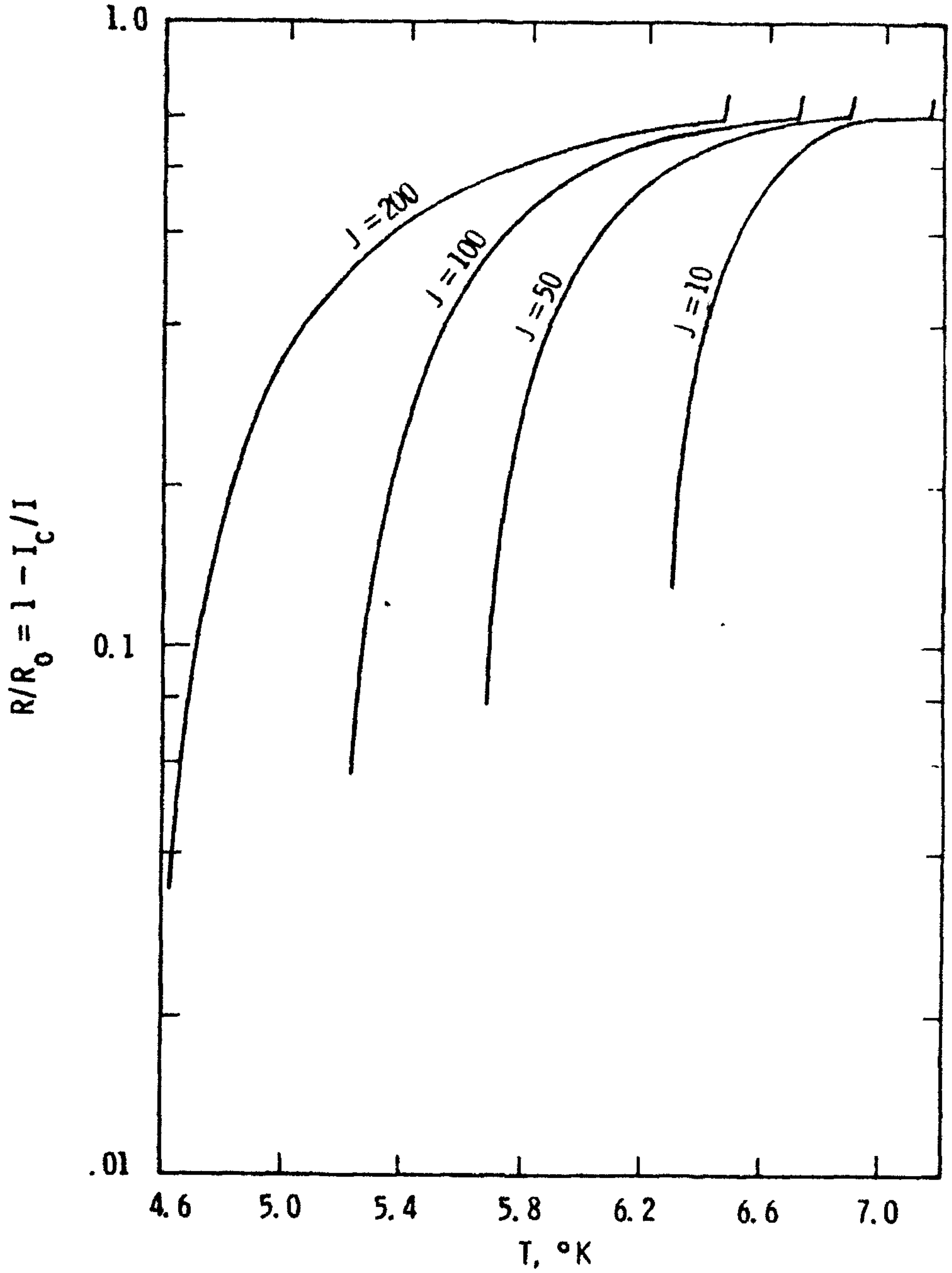

Fig. 6 — Temperature dependence of R/R_0 between T_1 and T_2

REFERENCES

1. C. J. Lobb, M. Tinkham, and W. J. Skocpol, Solid State Comm. 27, 1273 (1978).

2. W. J. Carr, Jr., submitted to J. Appl. Phys.

3. A. Davidson, M. R. Beasley and M. Tinkham, IEEE Trans. MAG-11, 276 (1975).

4. J. Bevk, M. Tinkham, F. Habbal, C. J. Lobb, and J. P. Harbison, IEEE Trans. MAG-17, 235 (1981).

5. G. Deutscher and P. G. DeGennes, Superconductivity, Vol. 2, Ed. by R. D. Parks, Marcel Dekker, New York (1969).

6. T. J. Callaghan and L. E. Toth, J. Appl. Phys. 46, 4013 (1975).

7. T. Luhman and M. Suenaga, Appl. Phys. Letters 29, 61 (1976).

8. A. Février and J. C. Renard, Ad. in Cry. Eng. 24, 363, Ed. by K. D. Timmerhaus, R. P. Reed, and A. F. Clark, Plenum Press, New York (1978).

9. P. R. Aron and G. W. Ahlgren, Ad. in Cry. Eng. 13, 21, Ed. by K. D. Timmerhaus, R. P. Reed, and A. F. Clark, Plenum Press, New York (1968).

Published in J. Appl. Phys. 54, 6549 (1983).

APPENDIX C

EFFECT OF TWIST ON WIRES MADE FROM IN SITU SUPERCONDUCTORS*

W. J. Carr, Jr.

Westinghouse R&D Center
Pittsburgh, Pennsylvania 15235

ABSTRACT

The effect of twist on the transverse field hysteresis of in situ superconducting wires is assumed to result from a lowering of the axial critical current density due to anisotropy of critical current density in the material. In weak transverse magnetic fields the twist raises the hysteresis loss, while in stronger fields the twist lowers the loss. It is shown that the axial critical current density determined from hysteresis or magnetic moment measurements in a twisted wire can be lower than the value obtained from transport measurements.

*Supported by the Air Force Aero Propulsion Laboratory, Contract No. F33615-81-C-2040.

INTRODUCTION

Measurements in a transverse magnetic field of the dc hysteresis for in situ superconductors indicate that in many samples the loss is that which would exist in a pure superconductor of the same dimensions and critical current density,[1,2] and, therefore, much larger than the hysteresis of an ordinary multifilament conductor. Nevertheless, it has been shown[1-5] that twisting the conductor can change the hysteresis, sometimes by as much as a factor of ten. A model for an in situ superconductor was recently proposed by the author,[6] and it was suggested that the effect of twist is related to a large anisotropy in critical current density which may be present in in situ materials. A more detailed analysis of this effect is presented here.

THE CRITICAL CURRENT DENSITIES

In the model referred to it is assumed that in an in situ material the filaments are in the shape of ribbons[7,8] with the principal axes denoted by 1, 2, 3 where the 1 axis is along the length, the 2 axis along the width and the 3 axis along the thickness. A vanishingly small electric field along the 1 axis produces a critical current density j_{c1}, which, of course, depends upon the temperature and the magnitude and direction of the magnetic field. If the in situ material is superconducting in all three directions critical current densities j_{c2} and j_{c3} exist for the other principal directions.

Neighboring filaments along a given chain are assumed to be electrically connected by the proximity effect via filaments in a different chain. The critical current density is determined by either the filament or the proximity layer. If the wire has been subjected to a large mechanical reduction to produce very long filaments, one may postulate that in the 1 direction j_c is determined by the filament, and[6]

$$j_{c1} \approx \frac{\lambda}{2} j_{c1f} \tag{1}$$

where λ is the fraction of superconductor in the composite and j_{c1f} is the critical current density of a filament along its length. The factor $\frac{1}{2}$ comes from an average over the length. In a direction through the thickness of the filament the critical current density j_{cp} of the proximity layer will dominate, providing j_{cp} is small compared with the filament critical current density, and

$$j_{c3} \approx j_{cp}' \; . \tag{2}$$

For a ribbon where the ratio of width to thickness w/d is less than the order of 10, one would expect that j_{c2} is the order of[6] $\lambda \; j_{cp} \; w/4d$, assuming the filaments are arranged uniformly enough to permit superconductivity in this direction. For typical values of λ and w/d, j_{c2} will be the smallest of the critical current densities. For simplicity it will be assumed that the wire is not superconducting along the 2 direction, and

$$j_{c2} = 0 \; . \tag{3}$$

When small electric field components exist simultaneously in more than one principal direction the assumption will be made that the critical current densities are the same order of magnitude as those measured for a single electric field component. In the case of j_{c1} and j_{c3} this assumption is reasonable because the two critical current densities are determined by different mechanisms. The argument is as follows: in the case of j_{c1} alone the current density flowing across the proximity layer surrounding a very long filament is much smaller than the critical current density of the proximity layer and, therefore, when an additional field component E_3 is applied, tending to produce a unidirectional current density j_{c3} through the proximity layer, this current is not seriously restricted by the presence of j_{c1}. j_{c2} may interact more strongly with the other components but its value is less important.

It follows from the assumption of independent values for j_{c1}, j_{c2} and j_{c3} that the critical current can now be specified in any direction; for insofar as the approximation is valid, the magnitude of the current density which can flow in an arbitrary direction is determined by the fact that its components along the principal axes of the filaments cannot exceed the critical values approximated by Eqs. (1), (2) and (3).

ORIENTATION OF FILAMENTS IN A WIRE AND THE AXIAL CRITICAL CURRENT DENSITY

It is reasonable to expect that in a highly reduced untwisted wire the filaments tend to be packed as idealized in Fig. 1, where the width is along the radial direction, the filament thickness is along the circumferential direction and the filament length is along the length of the wire, or z direction, in cylindrical coordinates R, θ, z. Electron micrographs (Fig. 2) seem to confirm this assumption near the surface, although the packing is far from ideal.

Consider now the effect of twist in the wire as in Fig. 3. For ideal packing the unit vectors $\hat{a}_1$, $\hat{a}_2$ and $\hat{a}_3$ for the filaments are given in terms of the unit vectors for the wire coordinates by[9]

$$\hat{a}_1 = \frac{\hat{a}_z + \frac{2\pi R}{L}\hat{a}_\theta}{\left[1 + \left(\frac{2\pi R}{L}\right)^2\right]^{1/2}} \qquad (4)$$

$$\hat{a}_2 = \hat{a}_R \qquad (5)$$

$$\hat{a}_3 = \frac{\hat{a}_\theta - \frac{2\pi R}{L}\hat{a}_z}{\left[1 + \left(\frac{2\pi R}{L}\right)^2\right]^{1/2}} \qquad (6)$$

Dwg. 7773A43

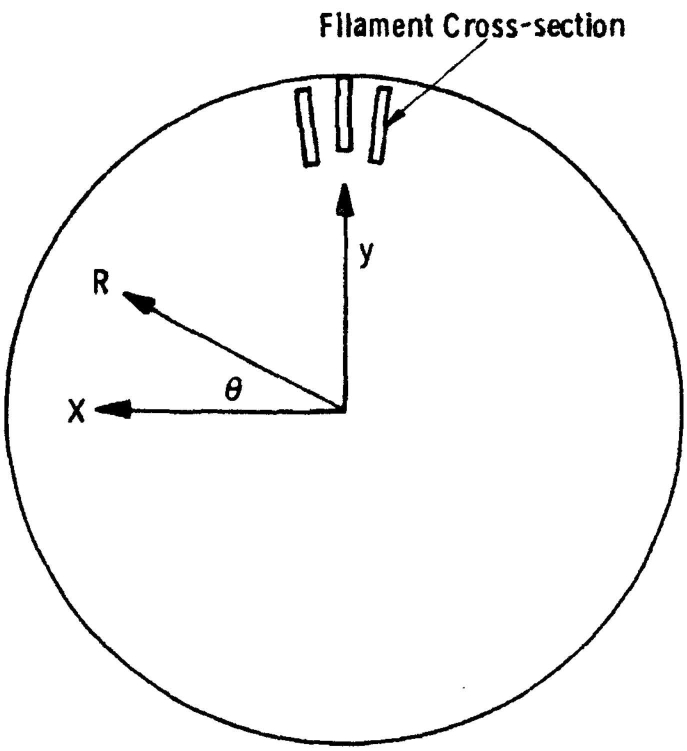

Fig. 1—The packing of filaments in an untwisted wire. (The angle θ is taken to conform with that of clock-wise twist of Fig. 3)

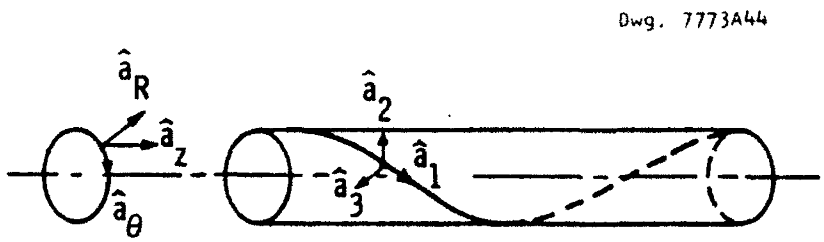

Fig. 3 —Unit vectors $\hat{a}_1$, $\hat{a}_2$, and $\hat{a}_3$ for the twisted filaments and the unit vectors $\hat{a}_R$, $\hat{a}_\theta$, $\hat{a}_z$ for the cylindrical conductor.

where L is the twist length. If a current density $\mathbf{j} = j\,\hat{a}_z$ flows down the wire it has components

$$j\left[1 + \left(\frac{2\pi\ R}{L}\right)^2\right]^{-1/2} \quad \text{and} \quad -j\left(\frac{2\pi\ R}{L}\right)\left[1 + \left(\frac{2\pi\ R}{L}\right)^2\right]^{-1/2}$$

in the 1 and 3 directions of the filaments. For relatively large twist lengths the components reduce to j and $-j\ 2\pi\ R/L$. But the magnitude of these components must be less than the critical current densities j_{c1} and j_{c3} respectively, and the maximum value that j can take if it flows entirely along the z axis is either

$$j = j_{c1} \tag{7}$$

$$\approx \frac{\lambda}{2}\, j_{c1f}$$

or

$$j = \frac{L}{2\pi\ R}\, j_{c3} \tag{8}$$

$$\approx \frac{L}{2\pi\ R}\, j_{cp}\ ,$$

whichever is smaller. In anticipation of later results, one may call this value of j the axial critical current density j'_{cz} obtained from a hysteresis measurement. When the twist length is very long j'_{cz} is given by (7), but for smaller L, j'_{cz} is determined by (8), except near the axis of the wire.

HYSTERESIS LOSS

For the case of full penetration, it is shown in the Appendix that in order to avoid divergence of current when a changing transverse magnetic field is applied to the wire, one component of the current density must be free to take arbitrary values. It follows, therefore, that one of the electric field components E_1 and E_3 must vanish. (An idea along these lines has been investigated independently by Murphy.)[10] If $E_1 = 0$, the power density $\underset{\sim}{E} \cdot \underset{\sim}{j}$ is equal to $|E_3|\ j_{c3}$, and if $E_3 = 0$, $\underset{\sim}{E} \cdot \underset{\sim}{j} = |E_1|\ j_{c1}$. In terms of the components for the wire coordinates, it is shown in the Appendix that $\underset{\sim}{E} \cdot \underset{\sim}{j} = E_z\ j_z$ in both cases, nd j_z is the only non-vanishing current component. In other words, the current induced by a transverse magnetic field is a "shielding" current which flows down the axis of the wire on one side and returns on the other side. If this is assumed to be the case in general the hysteresis loss is the same as in an ordinary bulk superconductor, and the critical value of j_z is j'_{cz} calculated in the previous section.

In weak magnetic fields the hysteresis loss depends inversely on j'_{cz}, because larger values provide more efficient shielding and allow less penetration. Since for $L = \infty$, $j'_{cz} = j_{c1}$, it follows that for heavily twisted wires where $j'_{cz} \approx L\ j_{cp}/2\pi\ R_o < j_{c1}$ the hysteresis Q is given by

$$Q(L) = \frac{2\pi\ R_o\ j_{c1}}{L\ j_{cp}}\ Q(\infty) \tag{9}$$

in weak applied fields H_A small compared with the penetration field. R_o is the radius of the wire, and for a Bean model $Q(\infty)$ is proportional to $H_A{}^3$.

For the case where H_A is large compared with the penetration field, the loss is directly proportional to j'_{cz}, and

$$Q(L) \approx \frac{L\ j_{cp}}{2\pi\ R_o\ j_{cl}}\ Q(\infty) \qquad (10)$$

where $Q(\infty)$ is now proportional to H_A. In reality, an average value of j'_{cz} over the wire should be used in (10), but since most of the area is near the outside, the result is approximately given by (10).

In a qualitative sense the behavior described by (9) and (10) is just that observed in the measurements of Braginski and Wagner[1] shown in Fig. 4, and Shen and Verhoeven[2] in Fig. 5. The data indicate in the latter case a value of j_{cl}/j_{cp} of about 30, while in the former it is in the neighborhood of 10 to 20, with the high field value smaller than the low field value. Since $\lambda \sim 0.2$ for these samples it follows that j_{clf}/j_{cp} is in the range of 100 to 300.

It is of interest to compare the behavior of twisted in situ wires with continuous filament conductors. When the latter are twisted a normal resistance is introduced into the path along the axis, and the critical current density j'_{cz} goes to zero. When the in situ wires are twisted j'_{cz} does not go to zero, but it does fall to a smaller value.

Curve 724315-B

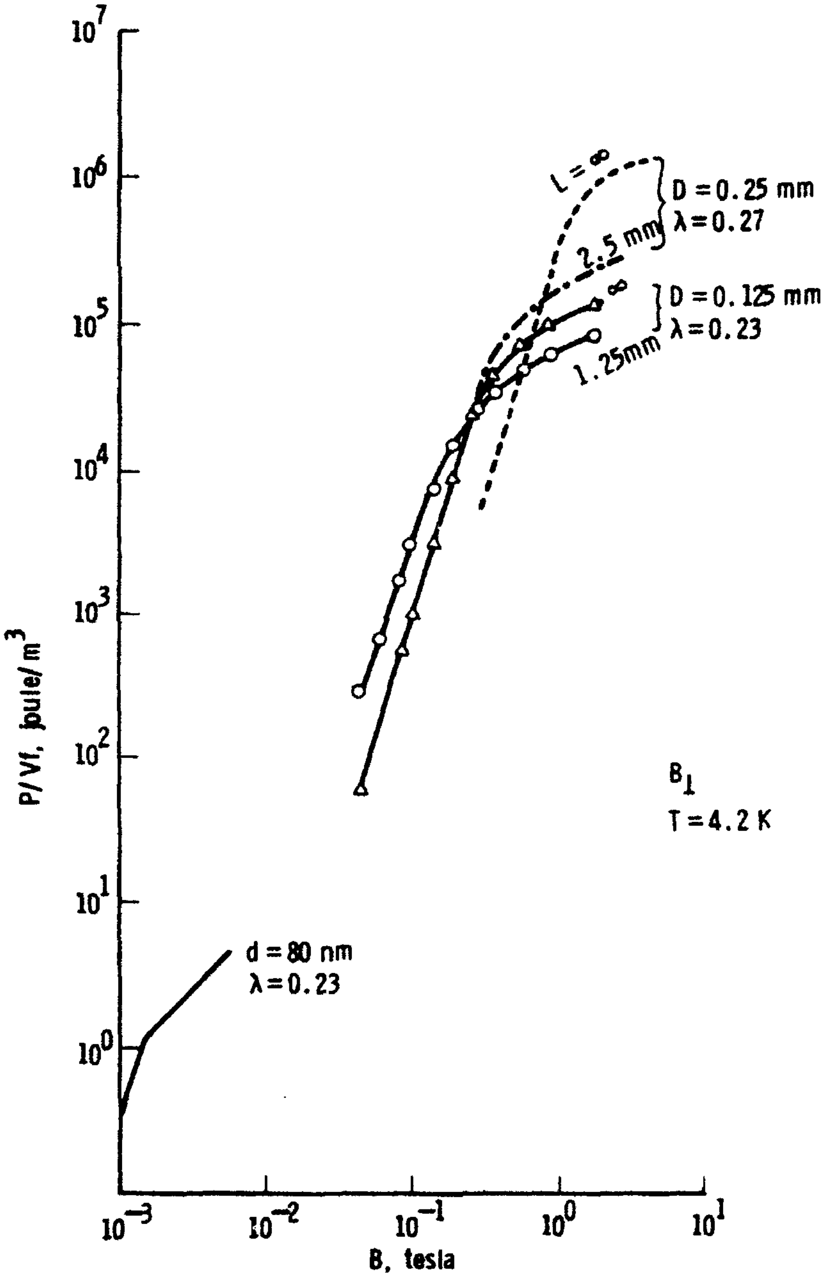

Fig. 4—Hysteretic loss per cycle vs the perpendicular field intensity in untwisted ($L = \infty$) and twisted conductors. (Taken from Braginski and Wagner[1])

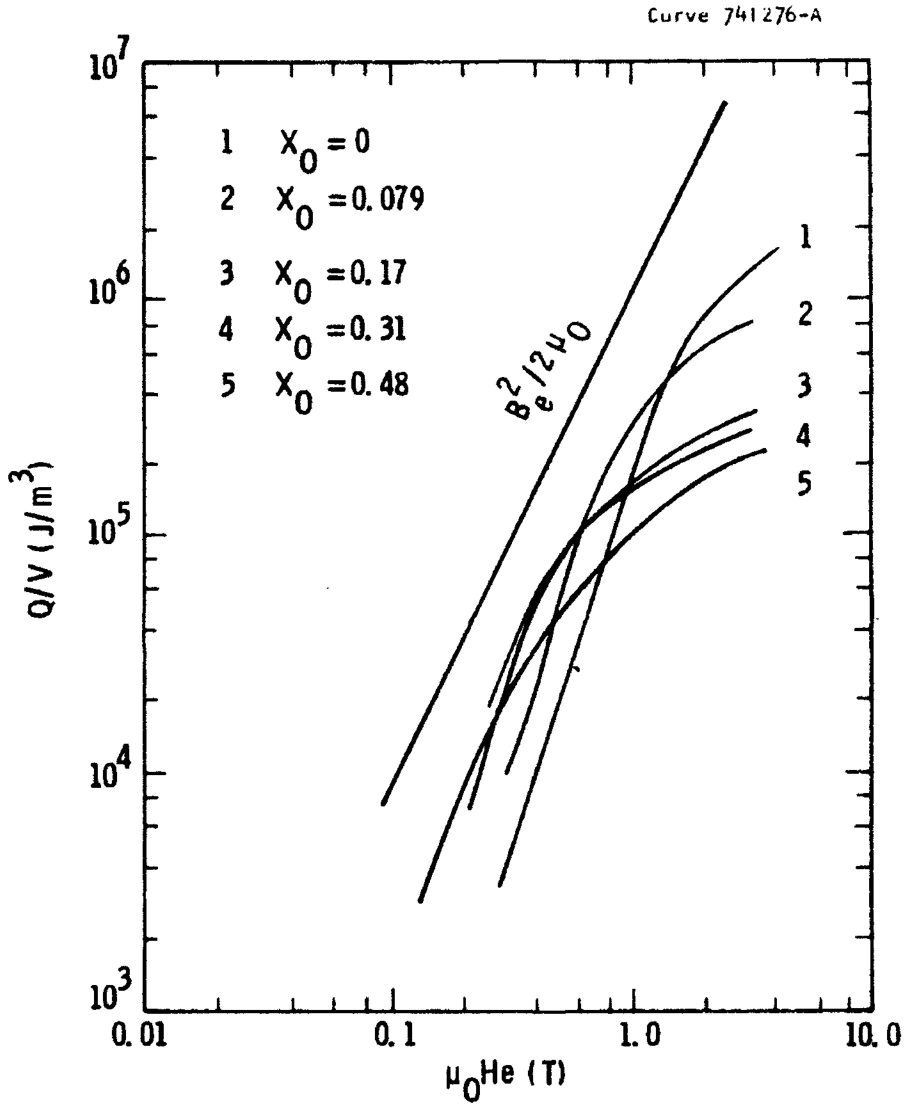

Fig. 5—Hysteresis losses of composites with different twist parameters. $X_0 = 2\pi R_0/L$. Taken from Shen and Verhoeven[2]

THE CRITICAL CURRENT DENSITY FOR TRANSPORT

When critical current density is measured from transport in a well-twisted in situ wire, a value different from the value obtained from the hysteresis or magnetic moment can be expected. When a small uniform electric field is applied along the z axis, the current density is simply

$$\underset{\sim}{j} = j_{c1} \operatorname{sgn} E_1 \hat{a}_1 + j_{c3} \operatorname{sgn} E_3 \hat{a}_3 \ . \tag{11}$$

and (see the Appendix)

$$j_z = \frac{\left(j_{c1} + \frac{2\pi R}{L} j_{c3}\right)}{\sqrt{1 + \left(\frac{2\pi R}{L}\right)^2}} \operatorname{sgn} E_z \tag{12}$$

where $\operatorname{sgn} E_1 = -\operatorname{sgn} E_3 = \operatorname{sgn} E_z$. Thus, for small $2\pi R_o/L$, as measured by transport

$$j_{cz} \approx j_{c1} \ , \tag{13}$$

which can be considerably larger than j'_{cz} when Eq. (8) applies. The source of the difference lies in the fact that in the transport measurement the electric field is independent of θ, and no problem exists with the divergence of $\underset{\sim}{j}$.

REFERENCES

1. A. I. Braginski and G. R. Wagner, IEEE Trans. MAG 17, 243 (1981).
2. S. S. Shen and J. D. Verhoeven, IEEE Trans. MAG 17, 248 (1981).
3. S. S. Shen, Filamentary A15 Superconductors, Ed. M. Suenaga and A. F. Clark, Plenum Press, New York (1980).
4. A. I. Braginski and J. Bevk, Filamentary A15 Superconductors, Ed. M. Suenaga and A. F. Clark, Plenum Press, New York (1980).
5. K. Yasohama, H. Ohkubo, T. Ogasawara, and Kō Yasukōchi, Ad. in Cry. Eng., Vol. 28, Ed. R. P. Reed and A. F. Clark, Plenum Press, New York (1982).
6. W. J. Carr, Jr., to be published.
7. J. Bevk, M. Tinkham, F. Habbal, C. J. Lobb, and J. P. Harbison, IEEE Trans. MAG 17, 235 (1981).
8. J. D. Verhoeven, D. K. Finnemore, E. D. Gibson, J. E. Ostenson, and L. F. Goodrich, Appl. Phys. Lett. 33, 101 (1978).
9. W. J. Carr, Jr., AC Loss and Macroscopic Theory of Superconductors, Gordon and Breech, London (in press).
10. J. H. Murphy - unpublished.

APPENDIX

If the rate of change of applied field $\dot{H}_A$ is very small all resistive currents can be neglected in a zeroth order approximation, and for the two-directional superconductor considered here,

$$\underset{\sim}{j} = j_1 \, \dot{a}_1 + j_3 \, \dot{a}_3 \tag{A-1}$$

where in cylindrical coordinates of the wire the components are

$$j_z = \left(j_1 - \frac{2\pi \; R}{L} \, j_3\right)\left[1 + \left(\frac{2\pi \; R}{L}\right)^2\right]^{-1/2} \tag{A-2}$$

$$j_\theta = \left(\frac{2\pi \; R}{L} \, j_1 + j_3\right)\left[1 + \left(\frac{2\pi \; R}{L}\right)^2\right]^{-1/2} \tag{A-3}$$

$$j_R = 0 \; . \tag{A-4}$$

j_1 and j_3 are given by the critical current densities, unless the electric field along one of the principal directions vanishes, in which case, if $E_i = 0$, the current component j_i can take any value between $\pm \, j_{ci}$. The current density must satisfy div $\underset{\sim}{j} = 0$, which reduces to $\partial j_\theta / \partial \theta = 0$, since for a long wire the current density is independent of z. In addition it will be assumed that the average value of j_z must vanish, corresponding to no net transport current.

After full penetration of the wire $\dot{\underset{\sim}{B}} \approx \dot{\underset{\sim}{H}}_A$ and the electric field in this approximation is

$$\underset{\sim}{E} = -\dot{H}_A R \sin\theta \, \hat{a}_z + \nabla\phi \tag{A-5}$$

where ϕ depends only on R and θ. The components of electric field along the filament axes are

$$E_1 = \left(-\dot{H}_A R \sin\theta + \frac{2\pi}{L}\frac{\partial\phi}{\partial\theta}\right)\left[1 + \left(\frac{2\pi R}{L}\right)^2\right]^{-1/2} \tag{A-6}$$

$$E_3 = \left(\frac{2\pi}{L}\dot{H}_A R^2 \sin\theta + \frac{1}{R}\frac{\partial\phi}{\partial\theta}\right)\left[1 + \left(\frac{2\pi R}{L}\right)^2\right]^{-1/2} \tag{A-7}$$

$$E_2 = \frac{\partial\phi}{\partial R} \tag{A-8}$$

Solutions can be investigated for four cases where (a) $E_1 = 0$, $E_3 \neq 0$; (b) $E_3 = 0$, $E_1 \neq 0$; (c) $E_1 \neq 0$, $E_3 \neq 0$ and (d) $E_1 = E_3 = 0$. But for non-vanishing $\dot{H}_A$ (d) is not allowed by (A-6) and (A-7), and since the signs of E_1 and E_3 change with θ, no divergenceless solution for $\underset{\sim}{j}$ can be found in case (c). Thus only (a) and (b) need be considered.

For case (b), $j_1 = j_{c1}$ sgn E_1 where

$$E_1 = -\dot{H}_A R \sin \theta \left[1 + \left(\frac{2\pi R}{L}\right)^2\right]^{1/2} \qquad \text{(A-9)}$$

and sgn E_1 is equal to $-\dot{H}_A \sin \theta / |\dot{H}_A \sin \theta|$. Then since $\partial j_\theta / \partial \theta$ must vanish it follows from (A-3) that

$$j_3 = \frac{2\pi R}{L} j_{c1} \frac{\dot{H}_A \sin \theta}{|\dot{H}_A \sin \theta|} + f(R) \qquad \text{(A-10)}$$

But (A-10) can apply only when the magnitude of the right-hand side is equal to or smaller than j_{c3}. The maximum value of the magnitude of the right-hand side at a fixed value of R is $2\pi R j_{c1}/L + |f(R)|$, and the range of the solution is given by

$$R \leqslant \frac{L}{2\pi j_{c1}} \left(j_{c3} - |f(R)|\right) \qquad \text{(A-11)}$$

where the maximum range corresponds to $f(R) = 0$. With this choice

$$j_\theta = 0 \qquad \text{(A-12)}$$

$$j_z = -j_{c1} \frac{\dot{H}_A \sin \theta}{|\dot{H}_A \sin \theta|} \left[1 + \left(\frac{2\pi R}{L}\right)^2\right]^{1/2} \qquad \text{(A-13)}$$

which leads to no net transport current. The power density $\underset{\sim}{E} \cdot \underset{\sim}{j}$ is equal to $E_1\ j_1$ (or $E_z\ j_z$) which is obtained with the aid of (A-9). Therefore, for $R < L\ j_{c3}/2\pi\ j_{c1}$

$$\underset{\sim}{E} \cdot \underset{\sim}{j} = j_{c1}\ |\dot{H}_A \sin\theta|\ R \left[1 + \left(\frac{2\pi\ R}{L}\right)^2\right]^{1/2} , \tag{A-14}$$

and if $L/2\pi\ R_o > j_{c1}/j_{c3}$, where R_o is the radius of the wire, this solution holds over the entire wire.

For smaller values of $L/2\pi\ R_o$ case (a) must be examined. In a similar way one obtains a solution valid for $R > L\ j_{c3}/2\pi\ j_{c1}$ where

$$E_1 = 0 \tag{A-15}$$

$$E_3 = \frac{L}{2\pi}\ \dot{H}_A \sin\theta \left[1 + \left(\frac{2\pi\ R}{L}\right)^2\right]^{1/2} \tag{A-16}$$

$$j_1 = -\frac{L}{2\pi\ R}\ j_{c3}\ \frac{\dot{H}_A \sin\theta}{|\dot{H}_A \sin\theta|} \tag{A-17}$$

$$j_3 = j_{c3}\ \frac{\dot{H}_A \sin\theta}{|\dot{H}_A \sin\theta|} \tag{A-18}$$

$$\underset{\sim}{E} \cdot \underset{\sim}{j} = \frac{L}{2\pi}\ j_{c3}\ |\dot{H}_A \sin\theta| \left[1 + \left(\frac{2\pi\ R}{L}\right)^2\right]^{1/2} . \tag{A-19}$$

(A-19) has the form of (A-14) with j_{c1} replaced by $L\ j_{c3}/2\pi\ R$, and in both cases current flows only along the z axis. The values of the current correspond to those given by (7) and (8) in the text.

If $L\ j_{c3}/2\pi\ j_{c1}$ is small compared with R_o the last solution holds over most of the volume of the wire, but unfortunately it does not include the origin. One may note that the model for the packing of filaments is most plausible near the outside of the wire. Near the center of the wire it becomes rather implausible, and, indeed, it seems to provide no simple solution for the electric field that matches the boundary conditions for the solution obtained at larger radii. However, to avoid the complication of modifying the model one can imagine a wire with a small hole bored down the center. The solution given by (A-15) to (A-18) then applies for small values of L over the entire hollow wire.

Published in Cryogenics 24, 183 (1984).

APPENDIX D

EFFECT OF TWIST ON THE LONGITUDINAL FIELD LOSS FOR AN IN SITU SUPERCONDUCTOR*

W. J. Carr, Jr.

Westinghouse R&D Center
Pittsburgh, Pennsylvania 15235

ABSTRACT

The effect of twist on the full penetration loss of an in situ superconductor is calculated for the case of a longitudinal applied magnetic field. An increase in hysteresis with increasing twist is predicted due to a large anisotropy in the critical current density. The anisotropy results from the fact that the critical current density along the length of a filament in the in situ material is determined by the filament, while along the thickness it is determined by the proximity effect in the matrix surrounding the filament. From the measurements of Braginski and Wagner the ratio of these critical current densities is calculated to be about 70, which is in order of magnitude agreement with the value previously found from transverse field measurements.

*Supported by the Air Force Aero Propulsion Laboratory Contract No. F33615-81-C-2040.

INTRODUCTION

An explanation for the effect of twist on the hysteresis of an in situ superconducting wire in a changing transverse magnetic field has been given based on anisotropy of the critical current density.[1] In the model used for the calculation,[2] the in situ material is assumed to be made up of chains of superconducting ribbons embedded in a normal metal which exhibits a superconducting proximity effect. The principal axes of the filaments are labeled 1, 2, 3, where the 1 axis is the length, the 2 axis is the width, and the 3 is the thickness. The filaments are assumed to be packed into the wire such that for an untwisted wire the 1 axis corresponds to the z axis (length) of the wire, the 2 direction is radial, and the 3 direction circumferential. For a twisted wire with twist length L, the unit vectors $\hat{a}_1$, $\hat{a}_2$, $\hat{a}_3$ for the filaments are related to the unit vectors $\hat{a}_R$, $\hat{a}_\theta$, $\hat{a}_z$ in cylindrical coordinates for the wire by[1]

$$\hat{a}_1 = \left(\hat{a}_z + \frac{2\pi R}{L}\hat{a}_\theta\right)\left[1 + \left(\frac{2\pi R}{L}\right)^2\right]^{-1/2} \tag{1}$$

$$\hat{a}_2 = \hat{a}_R \tag{2}$$

$$\hat{a}_3 = \left(\hat{a}_\theta - \frac{2\pi R}{L}\hat{a}_z\right)\left[1 + \left(\frac{2\pi R}{L}\right)^2\right]^{-1/2} \tag{3}$$

where R is the radial distance.

A superconducting in situ material is assumed to have different critical current densities along the principal axes.[1,2] In the case of very long filaments

$$j_{c1} \sim \frac{\lambda}{2} j_{c1f} \tag{4}$$

where j_{c1f} is the critical current density of a filament and λ is the fraction of superconductor in the composite. In the direction of the thickness

$$j_{c3} \sim j_{cp} \tag{5}$$

where j_{cp} is the critical current density of the proximity layer. For simplicity it is assumed that the material is not superconducting in the 2 direction and

$$j_{c2} \sim 0 \ . \tag{6}$$

Further, it is assumed that j_{c1} and j_{c3} are independent of one another. In the present analysis this model is used to compute the effect of twist in the case of a longitudinal applied magnetic field.

CALCULATION FOR A FULLY PENETRATED WIRE

The case of a twisted filamentary wire in a changing longitudinal magnetic field is complicated by the fact that due to the twist a net transport current tends to be induced in the wire, and since the ends of the wire prevent the flow of transport current, the current distribution tends to be dominated by end effects. One way to avoid consideration of the ends is to imagine that the longitudinal applied magnetic field changes its direction along the length of the wire[3] or, alternatively, one can imagine a wire in which the direction of twist changes along the length.[4] However, for the present calculation a simpler model will be used where both the wire and the magnetic field are taken to be uniform, but a uniform longitudinal electric field is also applied of magnitude such that the net transport current vanishes for any given applied magnetic field. Only the case of a fully penetrated wire will be considered, since the case of partial penetration is a very much more difficult problem. For a fully penetrated wire the time rate of change of flux density $\dot{\underset{\sim}{B}}$ is equal to the time rate of change of the applied field $\dot{\underset{\sim}{H}}_A$ in a Bean model for the current densities. From symmetry the field components depend only the radial distance R from the center of the wire. The Maxwell equations which must be solved are

$$\text{curl } \underset{\sim}{E} = -\dot{\underset{\sim}{H}}_A \qquad (7)$$

$$\mathrm{curl}\ \underset{\sim}{H} = 4\pi\ \underset{\sim}{j}\ , \qquad (8)$$

since div $\underset{\sim}{H} = 0$ is automatically satisfied by taking $H_R = 0$. The equation for the divergence of $\underset{\sim}{E}$ is of minor interest because in the present approximation it simply defines the charge density from the solution already obtained for $\underset{\sim}{E}$. The constitutive equations are

$$j_1 = j_{c1}\ \mathrm{sgn}\ E_1 \qquad (9)$$

$$j_3 = j_{c3}\ \mathrm{sgn}\ E_3\ . \qquad (10)$$

In the cylindrical coordinates R, θ, z for the wire the electric field components are given by

$$E_\theta = -\frac{\dot{H}_A}{2} R \qquad (11)$$

$$E_z = \dot{H}_A \frac{\pi}{L} R_1^{\ 2} \qquad (12)$$

$$E_R = 0 \qquad (13)$$

while the components along the ribbon axes are

$$E_1 = \dot{H}_A \frac{\pi}{L}\left(R_1^{\ 2} - R^2\right)\left[1 + \left(\frac{2\pi R}{L}\right)^2\right]^{-1/2} \qquad (14)$$

$$E_3 = - \frac{\dot{H}_A R}{2}\left[1 + \left(\frac{2\pi R_1}{L}\right)^2\right]\left[1 + \left(\frac{2\pi R}{L}\right)^2\right]^{-1/2} \tag{15}$$

where R_1 is a constant, and $\dot{H}_A \pi R_1{}^2/L$ represents the applied electric field. The value of R_1 is found by demanding that

$$\int_0^{R_o} j_z R\, dR = 0 \tag{16}$$

which is the condition for no net transport current, where R_o is the radius of the wire. It is observed from (14) that at $R = R_1$ the component of current density j_1 changes sign, and this in turn tends to change the sign of j_z, which is given by

$$j_z = \left(j_1 - \frac{2\pi R}{L} j_3\right)\left[1 + \left(\frac{2\pi R}{L}\right)^2\right]^{-1/2} . \tag{17}$$

Under the assumption that j_{c1} is large compared with $2\pi R j_{c3}/L$, and that $(2\pi R/L)^2$ can be neglected compared with unity, $j_z \simeq j_1$, and

$$R_1{}^2 \simeq \frac{R_o{}^2}{2} . \tag{18}$$

CALCULATION OF THE LOSS

The power density is given by

$$\underset{\sim}{E} \cdot \underset{\sim}{j} = j_{c1} \; |E_1| + j_{c3} \; |E_3| \tag{19}$$

and with the previous approximations

$$\underset{\sim}{E} \cdot \underset{\sim}{j} \simeq \frac{|\dot{H}_A|}{2}\left[j_{c1} \frac{2\pi}{L} \left| \frac{R_o^2}{2} - R^2 \right| + j_{c3} \; R \right] . \tag{20}$$

One obtains for the hysteresis loss per cycle per unit volume

$$W \simeq H_o \; R_o \left(\frac{4 j_{c3}}{3} + \frac{\pi \; R_o}{L} \; j_{c1} \right) \tag{21}$$

where H_o is the peak value of the applied field. This result can be re-written as

$$W(L) = W(\infty) \left(1 + \frac{3}{4} \; \frac{\pi \; R_o}{L} \; \frac{j_{c1}}{j_{c3}} \right) \tag{22}$$

and it is observed that, contrary to the transverse field case,[1] twisting the wire should increase the full penetration longitudinal field loss, in agreement with the measurements of Braginski[5] and Wagner shown in Fig. 1. With the expressions (4) and (5) substituted into (22) one obtains

$$\frac{W(L) - W(\infty)}{W(\infty)} \approx \frac{3\pi R_o}{8L} \frac{\lambda j_{clf}}{j_{cp}} \tag{23}$$

from which, according to the measured results, j_{clf}/j_{cp} is about 70, in order of magnitude agreement with values previously[1] found from the transverse field loss. Exact agreement cannot be expected since the arrangement of filaments probably deviates considerably from the ideal arrangement.

Curve 724311-A

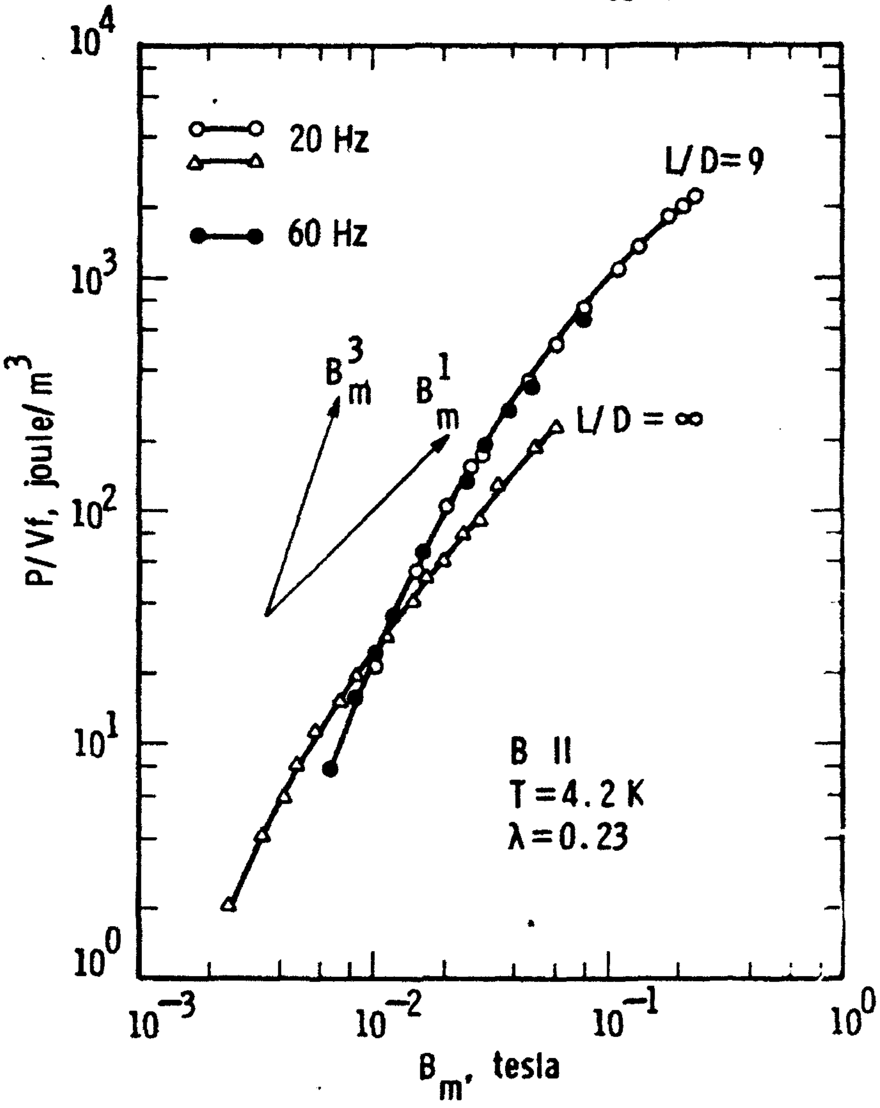

Fig. 1 – Low-frequency hysteretic loss vs. the amplitude of parallel field in untwisted and twisted wires ($D \simeq 0.13$ mm) having similar J_c. (Taken from Braginski and Wagner[5])

REFERENCES

1. W. J. Carr, Jr., to be published.
2. W. J. Carr, Jr., to be published.
3. W. J. Carr, Jr., J. Appl. Phys. 48, 2022 (1977).
4. K. P. Jüngst and G. Ries, IEEE Trans. MAG 13, 527 (1977).
5. A. I. Braginski and G. R. Wagner, IEEE Trans. MAG 17, 243 (1981).

Published in Adv. in Cryog. Eng. 30, 923 (1984).

APPENDIX E

HYSTERESIS IN A FINE FILAMENT NbTi COMPOSITE*

W. J. Carr, Jr. and G. R. Wagner

Westinghouse R&D Center
1310 Beulah Road
Pittsburgh, Pennsylvania 15235

INTRODUCTION AND SUMMARY

Recent progress has been made toward the development of multifilamentary superconductors having fine filaments which might be useful in ac applications because of their reduced losses. Eddy current losses have been reported for a mixed matrix NbTi conductor with 1.0 μm filaments having a tight twist.[1] Here we report the study of hysteresis in a conductor of the same configuration having filaments 1.6 μm in diameter. As in Ref. 1, the conductor was obtained from Oxford Airco Superconductors and its physical characteristics are given in Table I.

Table I

Conductor diameter	0.036 cm
Filament diameter	1.6 μm
Separation between filaments	0.4 μm
Fractional volume of filaments	0.27
Twist pitch	0.1 cm

The magnetic hysteresis loop was studied for transverse fields and found to exhibit an unusual asymmetry which is attributed to the effect of surface currents, which cannot be neglected in filaments of this size. A theory is developed for the surface current density

*Supported in part by the Air Force Aero Propulsion Laboratory, Contract No. F33615-81-C-2040.

which allows a determination of both surface and bulk current densities from the hysteresis loop. The critical transport current density is obtained from such measurements and is in reasonably good agreement with direct measurements. For applied fields $\geq$ 10 kOe the surface current appears to dominate the bulk current in determining the critical transport current, and for fields $\geq$ 1 kOe the surface contribution dominates the hysteresis.

The initial slope of the hysteresis loop from a virgin state indicates that no proximity coupling exists between the filaments, as expected from their separation given in Table I. In addition, the loss obtained from hysteresis loops agrees with calorimetric loss measurements and is characteristic of the individual filaments.

THE INITIAL MAGNETIZATION CURVE

It was shown by Shen[2] that the initial slope of magnetization versus magnetic field can provide an accurate measure of λ, the fraction of superconducting material in a filamentary composite. Shen used the value $-2\lambda/(1+\lambda)$ for the initial slope in a transverse magnetic field. Actually this is in reference to the field H in Maxwell's equations,[3] which for a circular wire is related to the applied field H_A by $H = (1 + \lambda) H_A$. Thus

$$4\pi(dM_{\perp}/dH_A) = -2\lambda \qquad (1)$$

for a virgin material near $H_A = 0$, where $M_{\perp}$ is the transverse magnetization for the composite. This result may be compared with the case of a longitudinal field in an untwisted wire where

$$4\pi(dM_{\parallel}/dH_A) = -\lambda \ . \qquad (2)$$

The applied field in both cases indicates the field applied to the wire, and in the present measurements, where the sample was in the form of a loosely wound coil, a small correction was necessary for the field due to neighboring turns in the sample. Because of the relatively tight twist in the sample, only the transverse case was analyzed and the twist was ignored. Using the initial slope obtained from Fig. 1 a corrected value of $\lambda = 0.23$ is obtained from Eq. (1) which is in good agreement with the value of $\lambda = 0.27$ expected for uncoupled, individual filaments.

In addition, Fig. 1 shows that the field H_p required to fully penetrate a filament is approximately 280 Oe. The linear part of the curve extends to about 50 Oe, indicating that this is the applied field where flux penetration begins. (The value should be corrected slightly to account for the dependence of the London penetration depth on the magnetic field but this correction has been ignored.) Since the maximum field on the surface of a superconducting filament is $2H_A$ for a transverse applied field, the measurement indicates that

$H_{c1} \approx 100$ Oe, if H_{c1} is defined as the field for initial flux penetration. Assuming that the surface current shields about 50 Oe of the applied field, one obtains 230 Oe for the contribution to H_p of the bulk current density, j_c, which reduces to about 200 Oe when corrected for the field of neighboring turns in the sample. With the use of the expression for H_p estimated from a Bean model it follows that

$$0.4 \; d \; j_c \approx 200 \qquad (3)$$

where d is the filament diameter in cm, and $j_c \approx 3.1 \times 10^6$ A/cm^2 for the bulk critical current density in a field of the order of 200 Oe (plus the self-field, which is neglected).

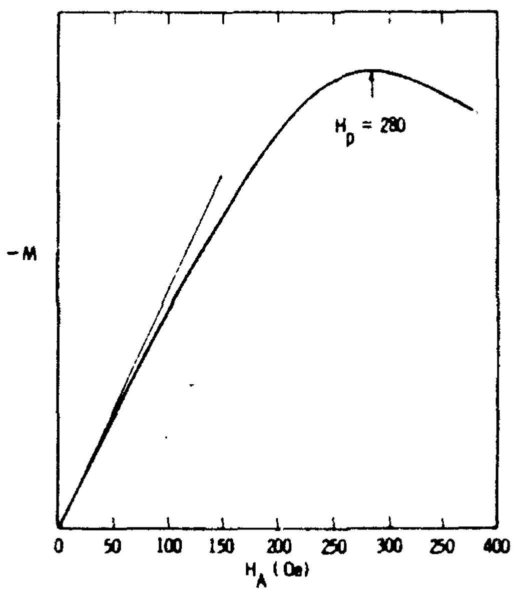

Fig. 1 — Measured magnetization for a virgin material in a transverse field.

THEORY OF THE SURFACE CURRENT

In the Meissner region of a type II superconductor only surface current density $\underset{\sim}{J}$ exists, but above the lower critical field H_{c1} bulk current density j_c penetrates into the conductor along with the flux. A question which remains moot in superconductivity theory is the behavior of the surface current density above H_{c1}.[4-7] Above H_{c1} in a changing transverse applied magnetic field, an electric field E exists at the surface, where $E \sim \pm \dot{H}_A w$, with $\dot{H}_A$ the time rate of change of applied field and w the depth of penetration. The plus sign applies over half the surface and the minus for the other half. In a macroscopic superconductor this electric field is generally large compared with the London electric field which is of the order $H_A \lambda_L$, where λ_L is the London penetration depth. The following assumption will be made here: if the macroscopic electric field acts in the direction of the surface current density it has a relatively small effect on the surface current density. If it acts against the surface current density over a period of time t such that $\int E \cdot J\,dt$ is greater than the energy density associated with the surface electrons, then the surface current density is destroyed. This behavior of the surface current is in contrast to the behavior of the volume current density, which reverses with the electric field. The difference in behavior results from the fact that the latter current arises from electrodynamics and the rate of change of magnetic field, while the former arises from equilibrium energy considerations, and it is governed by the vector potential, or the magnetic field itself. Over the course of a hysteresis loop starting from a virgin state, a distribution of surface current of opposite sign on the two halves of the conductor is first induced by the increasing magnetic field. The maximum in this current distribution reaches a critical value at H_{c1} and remains relatively constant as the applied field continues to increase, since the electric field is in the direction of the current flow. But when the applied magnetic field is reduced, a reversed electric field is established, bringing the surface current density to zero, where it remains until the magnetic field and vector potential change sign. At the latter point the surface current density reappears with opposite sign. This behavior is shown schematically in Fig. 2. The magnetic moment of current vortices in flux lines has been neglected.

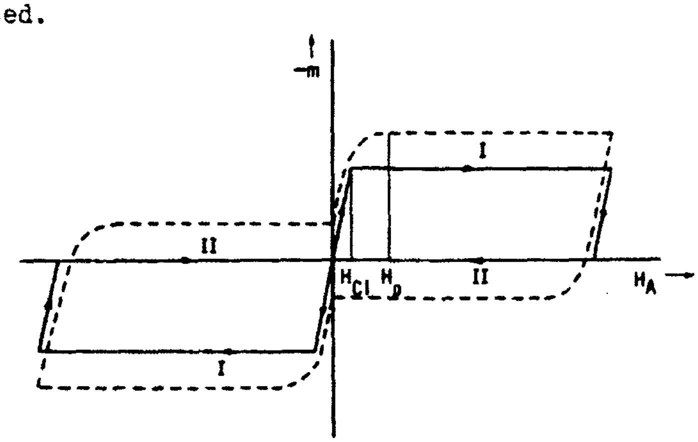

Fig. 2 — (Schematic) The solid curve gives the magnetic moment of a filament due to the surface current density and the dashed curve gives the total magnetic moment including the bulk current density contribution. Field dependence of the critical current density is neglected. On the paths marked I, H_A and $\dot{H}_A$ have the same sign, while on II they have opposite signs.

5

ANALYSIS OF THE MEASURED HYSTERESIS LOOP

Figure 3 shows a large hysteresis loop measured with a Foner type magnetometer, where the sample was initially in a virgin state, and care was taken to preserve the zero for magnetic moment. Several minor loops are included. The interesting feature of this loop is the extreme asymmetry about the m axis, in analogy with Fig. 2. From the previous analysis one may expect that the curve in the lower right-hand quadrant corresponds to a magnetic moment resulting only from the bulk current density. Also, the sum of the curve in the upper right-hand quadrant with the lower curve gives approximately the contribution of the surface current, where the analysis can only be carried out beyond the peak at 280 Oe, since in low fields below the peak various corrections should be applied.

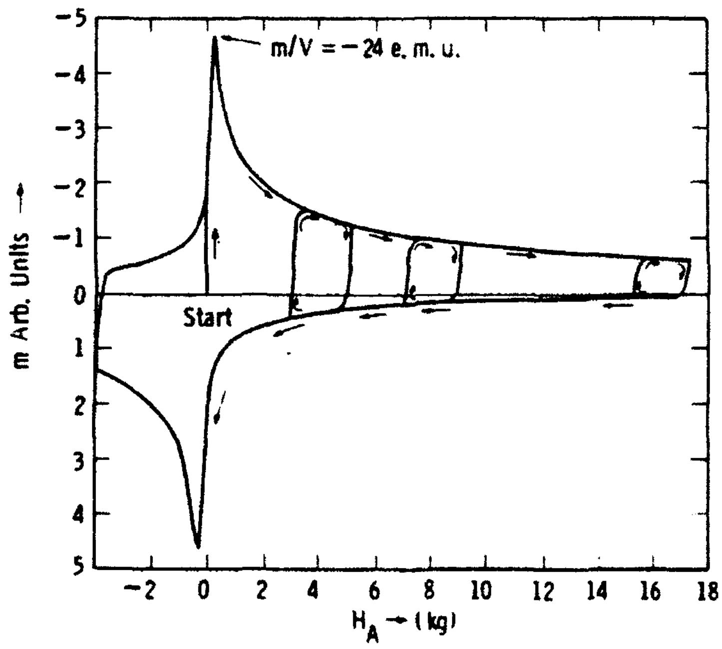

Fig. 3 — Measured hysteresis loop indicating several minor loops.

In a Bean-type approximation (constant j_c over the filament cross-section) the magnetic moment of the lower curve at any point is[8]

$$m/V = 0.2\, d\, j_c/(3\pi) \qquad (4)$$

where V is volume, and all quantities refer to an individual filament. From the measured values of m one can plot j_c as a function of H, and this is done in Fig. 4.

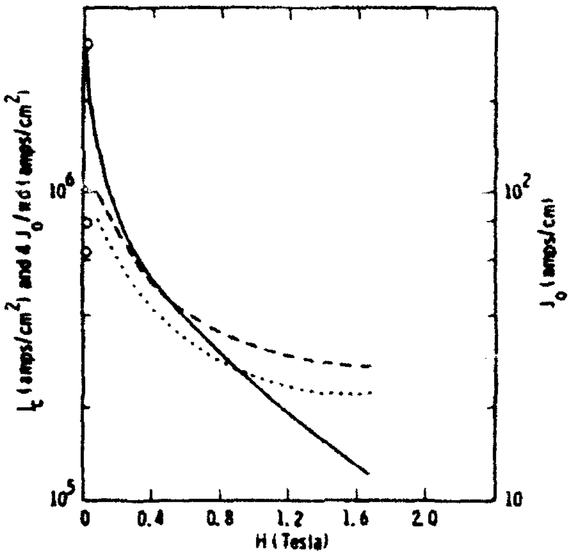

Fig. 4 — The bulk current density j_c, ——; the surface current density J_o, ---; $4J_o/\pi d$, $\cdots$. The points between 1 and 17 kOe were obtained from Fig. 3. The points marked with a circle at $H \approx 200$ Oe were obtained from Fig. 1, where $0.4\pi J_o = H_{c1}$ ($J_o \approx 80$ and $4J_o/\pi d \approx 6.4 \times 10^5$), and $j_c = 3.1 \times 10^6$ comes from Eq. (3).

For a sinusoidal distribution of surface current ($J = J_o \sin \theta$) one calculates the transverse magnetic moment of the surface current to be

$$m_s/V = 0.1J_o \quad . \tag{5}$$

and, thus, the surface current density J_o can also be obtained from the hysteresis measurement. This result is also plotted in Fig. 4, where the surface current density is observed to be less sensitive to magnetic field than the volume current density.

For the minor loop near 8 kOe about two thirds of the loss results from the surface current. The total loss is in good agreement with the value 0.93 mJ/cm^3/cycle obtained calorimetrically at this bias field for an ac field amplitude of 1 kOe.

TRANSPORT CURRENT

When a critical transport current is established in the absence of an applied field one expects a current distribution as indicated in Fig. 5(a), where a uniform surface current exists in addition to the bulk current. For an applied field smaller than the self field of the filament this distribution should remain relatively unchanged. However, for a large transverse applied field, in the absence of transport current the surface current is as indicated in Fig. 5(b), and when the transport current is now established, the dc electric field required to maintain the critical transport current is in the direction of the initial surface current density over one half the filament, and opposite to the initial surface current density over the other half. It is, again, assumed that the surface current is destroyed over half the surface, and that for the remaining half is assumed to distribute itself to minimize the energy. Since the exact distribution is not important, a sine wave distribution is assumed over half the surface, as in Fig. 5(c), and the effective current density of the filament is approximately[9]

$$j_{ceff} = j_c + (2J_o/\pi)(\pi d/2)(4/\pi d^2) = j_c + 4J_o/\pi d \ . \qquad (6)$$

With the results from Fig. 4 the effective j_c for transport current can be calculated, and this is compared with the measured values in Fig. 6. The calculated values are about 20% higher than the measured values, but otherwise they tend to follow the measured points. Below about 10 kOe the bulk current dominates, but above 10 kOe the surface current makes the largest contribution to the calculated curve:

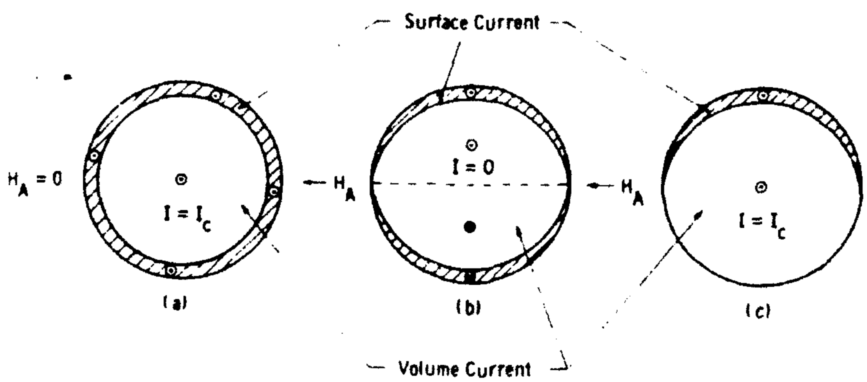

Fig. 5 – (a) Current distribution in filament cross section for a longitudinal applied electric field and no applied magnetic field; and current distribution in conductor cross-section for large transverse applied magnetic field with (b) no applied electric field and (c) longitudinal applied electric field. The thickness of the surface layer indicates the magnitude of the surface current, and is not intended to indicate the depth of penetration.

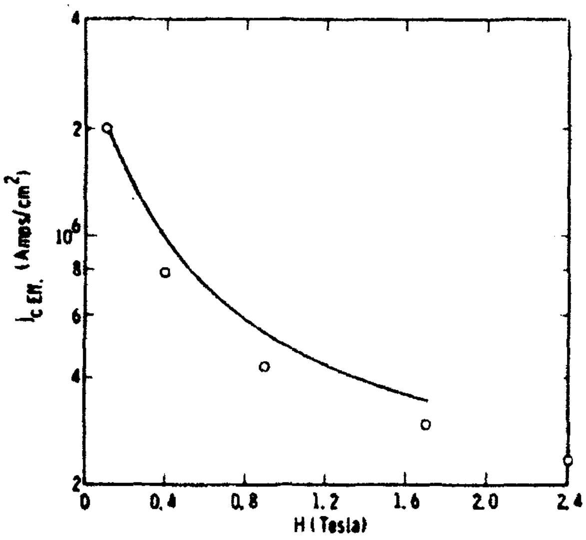

Fig. 6 — The effective critical transport current density. The solid line is calculated by adding the volume and surface parts given in Fig. 4, and the circles are measured points.

REFERENCES

1. T. Ogasawara, Y. Kubota, T. Makiura, T. Akachi, T. Hisanari, Y. Oda, and K. Yasukochi, IEEE Trans. MAG-19, 248 (1983).
2. S. S. Shen, Filamentary A15 Superconductors, Ed. by M. Suenaga and A. F. Clark, Plenum Press, New York (1980) p. 309.
3. W. J. Carr, Jr., Phys. Rev. B 11, 1547 (1975).
4. J. F. Bussiere, IEEE Trans. MAG-13, 131 (1977).
5. J. R. Clem, J. Appl. Phys., 3518 (1979).
6. J. P. Charlesworth and P. T. Sikora, IEEE Trans. MAG-15, 260 (1979).
7. G. Fournet and A. Mailfert, J. De Physique 31, 35 (1970).
8. W. J. Carr, Jr., J. H. Murphy and G. R. Wagner, Ad. in Cry. Eng. 24, Ed. K. D. Timmerhaus, R. P. Reed and A. F. Clark, Plenum Press, New York (1978) p. 415.
9. In a more precise analysis one should correct for the fact that the "surface" current really occupies a layer of thickness $\lambda_\perp$, and therefore the volume for the bulk current is slightly reduced. For simplicity, this correction has been ignored throughout the analysis.

Published in Adv. in Cryog.
30, 899 (1984).

APPENDIX F

ELECTROMAGNETIC THEORY FOR IN SITU SUPERCONDUCTORS*

W. J. Carr, Jr.

Westinghouse R&D Center
1310 Beulah Road
Pittsburgh, Pennsylvania 15235

INTRODUCTION

The remarkable fact that fine disconnected superconducting filaments embedded in a normal metal matrix can lead to bulk superconductivity was first reported by Tsuei[1] in 1973. Materials of this type are referred to as in situ superconductors, since the filaments arise from a precipitate in the matrix, which is made filamentary by drawing out the composite. The filaments typically take the shape of ribbons.[2,3] Although much remains to be learned concerning the microscopic electromagnetic behavior of in situ materials, some technologically important bulk properties can be described with only minimal knowledge of the microscopic physics. To do so one needs only to construct a macroscopic set of Maxwell equations, and postulate a set of constitutive relations which allow the equations to be solved. Since the Maxwell equations and constitutive relations involve only averages over the microscopic details, even a rough microscopic picture can lead to useful results. The present analysis is concerned with the bulk behavior.

CONSTITUTIVE RELATIONS

In continuous filament material the macroscopic fields are obtained by averaging over a volume element large enough to contain the cross section of a few filaments and their surrounding matrix as in Fig. 1(a). In contrast, for the case of discontinuous filaments one

---

*Supported by the Air Force Aero Propulsion Laboratory, Contract No. F33615-81-C-2040.

must choose a volume element which contains entire filaments, and since the filaments can be longer than the thickness of the conductor, a "microscopic" dimension along the length of the conductor is quite different from a microscopic dimension through the thickness. One must choose a very elongated volume element for making averages as in Fig. 1(b). The constitutive relations needed for a material which exhibits full bulk superconductivity correspond simply to a description of the bulk critical current density. Because the in situ material is expected to be highly anisotropic, a critical current density is needed along each of the three directions defined at any macroscopic point by the average principal axes of the filaments. In an electric field which has components along more than one principal axis it is likely that the critical current densities are interrelated: the current density along one principal axis can be affected by the value along a different axis. In the present simplified analysis, however, such interrelations are ignored, and the critical current densities are taken to be independent of one another, depending only on temperature and the magnetic field.

For bulk material which is not a bulk superconductor, the constitutive equations must take the form of a specification of resistivity along the three principal axes, which, if the filaments are still in a superconducting state, can be very much smaller than a normal resistivity. In addition, it is expected that in a resistive state which is approaching bulk superconductivity, closed superconducting paths will exist, which can carry magnetization current, even though no continuous superconducting paths exist through the conductor. Therefore, in this case it is also necessary to specify three components of the true magnetization.

Clearly, in an in situ material one can imagine intermediate states between fully superconducting and fully resistive, and these states correspond to superconductivity in one principal direction, with resistance along a different principal direction. In general, the superconductivity can be classified according to whether it exists in one, two or three directions.

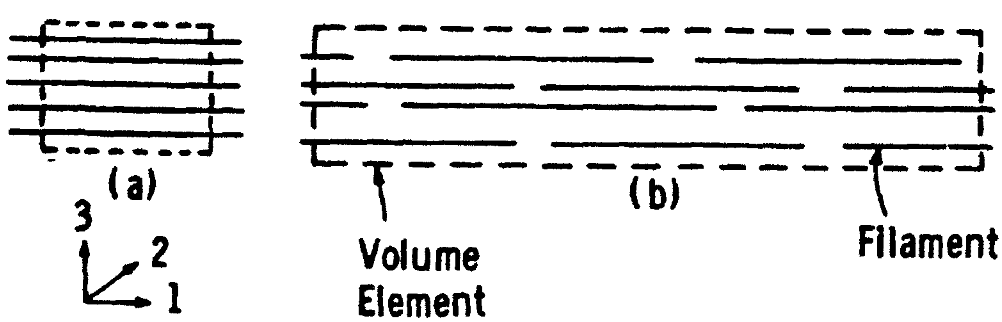

Fig. 1 — Cross-section of volume element for making averages for (a) continuous filament material and (b) in situ material.

NATURE OF THE FILAMENT COUPLING

Because of the method of preparation, a clean interface between filament and matrix exists in in situ materials, in the sense that no oxide layers are present, and under these conditions a strong proximity effect[2,4] should be observed, where superconductivity spills out of the filaments into the surrounding matrix, leading to superconducting electrons in the matrix within a thickness the order of 0.1 μm. The pattern of longitudinal current flow between filaments in the case of resistive material has been considered by Davidson, Beasley and Tinkham,[5] where current flow occurs via the low resistance path through a third filament as shown in Fig. 2. The same pattern is assumed to exist in the case of supercurrent. One can imagine the filaments in the in situ material to be arranged in chains as in Fig. 3. If the proximity layers of a pair of chains overlap, the chains are superconducting; otherwise, the bulk current they carry is resistive. For the pattern of current flow in Fig. 2 the transverse microscopic electric field and current density both average to zero. The average longitudinal electric field in the resistive case is determined by the longitudinal electric field which exists between the ends of the filaments, giving the voltage v between n and b shown in Fig. 2. If d is the thickness of the filament, w the width and ℓ the length, the average electric field is the order of* vdw divided by the volume over which the average is made. The latter is the volume $dw\ell/\lambda_n$ of a unit cell about a filament, where λ_n is the fraction of filament volume in the unit cell for the n^{th} filament. Then the longitudinal macroscopic electric field at the point of the n^{th} filament is

$$E_1 \sim \frac{v\,\lambda_n}{\ell} \; . \tag{1}$$

Since the voltage v between filaments n and b is twice the voltage between n and c, $v \approx 2(j_{1fn}\, dw)(2/\ell w)\, s_n''\, \rho_m$ where j_{1fn} is the current density at the middle of the n^{th} filament, $j_{1fn}\, dw$ is the filament current at the middle, $\ell w/2$ is the area for current flow between filaments n and c, s_n'' is the thickness of the normal region in the matrix (see Fig. 2) and ρ_m the normal matrix resistivity. Thus, if the n^{th} filament is centered about $\underset{\sim}{r}_n$**

$$E_1(\underset{\sim}{r}_n) \sim \frac{4d\,\rho_m}{\ell^2}\,\lambda_n\, j_{1fn}\, s_n'' \; . \tag{2}$$

*This estimate is made for the case where the separation between ends is the order of or less than the thickness d.

**A smooth function of $\underset{\sim}{r}$ can be constructed by further averaging over all n in the neighborhood of $\underset{\sim}{r}$.

4

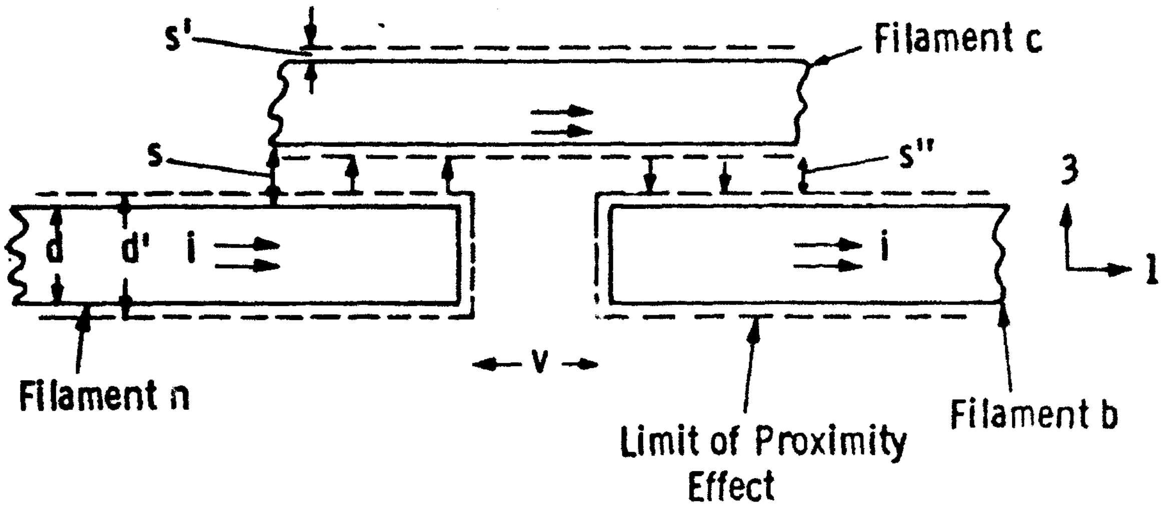

Fig. 2 — Model for the pattern of microscopic current flow in response to an applied electric field along the 1 axis. Filament c is the closest filament to the pair nb. The figure shows the cross-section of the ribbon-like filaments where d is the thickness. d' is a thickness which includes the proximity effect, s is the separation between filaments, s' is the thickness of the proximity layer, and s" is the thickness of the normal region between filaments.

When the proximity regions overlap, s" = 0, and the filaments at this point have bulk superconductivity. In general s" = s - 2s' where s is the local filament spacing, and s' = s'(H, T) is the effective proximity layer thickness, depending upon the magnetic field H and temperature T.

AVERAGE FILAMENT SPACING LARGE COMPARED WITH PROXIMITY LAYER THICKNESS

The behavior of in situ material can best be examined in two limiting cases: (a) where the average separation between filaments s_{av} is large compared with twice the maximum thickness s' of the proximity layer, and (b) where s_{av} is smaller than 2s'. The average spacing depends upon the fraction of filament volume in the composite, and the amount of mechanical reduction.[2,6] In the first case the distribution of s within a cross-section of the conductor is quite important, whereas in the second, the distribution can be ignored. In case (a) only the relatively small number of filament chains which are closer together than 2s' can carry supercurrent, as indicated in Fig. 3. Thus, a superconducting in situ material of this kind should exhibit a critical current which is quite small, and further, one would expect superconductivity only in one direction. Details of the calculation for this type of material may be found elsewhere.[7]

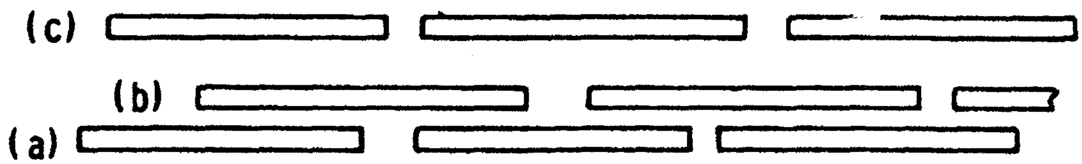

Fig. 3 — Three chains of filaments. (a) and (b) are superconducting, (c) is resistive.

CLOSELY SPACED FILAMENTS AND ANISOTROPY IN THE CRITICAL CURRENT DENSITY

When the average spacing between filaments is less than twice the proximity layer thickness not only the filament volume but also most of the matrix is superconducting, and bulk superconductivity is allowed in any direction. In this case the superconductivity of in situ material is distinguished from that of other bulk superconductors only by a high degree of anisotropy in the critical current density. Consider first the critical current density along the axis of the filaments (the 1 axis), which is computed with reference to Fig. 2. If j_{1f} again denotes the longitudinal current density in a filament at its mid-point, then averaging over the area of filament and matrix reduces this value to λj_{1f}. It is assumed that any longitudinal current flowing in the matrix can be neglected. A further average over the length gives $\lambda j_{1f}/2$, since the longitudinal current in the filament goes to zero at the ends. Thus the bulk critical current density j_{c1} is

$$j_{c1} \approx \frac{\lambda j_{1f}}{2} \, . \tag{3}$$

If the current at the mid-point of the filament is limited by the filament itself then $j_{1f} = j_{c1f}$ where j_{c1f} is the filament critical current density. On the contrary, if the current flow is limited by the matrix, j_{1f} is less than j_{c1f} and the transverse current density in the matrix takes a critical value j_{cp}. Then $dwj_{1f} = (w\ell/2)\, j_{cp}$ and $j_{1f} = (\ell/2d)\, j_{cp}$ for this case. It follows that the bulk critical current density in the 1 direction is the smaller of the two values $\lambda j_{c1f}/2$ and $\lambda \ell j_{cp}/4d$. If one is concerned only with an order of magnitude, the result can be summarized by

$$\frac{1}{j_{c1}} \sim \frac{2}{\lambda j_{c1f}} + \frac{4d}{\lambda \ell j_{cp}} \tag{4}$$

where for a typical material ℓ/d is usually large enough so that

$$j_{c1} \approx \frac{\lambda j_{c1f}}{2} . \tag{5}$$

For an electric field along the width of the filament (2 direction) the critical current density is more difficult to estimate, but in the special case where $w >> d$ it can be assumed that the order of magnitude is given by replacing ℓ with w in (4) and

$$\frac{1}{j_{c2}} \sim \frac{2}{\lambda j_{c2f}} + \frac{4d}{\lambda w j_{cp}} . \tag{6}$$

To estimate the critical current density in the direction of filament thickness, the 3 direction, consider the flow in Fig. 4. The area of filaments through which the current flows is nearly the same as the area of matrix, and the critical current density is either j_{c3f} or j_{cp}. Since the latter is anticipated to be smaller

$$j_{c3} \approx j_{cp} . \tag{7}$$

As of the present, no theory has been developed for the value of the critical current density of the matrix, and therefore j_{cp} must be obtained from experiment.

EFFECT OF TWIST ON THE HYSTERESIS

Because of the anisotropy in critical current density, the hysteresis loss of a fully superconducting in situ filamentary wire will depend upon the amount of twist in the wire. To understand this behavior it is expedient to review the behavior of an ordinary twisted continuous filament material, since the latter represents an extreme case of anisotropy, where the transverse critical current density goes to zero.

(a) Continuous Filament Material

An untwisted continuous filament material in a transverse applied magnetic field exhibits the hysteresis of a bulk superconductor above

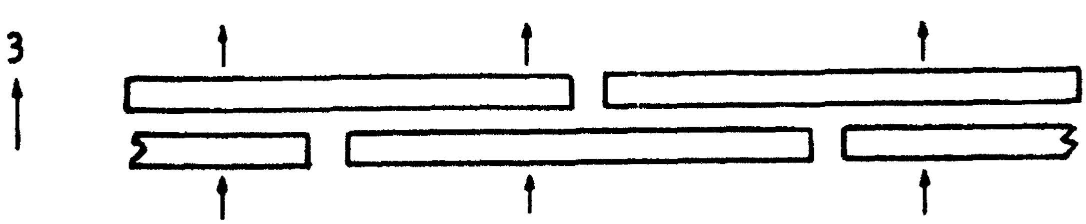

Fig. 4 — Pattern of current flow for an electric field in the 3 direction.

a frequency greater than the reciprocal relaxation time due to end resistance. For an infinite wire, or a wire with superconducting caps on the ends, this behavior would exist down to zero frequency. The current which leads to the hysteresis loss flows down the wire axis in one half the cross-section and back along the axis in the other half as in Fig. 5(a). At zero frequency the slightest twist in the wire will destroy this bulk behavior since it introduces resistance into the path along the wire axis, preventing the flow of supercurrent in this direction. The important point is that a changing transverse magnetic field tends to introduce current which shields the applied field, and only axial current, which changes sign over the two halves of the conductor, can perform this function. While this result is purely a consequence of the macroscopic Maxwell equations, one can understand in a simple way why the bulk supercurrent is destroyed by the twist by referring to Fig. 5(b). To avoid divergence, current in the filamen s tending to shield the conductor must leave the filaments and flow through a path which includes the matrix.

(b) <u>In Situ Material</u>

For in situ material twist does not destroy the bulk supercurrent tending to shield the wire, but it can change the magnitude.

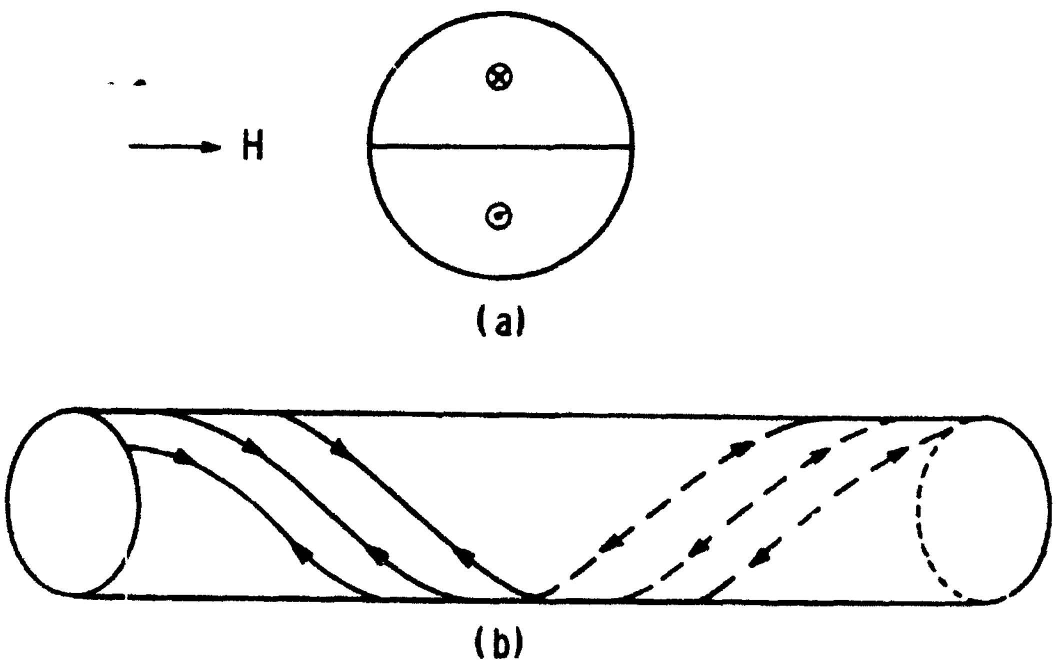

Fig. 5 — Shielding current induced by the transverse field H.
(a) Untwisted filaments, (b) the breakdown of bulk shielding as a result of twist in a continuous filament conductor.

For an ideal packing of the filamentary ribbons as in Fig. 6, if a current j_z flows down the axis of the wire it may be resolved into components along the principal filament directions 1 and 3 when the wire is twisted. The cosine of the angle between the wire axis and the 1 direction of the filament is approximately unity, while the cosine of the angle between the wire axis and the 3 direction is approximately[7] 2π R/L, where L is the twist length and R is radial distance from the axis. Since both components must be equal to or less than their critical values

$$j_z \leqslant \frac{\lambda}{2} j_{c1f} \tag{7}$$

and

$$\frac{2\pi R}{L} j_z \leqslant j_{cp} \; . \tag{8}$$

For large values of L, j_z takes the value $\lambda j_{c1f}/2$, while for small values of L, $j_z = Lj_{cp}/2\pi R$ except near the axis. At the surface of the wire R_o, the ratio of the two values is $\pi R_o \lambda j_{c1f}/Lj_{cp}$ corresponding to the ratio $j_z(\infty)/j_z(L)$ for a tight twist. One can use this ratio in the hysteresis expressions derived for continuous filament material, where it is found that the hysteresis loss W is proportional to j_z for full penetration, and to $1/j_z$ for the case of partial penetration of the magnetic field.[8] Thus in heavily twisted wires where (8) limits the current density, for partial penetration

$$W(L) = \frac{\pi R_o \lambda}{L} \frac{j_{c1f}}{j_{cp}} W(\infty) \tag{9}$$

while for full penetration

$$W(L) \approx \frac{L}{\pi R_o \lambda} \frac{j_{cp}}{j_{c1f}} W(\infty) \; . \tag{10}$$

For large L where (7) limits j_z, $W(L) \approx W(\infty)$. The behavior described by (9) and (10) is found in the data of Braginski and Wagner,[9] and Shen and Verhoeven.[10] From these data one finds that j_{cp} is about two orders of magnitude smaller than j_{c1f}. In the case of full penetration twisting the wire decreases the transverse field loss, while for partial penetration the loss is increased.

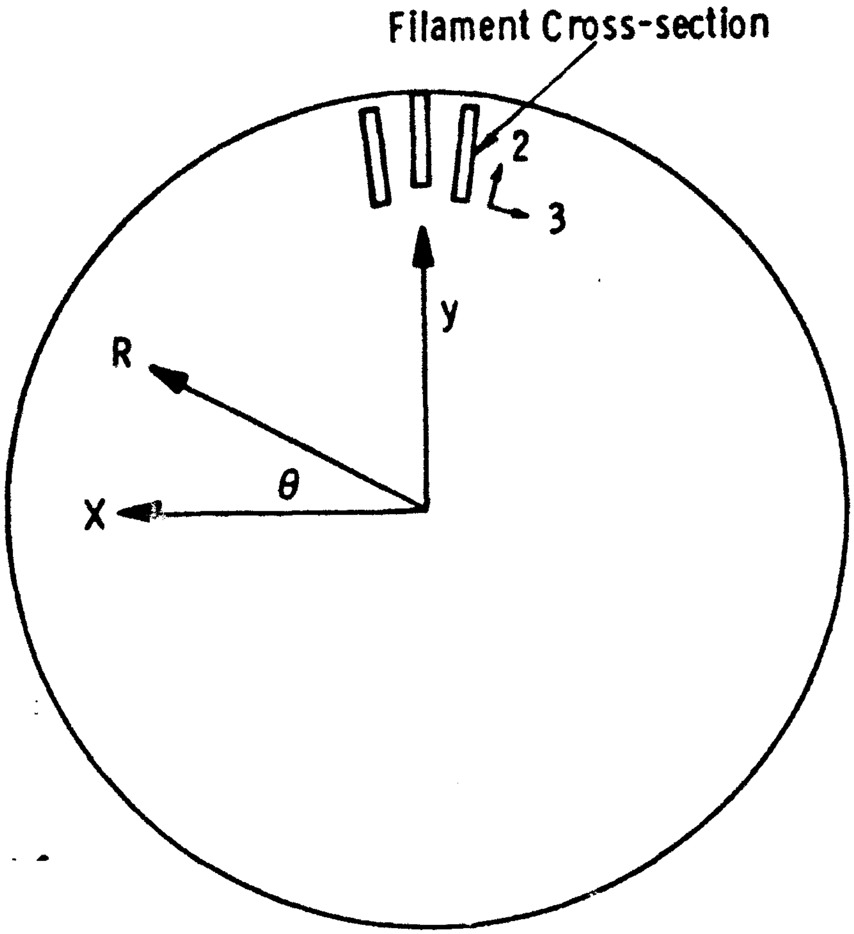

Fig. 6 — The packing of filaments in an untwisted wire.

COMPARISON OF CRITICAL CURRENT DENSITY FROM HYSTERESIS AND TRANSPORT MEASUREMENTS

In a direct measurement of the transport current for a twisted wire the symmetry restrictions discussed for the shielding current do not apply, since the current can simply follow the spiral path of the filaments. Thus the critical value of j_z obtained from direct transport measurements is ~ λj_{clf}, which will be considerably higher than the value obtained from hysteresis measurements, in the case of a tight twist pitch.

REFERENCES

1. C. C. Tsuei, Science 180, 57 (1973).

2. J. Bevk, M. Tinkham, F. Habbal, C. J. Lobb and J. P. Harbison, IEEE Trans. MAG-17, 235 (1981).
3. J. D. Verhoeven, D. K. Finnemore, E. D. Gibson, J. E. Ostenson and L. F. Goodrich, Appl. Phys. Lett. 33, 101 (1978).
4. G. Deutscher and P. G. De Gennes, Superconductivity, Vol. 2, Ed. by R. D. Parks, Marcel Dekker, New York (1969).
5. A. Davidson, M. R. Beasley and M. Tinkham, IEEE Trans. MAG-11, 276 (1975).
6. T. J. Callaghan and L. E. Toth, J. Appl. Phys. 46, 4013 (1975).
7. W. J. Carr, Jr., to appear in J. Appl. Phys.
8. See for example W. J. Carr, Jr., AC Loss and Macroscopic Theory of Superconductors, Gordon and Breach, New York (1983).
9. A. I. Braginski and G. R. Wagner, IEEE MAG-17, 243 (1981).
10. S. S. Shen and J. D. Verhoeven, IEEE Trans. MAG-17, 248 (1981).

APPENDIX G

Published in IEEE Trans. on Mag., MAG-21 355 (1985).

SURFACE CURRENTS IN FINE SUPERCONDUCTING FILAMENTS*

W. J. Carr Jr.

Westinghouse R&D Center
1310 Beulah Road
Pittsburgh, Pennsylvania 15235

Abstract

Measurements were made of the magnetic moment observed in a fine filament NbTi superconductor upon cooling through the transition temperature in a magnetic field large compared with H_{c1}. A partial Meissner effect was observed and this effect is interpreted in terms of surface current, body current and the magnetic moment of the flux lines. The interpretation is used to study the surface current behavior.

Introduction

For intermediate magnetic fields ($H_{c1} << H_a << H_{c2}$ where H_a is the applied field) in a soft type II superconductor the Ginzburg-Landau equations give for the flux density B[1]

$$B = H_a - H_{c1} + (\phi_o/8\pi\lambda^2)\left\{\ln[4\pi(H_a - H_{c1})\lambda^2/\phi_o] + 0.846\right\} \quad (1)$$

where ϕ_o is the flux quantum and λ the penetration depth. The equation applies for an isolated rod with the magnetic field along the axis of the rod. The result given in (1) may be interpreted as follows. Two types of current flow contribute to the flux density: a surface current and the current circulating in the vortex structure. The vortex current leads to a magnetization M_v given by

$$4\pi M_v = (\phi_o/8\pi\lambda^2)\left\{\ln[4\pi(H_a - H_{c1})\lambda^2/\phi_o] + 0.846\right\} \quad (2)$$

while the surface current produces a magnetic moment equivalent to an effective magnetization

$$4\pi M_s = - H_{c1} \quad (3)$$

Thus, if V is the volume, the magnetic moment of the rod is

$$m = (M_v - H_{c1}/4\pi)\ V\ , \quad (4)$$

which with measured values of the moment may be used to infer the behavior of the currents in the system. However, for hard type II superconductors Eq. (4) no longer applies because of several reasons: (1) it omits the magnetic moment m_b due to the body (bulk) current density j_c, (2) the thermodynamics used in the development of Eq. (1) fail to allow for the components to have separate constitutive equations,[2] and (3) the theory does not allow for the effects of electric fields which result from flux penetration in changing magnetic fields. At present no comparable theory exists which describes the magnetic moment and current flow in a hard superconductor, particularly in the case of filamentary conductors with filaments of such size that both surface and body currents are important.

Recently,[1] an experimental attempt was made to examine the various contributions to the magnetic moment of a superconductor by investigating the hysteresis loops of a fine filament NbTi superconductor, and the present paper represents a continuation of this study. A knowledge of this breakdown is important for the design of practical superconductors with superior critical current and loss characteristics. The details of the conductor, which was obtained from Oxford Airco Superconductors, are shown in Table I.

Table I

Conductor diameter	0.036 cm
Filament diameter	1.6 μm
Separation between filaments	0.4 μm
Fractional volume of filaments	0.27
Twist pitch	0.1 cm

Constitutive Relations

In the absence of a systematic theory for a hard superconductor it is necessary to make assumptions concerning the magnitude and direction of the three current systems:

A. Body Current

In the critical state model the body current density has its magnitude determined by the magnetic field and its direction by the electric field $\underline{E}$, i.e.

$$\underline{j}_b = j_c(H)\ \underline{E}/E \quad (5)$$

where if E is zero the direction is determined by the electrical history. The magnetic moment of the body current for an isolated body in a changing magnetic field is either diamagnetic or paramagnetic depending on whether the magnetic field is increasing or decreasing.

B. Vortex Current

In Abrikosov theory the vortex currents circulate around the direction of the flux density, and extension of the theory to a hard superconductor implies a paramagnetic moment depending only on the magnetic field.

C. Surface Current

In the absence of an electric field the surface current is diamagnetic, and the question arises as to how this current behaves when macroscopic electric fields exist. In Ref. 3 it was postulated that an electric field in the direction of surface current flow has little effect on the surface current, but an electric field acting against the surface current brings it to zero. This behavior is in contrast to that of the body current which is reversed by a change in direction of the electric field. It is assumed that the surface current in an isolated body is inherently diamagnetic. Thus, the electric field can destroy the diamagnetism but cannot produce a paramagnetic surface contribution. For a body which is not isolated, but carries transport current in an applied magnetic field, it was further assumed that only portions of the surface exhibit a surface current, where these portions correspond to regions where E corresponds to the direction of surface current flow induced by H.

*Supported by the Air Force Aero Propulsion Laboratory, Contract No. F33615-81-C-2040.

Manuscript received September 10, 1984.

Description of the Experiment

At various points corresponding to intermediate fields on the m-H_a hysteresis loop a sample of wire wound on a mandrel was heated above its critical temperature and then cooled below T_c in a constant magnetic field. The magnetic moment was measured with a Foner magnetometer, with the magnetic field transverse to the axis of the wire. Results of the measurements are shown in Figure 1. In order to detect the effect of cooling the magnetic field was slightly raised or lowered while the sample was warm as shown in the figure. After the change in moment with cooling to 4.2°K was observed, the magnetic field was then increased or decreased to show that the magnetic moment returns to its proper point on the major hysteresis loop. In each case a partial Meissner effect was observed upon cooling in a constant field, and the moment which was measured after the sample became superconducting is indicated by the dashes in the figures.

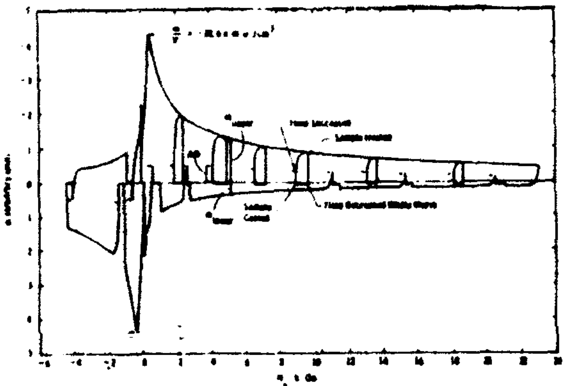

Fig. 1 — Plot of the major m-H_a hysteresis loop with minor loops obtained by (1) warming the sample above its critical temperature, (2) slightly shifting the field, (3) cooling to 4.2°K in a constant field and (4) increasing or decreasing the field to return to the major loop. V is the volume of superconductor in the sample.

Interpretation of the Results

When a hard superconductor is cooled below its critical temperature in a constant intermediate applied magnetic field, it is expected that diamagnetic surface currents will appear, and according to Eq. (2) paramagnetic vortex currents will form about the flux lines. The change in magnetic field inside the superconductor will be dominated by the surface currents, and this change is expected to induce body currents which oppose the change (contributing a paramagnetic moment). Thus, upon cooling in a positive fixed applied field, theory predicts that

$$\Delta m = -m_s + m_b + m_v \qquad (6)$$

where m_s, m_b and m_v are positive numbers. Δm corresponds to the interval between zero and the dash in Figure 1. The point on the upper major hysteresis curve for this field should correspond to a magnetic moment

$$m_{upper} = -m_s - m_b + m_v \qquad (7)$$

and therefore a change of state from (6) to (7) requires a reversal of m_b, which is accomplished by slightly increasing the applied magnetic field to give the required electric field. A point on the lower major hysteresis curve obtained by decreasing the magnetic field would be expected to be given by

$$m_{lower} = m_b + m_v \qquad (8)$$

where the electric field of the decreasing magnetic field, starting from the condition described by (6) destroys m_s. m_v is the same in (6), (7) and (8) since the magnetic field in the superconductor is essentially the same in all three cases.

Inasmuch as three theoretical equations are given for each value of H_a the three moments m_s, m_b and m_v can be obtained from the measurements. If Eq. (2) is assumed to hold for m_v then for $\lambda \sim 10^{-5}$ and $H_a = 10^4$ Oe a value $m_v/V \sim 30$ e.m.u. would be expected, but this value is nearly an order of magnitude too large to be compatible with any reasonable interpretation of the measurements. It must be concluded that either λ is larger than it is generally assumed to be in NbTi, or that Eq. (2) is not a good approximation. The use of equations (6), (7) and (8) to evaluate m_v shows it to be smaller than m_s and m_b but negative. Since a negative value of m_v is difficult to understand, it is postulated that the measurements are not sufficiently accurate to evaluate m_v (due perhaps to the twist which is present in the wire, which introduces a longitudinal component to the field, whereas a transverse field has been assumed). In the remaining analysis it will be assumed that the magnetic moment of the vortex structure can be neglected, and m_v will be set equal to zero. Thus,

$$\Delta m = m_{upper} + 2m_{lower} - 2m_v$$

$$\approx m_{upper} + 2m_{lower} \; . \qquad (9)$$

Then the calculated value of Δm given by (9) using the measured values of m_{upper} and m_{lower} can be compared with the measured value of Δm. The results are shown in Figure 2. Qualitative agreement is obtained with the theory, but a quantitative proof of the assumptions must await additional measurements on more well-defined samples. The values for m_s and m_b obtained in this way are given in Ref. 3.

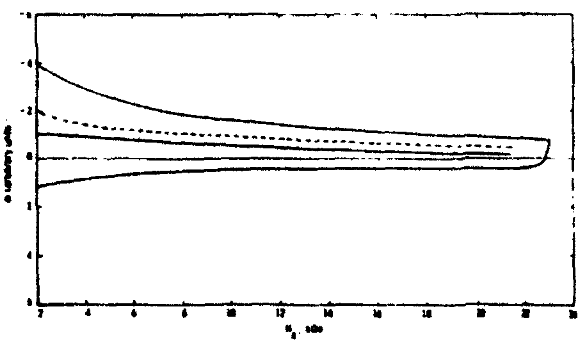

Fig. 2 — Plot of major hysteresis loop and measured values of Δm (——) vs the calculated curve (- - -).

The fact that the magnetic moment on the lower part of the major hysteresis loop in quite small is a good indication that m_v is very small, for in this region of positive magnetic field and decreasing H_a, no obvious reason exists for the presence of any diamagnetic currents which would tend to cancel to vortex moment. The results tend to indicate a need for revision in the theory of vortex structure.

Finally, it is noted from Figure 1 that the zero line for the superconducting moment established by warming the sample in various fields has a slight downward slope. This slope is attributed to a net paramagnetism in the sample holder and the conductor matrix.

<u>References</u>

1. A. L. Fetter and P. C. Hohenberg, Superconductivity, 2, p. 838, Ed. R. D. Parks, Marcel Dekker, New York (1969).

2. W. J. Carr Jr., Phys. Rev. B 23, 3208 (1981).

3. W. J. Carr Jr. and G. R. Wagner, Ad. in Cry. Eng. 30, 923, Eds. A. F. Clark and R. P. Reed, Plenum, New York (1984).

To be published in Adv. in Cryog. Eng. 32 (1986).

APPENDIX H

MAGNETIC BEHAVIOR OF A VERY FINE FILAMENT CONTINUOUS SUPERCONDUCTOR*

W. J. Carr, Jr. and G. R. Wagner

Westinghouse R&D Center
Pittsburgh, Pennsylvania

ABSTRACT

The magnetic moment of an untwisted multifilamentary superconductor consisting of 0.12 μm diameter Nb filaments in a copper matrix was studied as a function of applied magnetic field. The wire contains 72,102 filaments arranged in 61 bundles of 1182 each. In a transverse magnetic field the wire behaves as a solid superconductor yielding a moment characteristic of the wire diameter as expected for a long untwisted wire. But in a parallel field the moment is much smaller and is interpreted as arising from strong proximity coupled filaments within a bundle, with weak coupling between bundles. A Meissner effect was observed for the individual filaments but not for the bundles or wires.

INTRODUCTION AND SUMMARY

A study has been made of the magnetic moment in both weak and strong magnetic fields of a multifilament superconductor having 0.12 μm diameter filaments, presumed to be continuous through the wire. The conductor consists of Nb filaments embedded in a Cu matrix with the configuration shown in Fig. 1, except that the outer Cu and the Nb barrier have been etched away. The filaments are arranged in bundles with 61 bundles of 1182 filaments in the wire, giving a total of 72,102 filaments. Neither the filaments nor the bundles are twisted. Each bundle has a core of Sn but this fact is considered to be unimportant in the analysis. All measurements in the superconducting state were made at 4.2°K. The wire was obtained from Intermagnetics General Corporation.[1] The magnetic moment was measured with a Foner-type vibrating sample magnetometer.

Since the separation between filaments in a bundle is the order of 0.05 μm it is to be expected that the filaments are strongly coupled together via the proximity effect in the copper,[2] and for some purposes the bundle may be expected to act as a single large filament. It is found that for perpendicular magnetic fields the bundles can also be considered

*Supported by the Air Force Aero Propulsion Laboratory, Contract No. F33615-81-C-2040.

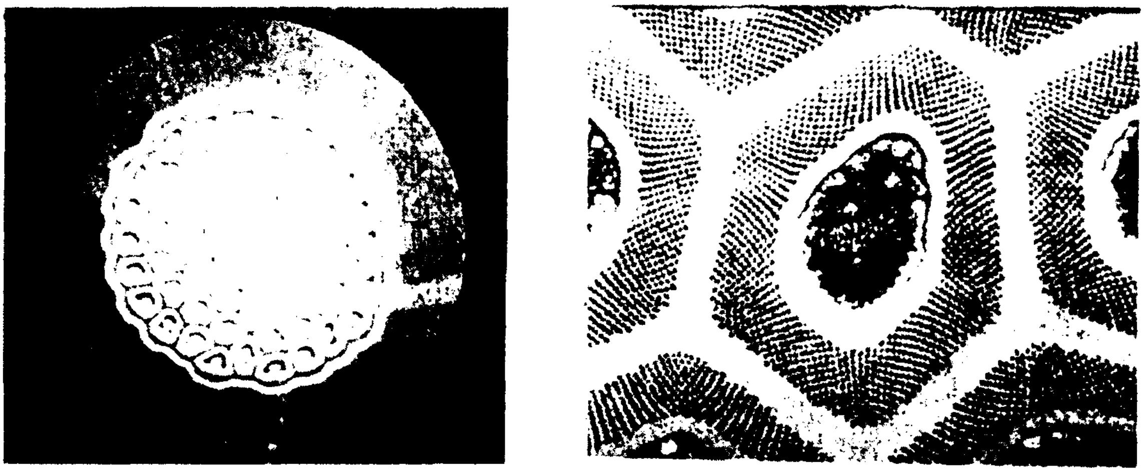

(a) (b)

Fig. 1. (a) Conductor cross-section showing 61 bundles of filaments with Sn central core, diffusion barrier, and outer stabilizing copper. (b) A bundle at higher magnification showing individual filaments.

as coupled together, and the magnetic moment is determined by the wire diameter. For parallel fields each bundle acts as a single filament, but the bundles are only weakly coupled and the magnetic moment is much smaller. In all magnetic fields a weak partial Meissner effect is observed for the parallel field case, but it occurs only in the filaments.

BEHAVIOR IN A TRANSVERSE FIELD

The initial slope of the magnetization curve as a function of applied magnetic field[3] is shown in Fig. 2, where the ordinate corresponds to -4π times the magnetic moment divided by the total volume V of the sample. For a solid superconductor, simple theory would predict an initial slope of two for this plot. Since, to good approximation, the measured curve fits this theoretical curve, it follows that the filamentary nature of the sample has no effect on the measured curve: i.e., the magnetic moment is the same as that for a solid superconductor with an equivalent current density. Thus the bundles are coupled together in addition to the filaments. This result is not entirely surprising, since for a long untwisted wire in a transverse field, the currents tend to flow parallel to the filaments and bundles, and these currents have the whole length of the wire to cross over from one bundle to another. Even a very small transverse supercurrent in the Cu matrix between bundles will lead to the observed result. In terms of the effective longitudinal current density j_c for the wire, the critical state model gives for the magnetic moment[4]

$$\frac{m}{V} = \frac{0.2}{3\pi} d \, j_c \qquad (1)$$

for full penetration of the current into the wire, where d is now the diameter of the wire (71×10^{-4} cm). The peak in the curve of Fig. 2 is taken to correspond to the point of full penetration, and using the measured value of m/V one obtains $j_c = 1.32 \times 10^6$ amps/cm^2. With the approximation $j_c = 0.23 \, j_{cf}$ where 0.23 is the fraction of superconductor in the wire, the value obtained for the critical current density j_{cf} of the filaments at H = 1500 Oe is

$$j_{cf} = 5.7 \times 10^6 \qquad (2)$$

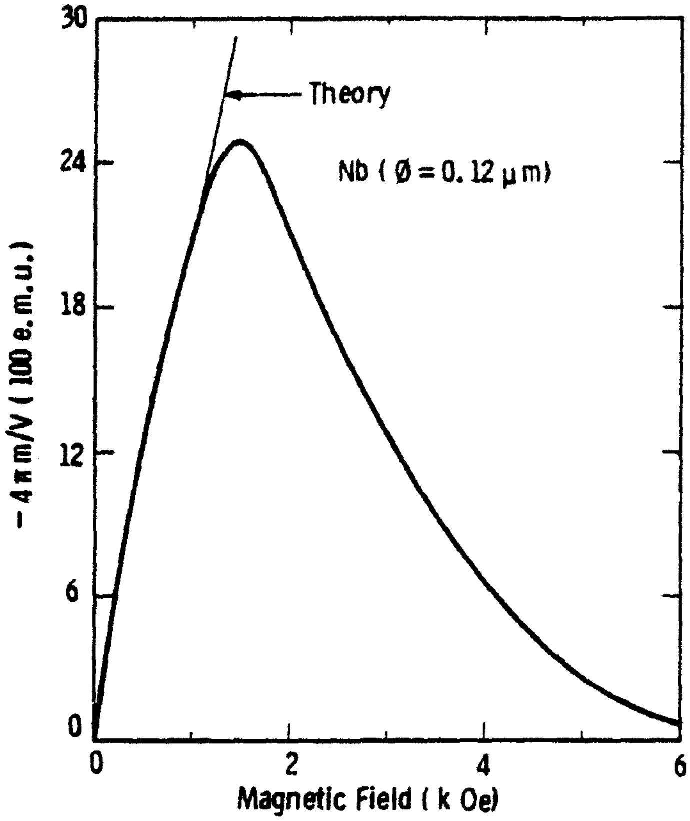

Fig. 2. Initial magnetization as a function of the applied transverse magnetic field, where m is the magnetic moment and V the sample volume.

in good agreement with the value measured for this wire as shown in Fig. 3.

Figure 4 shows the results of cooling the sample in various magnetic fields from a temperature above the critical temperature T_c. No bulk Meissner effect is observed, and, in fact, no effect at all is observed from cooling in a constant magnetic field. However, as discussed in the following section, it is believed that a small Meissner effect exists in the filaments, but the magnetic moment in a transverse field is so large that this small effect is not resolved.

BEHAVIOR IN A PARALLEL FIELD

A sample was prepared for parallel field measurements by cutting the wire into one centimeter lengths and using 77 segments to form a sample of nearly the same volume as that used for the transverse field measurements. The initial magnetization curve is shown in Fig. 5, where two peaks in the curve are observed, one at m = -0.057 e.m.u., H = 400 Oe; with the other at m = -0.084, H = 3000. It is observed that the magnetic moments tend to be an order of magnitude smaller than those for the transverse field. The interpretation assumed for this curve is the following: (1) each bundle acts like a single large superconducting filament which becomes fully penetrated at the lower peak, H = 400 Oe; and (2) bulk supercurrents also circulate around larger loops (Fig. 6) due to migration along favorable paths between bundles. The latter are presumably determined by some randomness in the spacing, and these current loops produce the additional moment leading to the second peak. One may check the first assumption as follows. The field for full penetration of a hollow filament of outer diameter d_{so} and inner diameter d_{si} is[5]

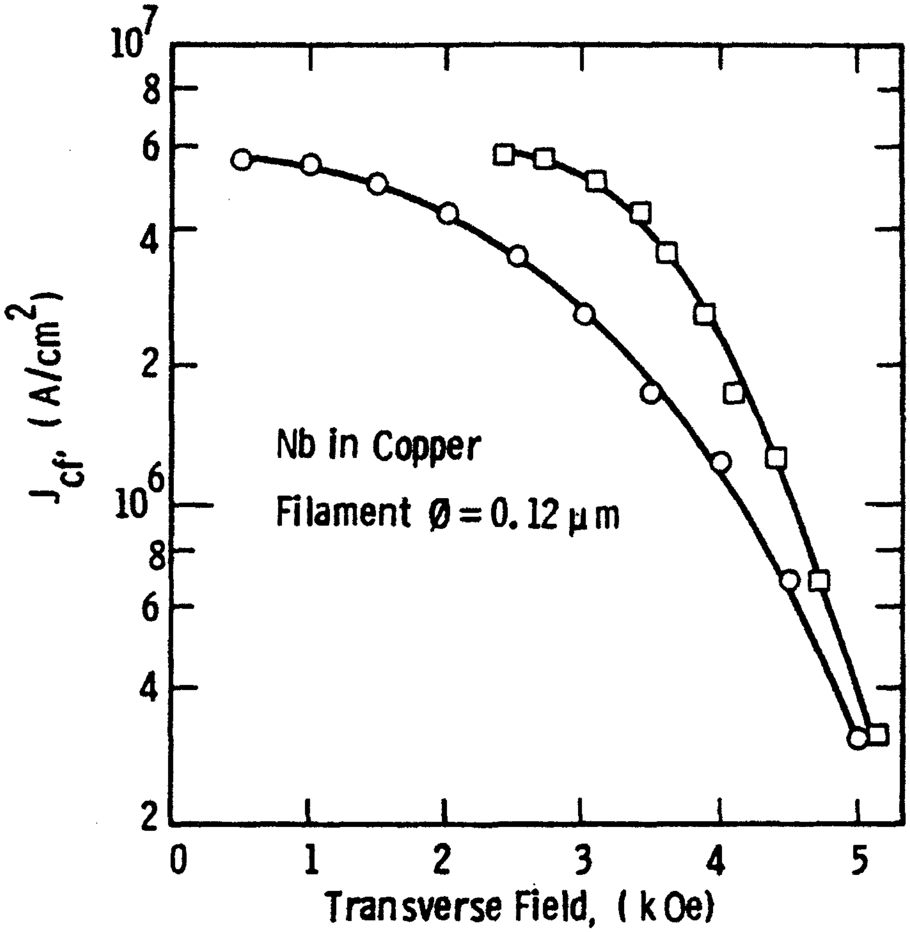

Fig. 3. Measured critical current density in the filaments vs. the applied transverse field. The circles are as measured and the squares are corrected for self field.

$$H_p = 0.2\pi \ j_c(d_{so} - d_{si}) \tag{3}$$

with j_c the current density in the filament. For the hollow filament formed by the bundle of Fig. 1, $d_{so} - d_{si} = 3.2 \times 10^{-4}$ cm, and for $H_p = 400$

$$j_c = 2 \times 10^6 \ \text{A/cm}^2 \tag{4}$$

for the critical current density circulating in the part of the bundle occupied by filaments. This value is smaller than the longitudinal critical current density given by (2), as expected, since the circumferential current density must flow, in part, through the matrix. However the two have the same order of magnitude. It is easily shown that the magnetic moment due to the critical current j_c of a fully penetrated cylinder in a longitudinal field is

$$m = \frac{0.1 \ j_c \ d}{6} V \ . \tag{5}$$

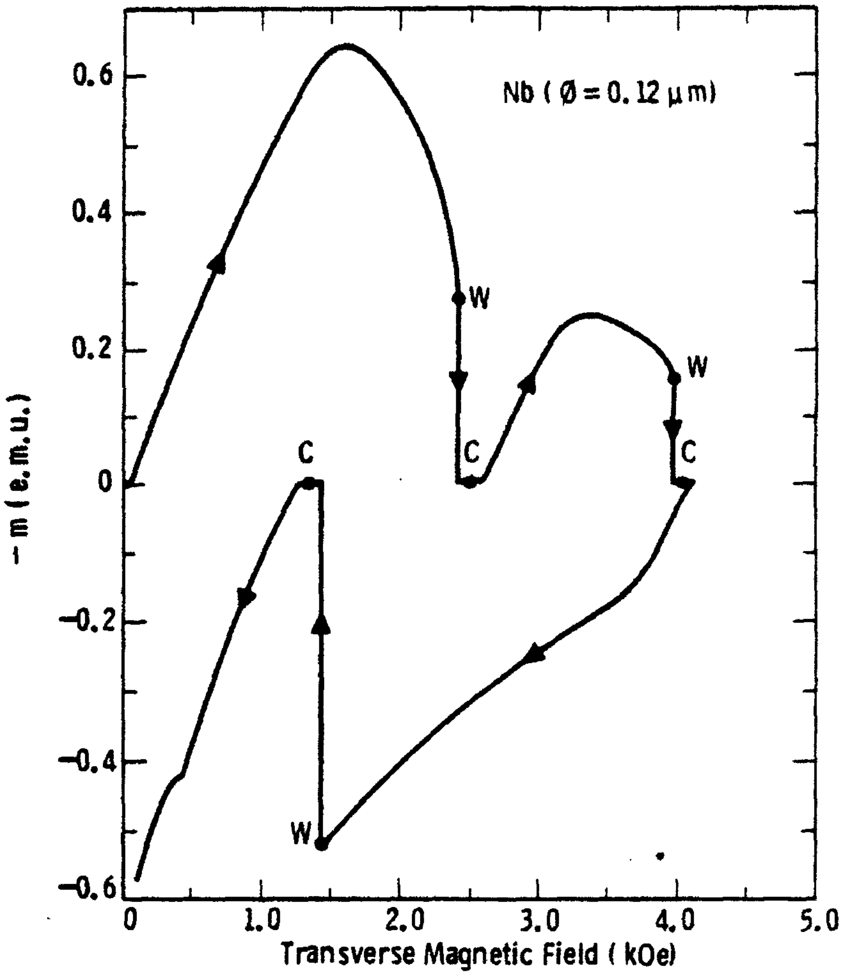

Fig. 4. Measured magnetic moment in a transverse magnetic field. At points indicated by W the sample was warmed above T_c at constant field. At points indicated by C the sample was recooled to 4.2°K at constant field. While the sample temperature was above T_c, the recorder pen was displaced horizontally to properly observe the effect of cooling, so the horizontal portions have no significance.

Thus for a hollow strand

$$m = \frac{0.1\ j_c}{6}\ \left[d_{so}\ \frac{\pi}{4}\ d_{so}^2\ \ell - d_{si}\ \frac{\pi}{4}\ d_{si}^2\ \ell\right]$$

$$= \frac{0.1\ j_c}{6}\ d_{so}\ V_s\left(1 - \frac{d^3_{si}}{d^3_{so}}\right) \tag{6}$$

where ℓ is the total length of the strand and V_s is the volume. One obtains using (4)

$$m = 2.75 \times 10^{-8}\ j_c \tag{7}$$

$$= 0.055$$

in excellent agreement with the measured value 0.057. The second assumption is more difficult to verify since the larger current loops involve a distribution of current paths.

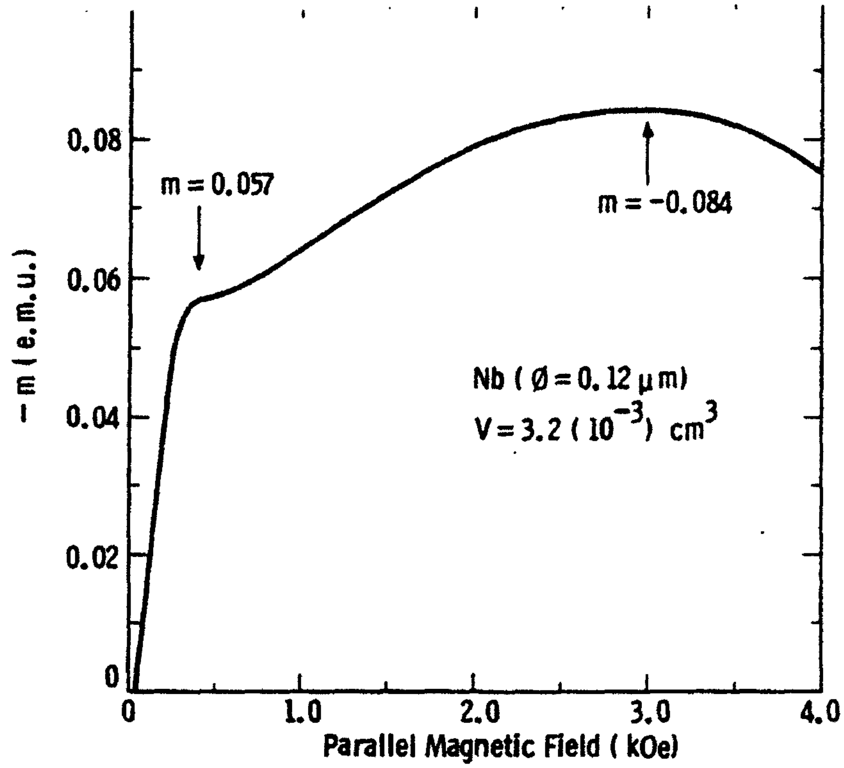

Fig. 5. Initial magnetization measured as a function of the applied field parallel to the filaments.

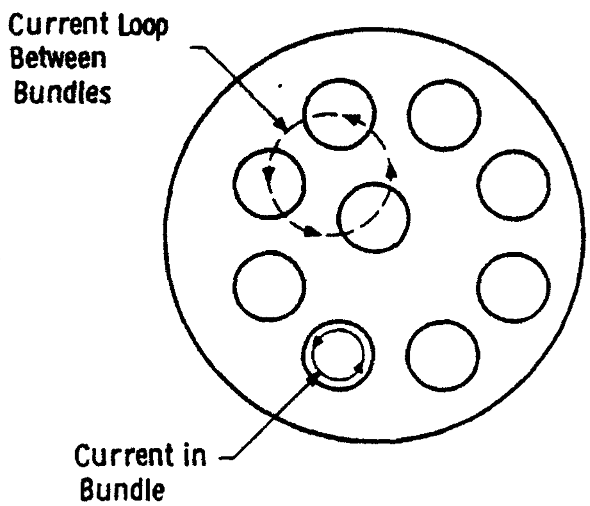

Fig. 6. Schematic picture indicating a current loop within a bundle and a larger loop between bundles.

Figure 7 shows an investigation of the Meissner effect in various parallel applied fields. It is clear that no bulk Meissner effect occurs in the wire or bundles, but a small effect is observed at all fields, which is attributed to a partial Meissner effect in the filaments. The change in magnetic moment observed on cooling through the critical temperature is $\Delta m \sim 2 \times 10^{-3}$ and the total volume of filaments is 0.67×10^{-3}. One finds that

$$\frac{4\pi\ \Delta m}{V_f} \sim 38 \qquad (8)$$

in e.m.u., which is less than the lower critical field H_{c1}, as expected.

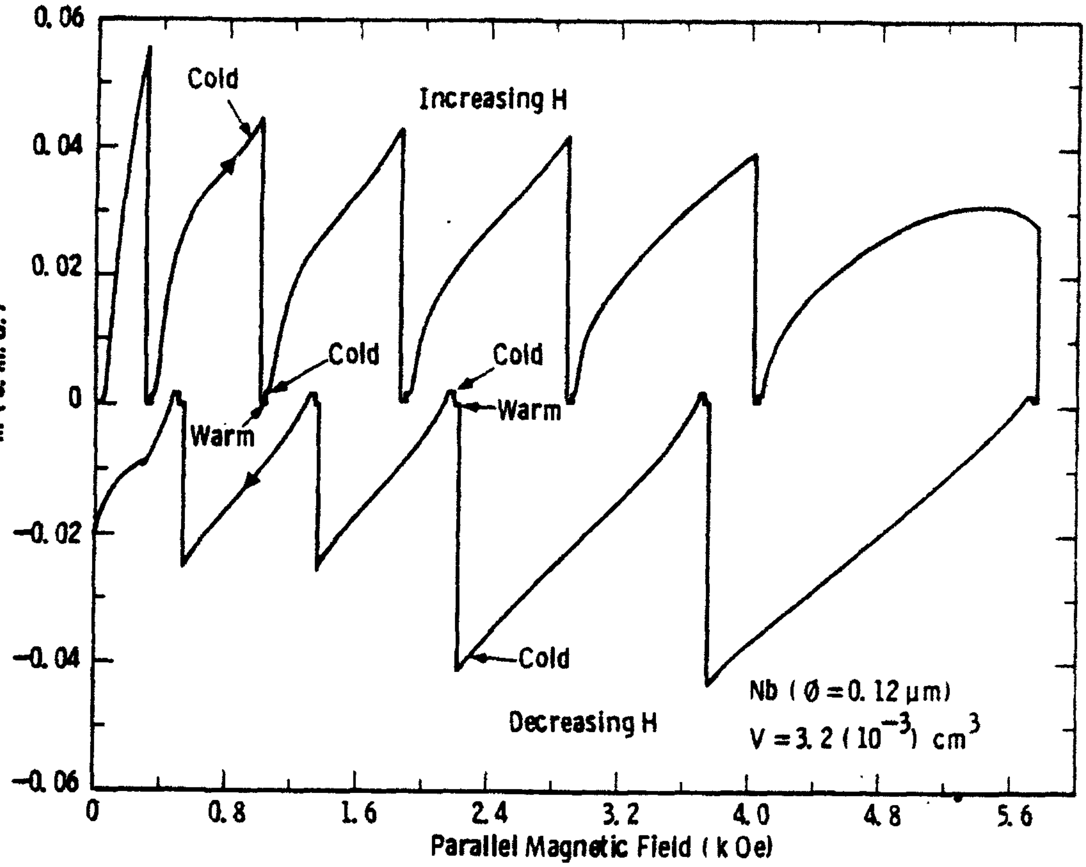

Fig. 7. The magnetization vs. applied field parallel to the filaments showing the partial expulsion of flux upon cooling through the critical temperatures at various values of field. Warm indicates the sample temperature is above T_c and cold is 4.2°K. The horizontal portions are due to a mechanical displacement of the recorder pen and have no significance. (See Fig. 4 caption)

REFERENCES AND FOOTNOTES

1. This conductor was manufactured by IGC to be subsequently heat treated to form Nb_3Sn by the internal tin technique. The results reported here are for the unreacted state with the outer copper stabilizer and diffusion barrier etched away leaving Nb filaments in a copper matrix with the tin core in the bundles. We thank Dr. G. M. Ozeryansky of IGC for supplying the wire.
2. It is interesting to compare these results with the hysteresis losses in similar fine filament conductors reported by P. Dubots, A. Fevrier, J. C. Renard and J. P. Tavergnier at the Applied Superconductivity Conference, San Diego (1984). In the latter the matrix consists of a Cu-Ni alloy which has a much weaker proximity effect, and filamentary behavior exists down to a smaller filament diameter.
3. The sample consisted of a wire coiled on a mandrel. A small correction was made to the applied magnetic field to account for the field of neighboring turns.
4. W. J. Carr Jr. and G. R. Wagner, Ad. in Cryogenic Eng., Ed. A. F. Clark and R. P. Reed, Plenum, New York, Vol. 30, 923 (1984).
5. W. J. Carr Jr., AC Loss and Macroscopic Theory of Superconductors, Gordon and Breach, New York (1983).

SURFACE CURRENT AND HYSTERESIS IN FINE FILAMENT NbTi SUPERCONDUCTORS

W. J. Carr Jr., G. R. Wagner

Westinghouse R&D Center
Pittsburgh, Pennsylvania 15235

Abstract - Measurements of hysteresis loops and critical currents were made on composite superconducting wires of NbTi filaments embedded in a Cu-CuNi matrix and on similar samples with the matrix etched away. Results were obtained for filament diameters of 1.6, 0.8 and 0.4 μm. The measurements indicate that in magnetic fields above several kilooersteds most of the current in the filaments is surface current.

INTRODUCTION

In previous work it has been shown [1-3] that in high magnetic fields the hysteresis loop of a fine filament NbTi superconductor is quite different in shape from that of a bulk conductor. Near zero field the shape is similar to that of a hard bulk conductor, but in large fields it becomes more reversible and the shape is intermediate between that for a hard bulk material and an ideal soft material. The results were interpreted in terms of surface currents which become relatively large compared with the bulk current as the filament diameter is made smaller, and they suggest a possible approach for obtaining superconductors with low loss and high critical current. Some further measurements on NbTi filaments of different diameters are reported here. The conductors, which were obtained from Oxford Airco Superconductors, are described in Table 1. Samples were prepared by winding the wire on a mandrel, and all measurements were made with a vibrating magnetometer in a transverse applied field. The filaments in the composite conductors were surrounded by a Cu-CuNi matrix. Studies on the 1.6 μm conductor were reported by the present authors and also, in a different context, by Ogasawara et al. [4] However, results for the wires with 0.8 and 0.4 μm filaments are new, and further, additional samples of all three conductors were prepared with the entire Cu and Cu-Ni matrix etched away. Unfortunately, the filaments were twisted in the composite samples; whereas in the etched samples an attempt was made to remove the twist. In the interpretation, twist has been ignored in all the samples.

Table 1

Sample	1	2	3
Conductor dia. (mm)	0.36	0.018	0.09
Filament dia. (μm)	1.6	0.8	0.4
Approximate Filament Separation (μm)	0.6	0.3	0.15
Approximate CuNi thickness (μm)	0.3	0.15	0.08

INITIAL MAGNETIZATION CURVES

In order to examine whether the observed magnetic moment results from individual filaments or from coupled filaments, measurements were made of the initial magnetization curves. The magnetic moment per unit filament volume (multiplied by 4π) for the 1.6 μm and 0.8 μm samples is plotted in Fig. 1 and for the 0.4 μm sample in Fig. 2. A small correction was made for neighboring turns in the sample to give the field applied to an individual turn. Simple theory gives an initial slope of two, which arises from an assumed perfect Meissner behavior and the demagnetizing factor of a cylinder.

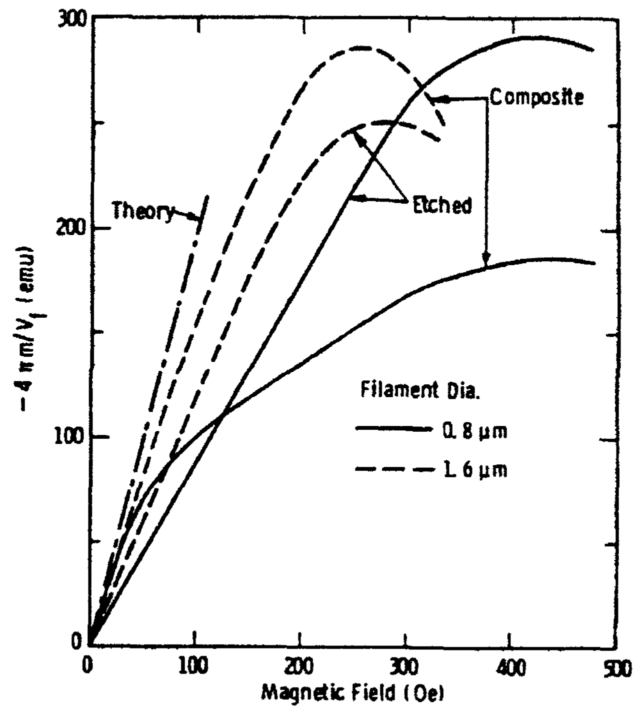

Fig. 1 - The measured initial magnetic moment per unit filament volume (multiplied by -4π) for the 1.6 and 0.8 μm composite and etched samples is plotted vs. the applied transverse field.

The 1.6 μm Samples

The magnetization curve for the composite sample with 1.6 μm filaments agrees with the theory reasonably well, which indicates that the magnetic moment indeed comes from individual filaments that are not coupled through the matrix. This conclusion is re-enforced by the fact that a similar sample with the matrix etched away leads to essentially the same results.

The magnetic field at which the peak in magnetic moment occurs (approximately 250 Oe) is presumed to be the field required to fully penetrate a filament. The lower critical field H_{c1} where flux lines and bulk currents begin to penetrate into the filaments is determined roughly by the point on the magnetization curve where linearity begins to break down. This seems to occur in the neighborhood of 100 Oe (within a factor of two) which is in order of magnitude agreement with previous estimates of H_{c1}.

The 0.8 μm Samples

The results for the 0.8 μm filaments are more difficult to understand, and the measurements for the etched sample differ considerably from those for filaments embedded in the matrix. However, since the initial slope of both curves falls below the theoretical value there is no evidence of filament coupling, and the magnetic moment appears to come from individual filaments as for the 1.6 μm filaments.

*Supported by the Air Force Aero Propulsion Laboratory, Contract No. F33615-81-C-2040.

In the etched sample no evidence of a full Meissner effect exists. The reason for this fact, and for the relatively large magnetic field required to reach the peak in magnetic moment is not known. In examining the difference between the composite and the etched samples it should be kept in mind that filaments embedded in the matrix are probably under stress, and also the condition of the filament surfaces in the two samples is probably considerably different.

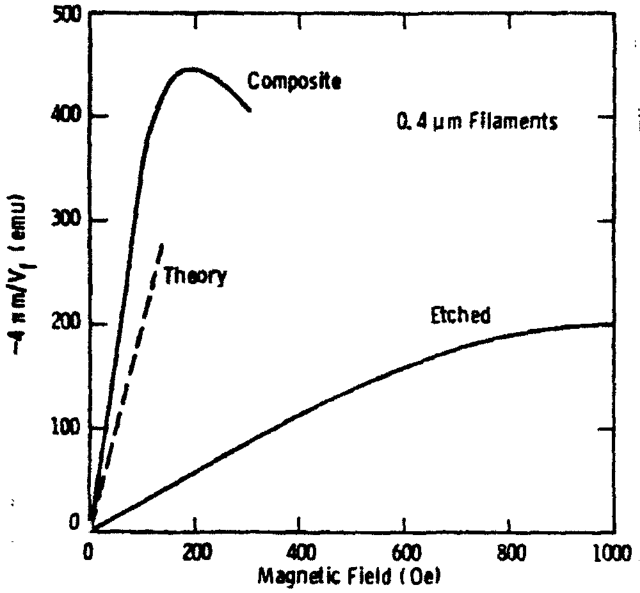

Fig. 2 - As Fig. 1, but for the 0.4 µm samples.

The 0.4 µm Samples

Since the curve for the composite sample rises above the theoretical curve, one is led to believe that some filament coupling through the matrix exists, leading to a magnetic moment larger than expected. However, in the following section it is found that the coupling apparently disappears in high fields. In the etched sample no coupling is observed, as would be anticipated, but again the field at the peak in magnetic moment is quite large and a full Meissner state is not observed.

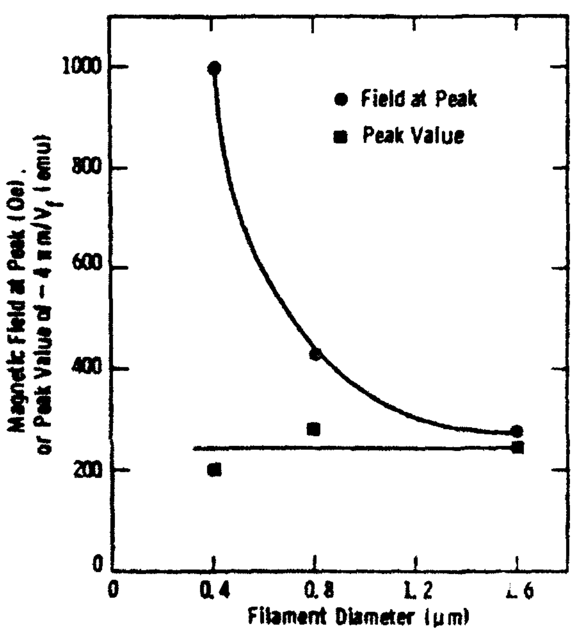

Fig. 3 - The measured peak value of $4\pi m/V_f$ and the magnetic field at which it occurs are plotted vs. filament diameter.

In Fig. 3 the magnitude of the peak in magnetic moment and the magnetic field required to reach it are plotted against filament diameter for the three etched samples. While the peak value is nearly the same for the three diameters, the field required to reach the peak increases with smaller diameter. This is opposite to the behavior expected from simple critical state theory for the full penetration field, and is also not understood.

HYSTERESIS IN HIGH FIELDS

In general, for filament radii greater than the London penetration depth, three types of current flow can exist in a superconductor with each producing its own magnetic moment: (1) body or bulk currents, (2) surface currents, and (3) currents circulating in the vortex structure. The first gives a magnetic moment per unit volume which is proportional to the filament diameter for a fixed current density. The other two give moments which are independent of diameter.

The surface current which is investigated here is assumed to be that which originates under the action of a magnetic field in order to lower the energy. This equilibrium type current is in contradistinction to the non-equilibrium type body currents resulting from flux pinning. Matsushita, et al [5] have studied surface currents in larger filaments that appear to result from surface pinning. The relationship between such surface current and that discussed here is unclear.

A wide range of assumptions have been made by various authors to discuss the hysteretic behavior of fine filaments. Some of the conflicting ideas proposed may be listed as follows: (a) the hysteresis loop is the superposition of a reversible equilibrium contribution and an irreversible contribution from flux line pinning, [3,6] (b) surface currents determine the hysteresis, [7] (c) surface and bulk currents both contribute, but the surface current flows only during half of the hysteresis cycle, being destroyed by an electric field over the other half of the cycle, [1] (d) both surface and bulk currents contribute, with the surface current making a symmetric contribution to the hysteresis loop [8,9] and (e) thermodynamic surface "barriers" to flux entrance and exit determine the shape of the hysteresis loop. [10,11]

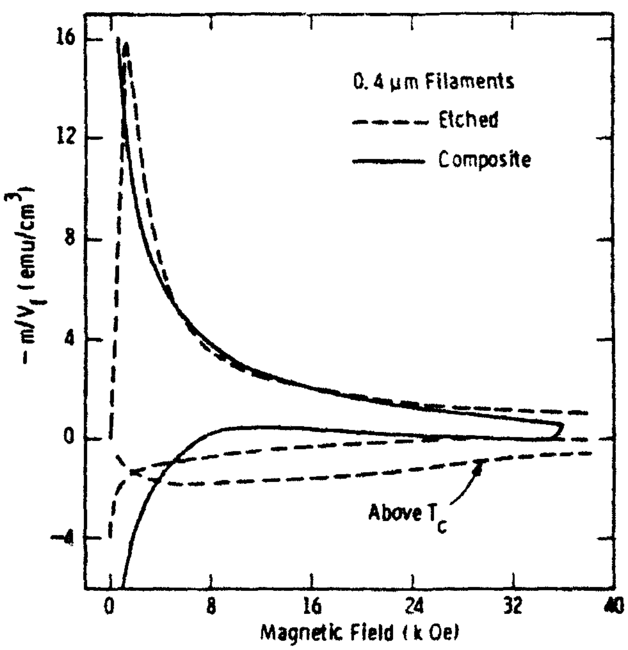

Fig. 4 - The measured magnetic moment per unit filament volume vs. the applied transverse field for the 0.4 µm samples. The solid curve is for the composite and the dashed curve is for the filaments alone (with the matrix etched away). The loops were taken at 4.2K and the lower dashed curve above T_c.

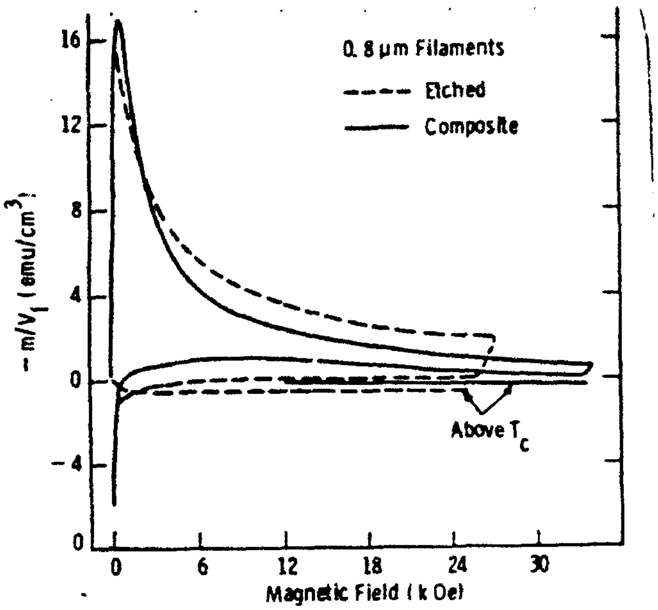

Fig. 5 - Same as Fig. 4, but for the 0.8 μm samples. The lower solid and dashed curves were taken above T_c.

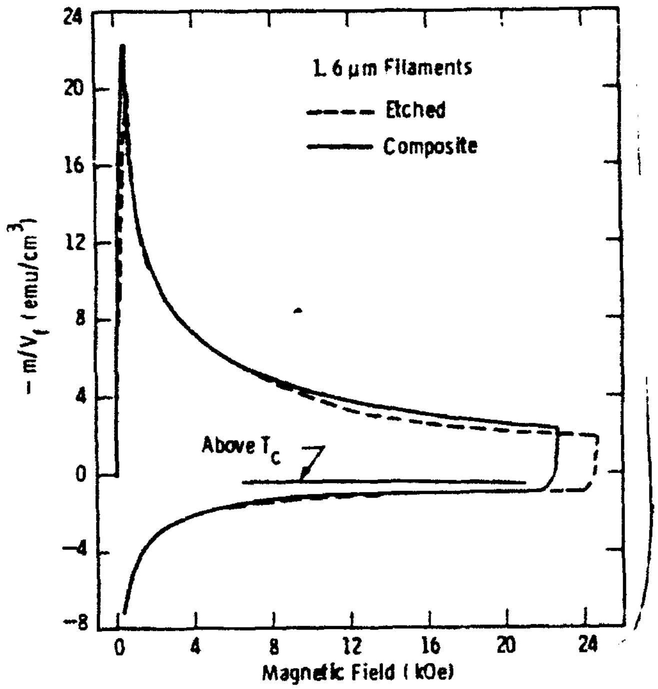

Fig. 6 - Same as Fig. 4, but for the 1.6 μm samples.

For the present material the hysteresis loops are shown in Figs. 4-6. The results for the composite samples in high fields are regarded as more reliable, since the etched samples appear to have some ferromagnetic contaminate, which is probably Ni. Nevertheless, in a qualitative sense the composite and etched samples are much the same. For the 0.8 and 0.4 μm filaments it appears that assumption (a) is more nearly correct, since the upper and lower parts of the hysteresis loop are both negative, and a tendency toward reversible behavior is observed. It is possible that (c) would apply if the loop were traversed more rapidly.

Inspection of the three hysteresis loops for the composite samples shows that in high fields the loops for the 0.8 and 0.4 μm filaments are essentially the considerably broader. The conclusion reached from these results is that for filaments considerably larger than 1 μm the body currents are important, while below 1 μm only the surface current is significant. This conclusion is also in agreement with the hysteresis loss measurements of Dubots et al. [12]

TRANSPORT CURRENT

It is now of interest to determine if the surface component also dominates the transport current of the 0.8 and 0.4 filaments. If this is the case, the critical current density in the filaments should be twice as large in the 0.4 μm filaments as in the 0.8 μm material, providing the surface current of the filaments is the same for both wires. The measured effective critical current densities of the wires are shown in Fig. 7. While the factor of two ratio does not persist over the entire curves, it does hold approximately over the lower portion. The fact that the 1.6 μm curve lies intermediate to the other two is attributed to the additional contribution of the body current in this sample.

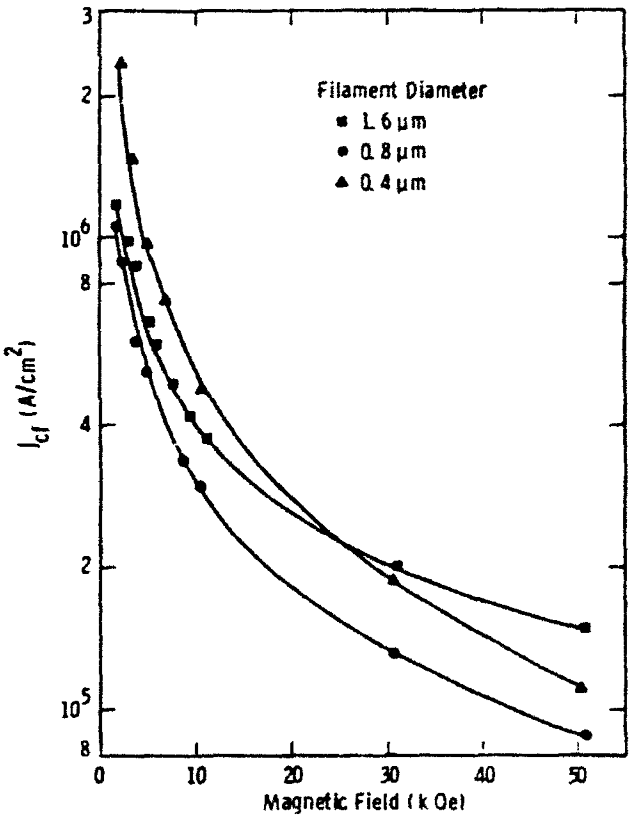

Fig. 7 - The measured critical current density in the filaments, corrected for self field, is plotted vs. magnetic field.

CONCLUSIONS

For NbTi filaments less than about 1 μm in diameter the current flow is dominated by the surface component. This conclusion implies that to obtain superconductors with high critical current density one should concentrate on examining the surface condition of the filaments rather than the internal pinning forces. For equivalent surface conditions the critical current density should increase proportional to 1/d (d the filament diameter) down to the point where the diameter becomes the order of twice the London penetration depth. Unfortunately, this predicted behavior is not observed in measurements of Dubots et al., [12] but it is possible that the effect is masked by other factors such as broken filaments.

REFERENCES

[1] W. J. Carr Jr. and G. R. Wagner, Adv. in Cry. Eng., Eds. A. F. Clark and R. P. Reed, Plenum Press, New York, Vol. 30, p. 923, (1983).

[2] W. J. Carr Jr., IEEE Trans. Magnetics, MAG-21, 355 (1985).

[3] Similar asymmetry was observed by P. S. Swartz, Phys. Rev. Letters 9, 448 (1962) in measurements on fine powders of other alloys.

[4] T. Ogasawara, Y. Kubota, T. Makiura, T. Akaci, T. Hisanari, Y. Oda and K. Yasukōchi, IEEE Trans. MAG-19, 248 (1983). The conductor measured by these authors was slightly smaller, and had 1 μm filaments.

[5] T. Matsushita, T. Honda, Y. Hasegawa, T. Akenaga and Y. Monju, Proc. ICMC, Kobe, p. 171, Eds. K. Tachikawa and A. Clark, Butterworths, UK (1982).

[6] J. Silcox and R. W. Rollins, Appl. Phys. Lett. 2, 231 (1963).

[7] L. J. Barnes and H. J. Fink, Phys. Lett. 20, 583 (1966).

[8] C. Fournet and A. Mailfert, J. Phys. Paris 31, 357 (1970).

[9] S. T. Sekula and J. H. Barrett, Appl. Phys. Lett. 17, 204 (1970).

[10] J. R. Clem, J. Appl. Phys. 50, 3518 (1979).

[11] M. A. R. LeBlanc and J. P. Lorrain, IEEE Trans. MAG-19, 256 (1983).

[12] P. Dubots, A. Février, J. C. Renard, J. P. Tavergnier, IEEE Trans. Magnetics, MAG-21, 177 (1985).

Submitted for publication in the Proc. of the Intl. Symp. on Flux Pinning and Electromagnetic Effects in Superconductors.

APPENDIX J

MECHANISM OF CURRENT TRANSPORT IN FINE NbTi FILAMENTS*

W. J. Carr, Jr. & G. R. Wagner
Westinghouse R&D Center
Pittsburgh, Pennsylvania 15235

ABSTRACT

Measurements of the hysteresis loops, the magnetic moments obtained by cooling in a constant field and the critical current density of submicron NbTi filaments are consistent with the assumption that surface current is the principal mechanism of current flow in these filaments.

*Supported by the Air Force Aero Propulsion Laboratory Contract No. F33615-81-C2040

1. INTRODUCTION

The development of fine filament superconductors having low loss and high current density in large magnetic fields has reached the point where further progress appears to demand a more fundamental understanding of the reversible and irreversible behavior of fine filaments. To study this behavior, a series of measurements of hysteresis loops and critical current densities have been made on the NbTi fine filament wires described in Table 1. The wires were obtained from Oxford Airco Superconductors, and described more fully in previous papers.[1-3] Loss measurements of an eddy current nature on a similar conductor have been reported by Ogasawara et al.;[4] and other recent work on submicron NbTi filaments have been published by Dubots et al.[5] Measurements on 1 to 5 μm material have been reported by Ghosh and Sampson[6]. In the present samples it was noted previously[1] that a high degree of asymmetry exists about the horizontal axis of the transverse field m-H hysteresis loop (m the magnetic moment), and in the 1.6 μm composite it was shown that a partial "Meissner effect" exists up to the highest magnetic fields that were investigated.[2] Both effects were attributed to surface current in the filaments. Additional measurements of these effects are presented here. To eliminate the possibility of proximity coupling of the filaments through the Cu and CuNi matrix, measurements have also been made on a similar set of samples with the

Table 1

	Sample 1	Sample 2	Sample 3
Conductor diameter (cm)	0.036	0.018	0.009
Filament diameter (μm)	1.6	0.8	0.4
Separation between filaments (μm)	~ 0.6	~ 0.3	~ 0.15
CuNi thickness between filaments (μm)	~ 0.3	~ 0.15	~ 0.08

entire matrix etched away. Results are given for the six samples, along with conclusions concerning the behavior of the transport current in these materials. Conclusions are necessarily qualitative in nature since, as pointed out in the following section, some questions concerning the theory for the behavior of very fine filaments remain to be answered.

Two types of surface current have been previously identified in the mixed state of a type II superconductor: one an irreversible current depending on strong flux pinning near the surface as described by Matsushita et al.,[7,8,9] the other a reversible surface current[10] which can be viewed as an extension of the Meissner current.* The latter is of principal interest here. Contrary to previous treatments, a surface part is assumed to exist in both the magnetization and transport measurements.

---

*In reality this theory postulates a reversible magnetization as calculated from Abrikosov theory (See also Reference 11,12) which therefore presumably includes a surface current and a series of vortex currents throughout the volume[(2)]. However, since the net Abrikosov magnetization is diamagnetic, one has reason to conclude that the surface current is dominant. Fietz et al.[(10)] lumped the entire magnetization into a surface current. However these authors ignored the possibility of a surface component in the transport current.

2. THEORIES OF HYSTERESIS AND TRANSPORT IN FINE FILAMENTS

A wide range of models have been proposed to discuss the hysteresis of fine superconducting filaments. These models include the following:

(a) The magnetic moment measured on the hysteresis loop is a superposition of a reversible equilibrium magnetization (mainly a surface current) and an irreversible contribution from flux line pinning.[10]

(b) Surface currents determine the hysteresis.[13]

(c) Surface and bulk currents both contribute, but the surface current flows only during half of the hysteresis cycle, being destroyed by an electric field over the other half of the cycle.[1]

(d) Both surface and bulk currents contribute, with the surface current making a symmetric contribution to the hysteresis loop.[14,15]

(e) Thermodynamic surface "barriers" to flux entrance and exit determine the shape of the hysteresis loop.[16,17]

Most of these models apply also for large filaments but in that case bulk pinning tends to mask the other effects. The model which seems to best fit the experimental data is model (a), although the reasons are not entirely obvious. The various models correspond to various degrees of reversibility of the surface terms, and to whether the problem is viewed as a problem in static field theory at zero frequency or a problem in electrodynamics at low frequency.

A hysteresis loop is typically measured by slowly but continuously varying the magnetic field. Thus a time rate of change of applied field $\dot{H}_a$ exists, and the electric field arising from $\dot{H}_a$, or more generally from $\dot{B}$, is the central feature of hysteresis. In particular the direction of the bulk current density j_c depends upon the electric field E, and this electric field acts on the surface as well as the bulk. In contrast, the sign of an equilibrium current depends upon the vector potential A, which is determined by B rather than $\dot{B}$. In a large magnetic field, $B \approx H_a$, and A is essentially the same for both the upper and lower branches of the hysteresis loop, but $\dot{H}_a$ and E change sign in the two branches. From an equilibrium point of view the surface current would be the same in both branches but from electrodynamics, any surface current might be expected to reverse with the bulk current density. Thus a dilemma exists. Carr and Wagner[1] (model c) made the assumption that a current can exist on the surface only if the signs of A and E are such as to make the current flow in the same direction, and this is the case only for one branch of the hysteresis loop. For a transport current measurement the theory would indicate that equilibrium surface current can flow only over one-half the circumference. While model (c) does not seem to describe the magnetization measurements it may apply for the transport case, since critical transport current measurements are made in the presence of a comparatively large dc electric field. The essential idea behind this model is the following. If a large transverse magnetic field is first applied and it produces, as in model (a), an equilibrium surface current, the surface current must be positive on one side of the filament and negative on the other. The application of a positive dc electric field to produce transport will then tend to destroy the negative surface current but leave the positive part approximately unchanged.

3. RESULTS FOR THE HYSTERESIS LOOPS AND CRITICAL CURRENT DENSITY

The measured critical current density for the three composite conductors is shown in Figure 1 where j_c is computed from the filament area. It is observed that the curve for the 1.6 μm filaments lies above that for the 0.8 μm filaments, but the critical current density of the 0.4 μm sample is also above the curve for the 0.8 μm. The latter is contrary to expectations based on previous measurements[5] and a possible explanation may be found in the integrity of the filaments.[18]

The transverse hysteresis loops for magnetic moment per unit filament volume vs. applied magnetic field for the three filament diameters are shown in Figures 2, 3, and 4, both for the composite samples and for the samples with the matrix etched away. The curves for the composite samples are regarded as more reliable because of the possibility of shorted turns, and because the etched 0.8 and 0.4 μm samples were found to have a ferromagnetic contaminate, which is presumed to be Ni. The essential features of the loops are (1) the loops for the 0.8 and 0.4 μm composite samples are nearly the same, and much more narrow than that for the 1.6 μm material, and (2) at high fields both branches of the loop for the 0.8 and 0.4 μm material correspond to a negative magnetic moment. The points marked with X are explained in Section 5.

4. RESULTS OF THE MEASUREMENTS FROM COOLING IN A CONSTANT MAGNETIC FIELD

In a true Meissner effect observed in bulk type I and type II superconductors, magnetic flux is almost completely expelled by surface current when the conductor is cooled below its critical temperature in a constant magnetic field of magnitude less than H_c or H_{c1} respectively. The surface current leads to a magnetic moment. The effect investigated here corresponds to a magnetic moment presumed to result from expulsion of a very small amount of flux in fields well above H_{c1} in the hysteretic region of a type II superconductor. The measurement consists of heating the sample above its critical temperature at various points along the hysteresis loop, and then measuring the magnetic moment as the sample is cooled in the constant magnetic field. The results obtained are given by the dotted curves shown in Figures 5, 6 and 7. Only the curves for the composite samples are shown but the results for the etched samples were similar. The small deviations from the origin for the normal state curves are believed to be the result of a slight amount of paramagnetism in either the matrix or the holder for these samples.

5. ANALYSIS OF THE DATA AND CONCLUSIONS

For any current density j_s that is concentrated near the surface of the filament, one may define a surface current density J by

$$J = \int_0^{R_o} j_s dR \qquad (1)$$

where R_o is the radius and R the radial distance from the axis. If j_s is assumed to be an equilibrium type current as postulated in model (a), then for a transverse applied magnetic field, the surface current has the symmetry

$$J = - J_o \sin \theta \qquad (2)$$

where θ is the angle measured from the direction of the transverse applied field and J_o is the maximum value. The magnetic moment per unit volume of filament produced by this surface current is[1]

$$\frac{m_s}{V} = - 0.1\ J_o \qquad (3)$$

for J_o in amp/cm and m/V in emu/cm^3. In terms of the average magnitude $J_{av} = 2\ J_o/\pi$

$$\frac{m_s}{V} = - 0.1\ \frac{\pi}{2}\ J_{av} \qquad (4)$$

Consider now the case of transport current in the same applied field. If the large transverse field leads to an equilibrium surface current in the absence of transport current, it is reasonable to expect a surface current of approximately the same magnitude in the case where a transport current exists, except that the symmetry may be changed. As a rough approximation, if the assumption of Carr and Wagner[1] is used for the latter case, i.e. J is found only over half the filament circumference, then an equilibrium contribution of $\pi R_o J_{av}$ to the transport current I would be expected. When a pinned surface current density J_p and the pinned bulk current density j_c are added, the critical transport current becomes

$$I_c \approx \pi R_o J_{av} + 2\pi R_o J_p + \pi R_o^2 j_c \tag{5}$$

and since the measured j_c is $I_c/\pi R_o^2$

$$(j_c)_{meas.} \approx \frac{J_{av}}{R_o} + \frac{2 J_p}{R_o} + j_c \tag{6}$$

For filaments with a large radius R_o the measured value is the same as the bulk j_c, but for small R_o, the surface part should dominate. The expression (6) is intended to apply as long as R_o is greater than the penetration depth λ.

In general the total magnetic moment m measured for no transport current will contain contributions due to the pinned currents and also due to vortex currents about the flux lines, but in the special case where the equilibrium current dominates, both m and I_c are determined roughly by the term in J_{av}. In this case m will then be reversible, and from (4), m/V will be independent of filament diameter $d = 2 R_o$, assuming the surface current density is the same in all filaments. However the measured j_c should be proportional to 1/d since from (6), (j_c) meas. $\approx 2 J_{av}/d$, and from (4) and (6) the value of m/V can be estimated from the measured j_c accorded to the expression

$$\frac{m}{V} \approx - 0.1 \frac{\pi}{4} d \, (j_c)_{meas.} \tag{7}$$

In the 0.8 and 0.4 μm filaments an approach toward reversibility indeed is observed, and the magnetic moment in high fields is roughly independent of d. Although the expected factor of two ratio is not obtained in the measured critical current density, the measured value for the 0.4 μm filaments is considerably higher than that for the 0.8 μm filaments. A plot of m/V calculated from Equation (7) using the measured critical current density is shown by the points marked by X in Figures 3 and 4 and, again, the result is in reasonable agreement with the measurements. Finally, if an equilibrium surface current is largely responsible for m, an appreciable "Meissner" effect would be expected, as observed in Figures 6 and 7.

The conclusion is that a model which assumes that the dominant current flow in submicron filaments is due to an equilibrium surface current is in reasonable agreement with the measurements. However, as noted in Section 2, a detailed theory for such a model remains to be given.

6. REFERENCES

(1) W. J. Carr, Jr. and G. R. Wagner, Adv. in Cry. Eng., Eds. A. F. Clark and R. P. Reed, Plenum Press, New York, Vol. 30, p. 923, (1983).

(2) W. J. Carr Jr., IEEE Trans. Magnetics, MAG-21. 355 (1985).

(3) W. J. Carr Jr. and G. R. Wagner, submitted to 9th Int. Conf. on Magnet Tech. (1985). (Paper not presented)

(4) T. Ogasawara, Y. Kubota, T. Makiura, T. Akaci, T. Hisanari, Y. Oda and K. Yasukochi, IEEE Trans. MAG-19, 248 (1983).

(5) P. Dubots, A. Fevrier, J. C. Renard, J. P. Tavergnier, IEEE Trans. MAG-21, 177 (1985).

(6) A. K. Ghosh and W. B. Sampson, Int. Cry. Mat'l Conf. (1985).

(7) T. Matsushita, T. Honda, Y. Hasegawa, Y. Akenaga and Y. Monju, Proc. ICMC Kobe, p. 171, Eds. K. Tachikawa and A. Clark, Butterworths, UK (1982).

(8) T. Matsushita, T. Tanaka and K. Yamafuji, J. Phys. Soc. Japan, 46, 756 (1979).

(9) T. Matsushita, T. Honda and Y. Hasegawa, J. Appl. Phys. 54, 6526 (1983).

(10) W. A. Fietz, M. R. Beasley, J. Silcox and W. W. Webb, Phys. Rev. 136, A335 (1964).

(11) P. S. Swartz, Phys. Rev. Letters 9, 448 (1962).

(12) J. Silcox and R. W. Rollins, Appl, Phys. Lett. 2, 231 (1963).

(13) L. J. Barnes and H. J. Fink, Phys. Lett. 20, 583 (1966).

(14) G. Fournet and A. Mailfert, J. Phys. Paris 31, 357 (1970).

(15) S. T. Sekula and J. H. Barrett, Appl. Phys. Lett. 17, 204 (1970).

(16) J. R. Clem, J. Appl, Phys. 50, 3518 (1979).

(17) M. A. R. LeBlanc and J. P. Lorrain, IEEE Trans. MAG-19, 256 (1983).

(18) D. C. Larbalestier, IEEE Trans. MAG-21. 257 (1985).

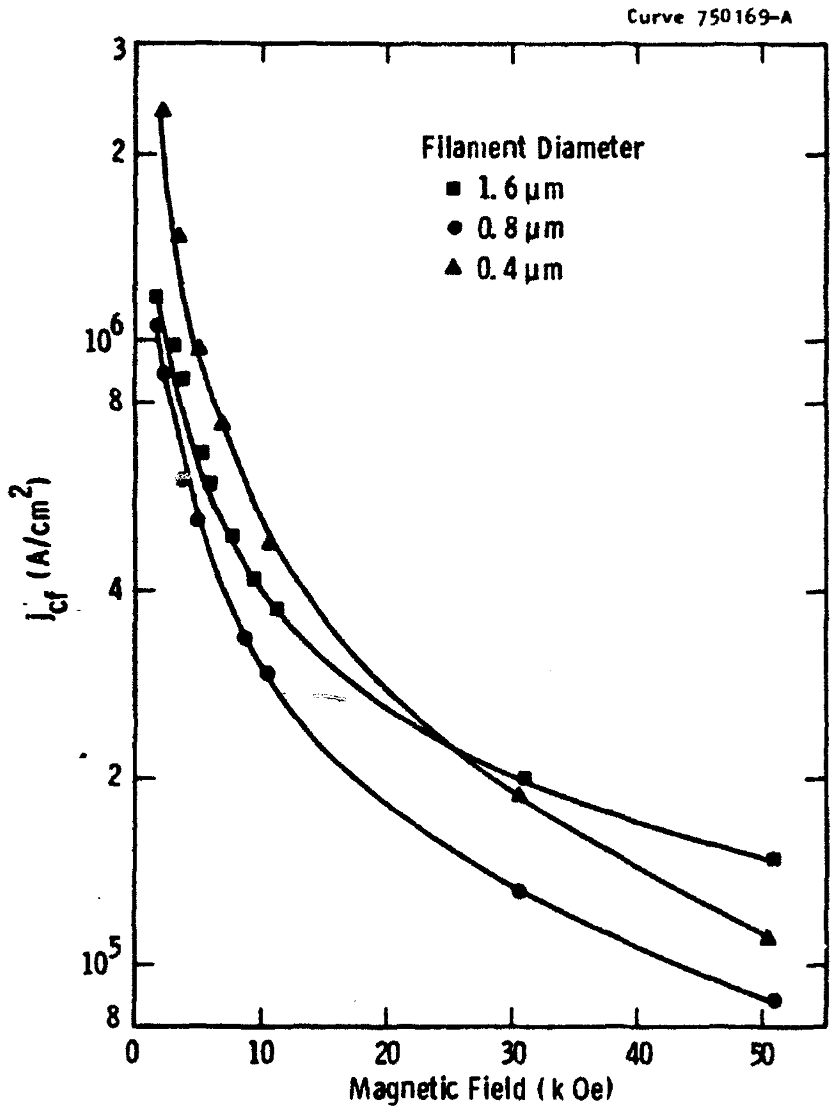

Figure 1. The measured critical current density in the filaments, corrected for self field, is plotted vs. magnetic field.

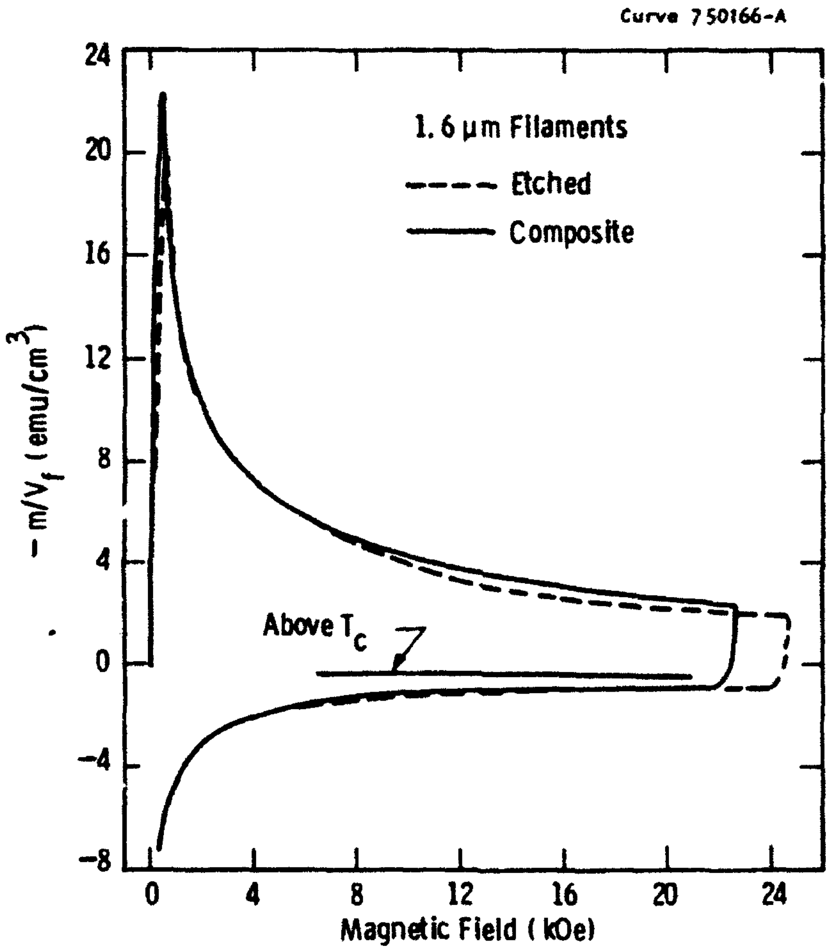

Figure 2. The measured magnetic moment per unit filament volume vs. the applied transverse field for the 1.6 um samples. The solid curve is for the composite and the dashed is for the filaments with the matrix etched away. The loops were taken at 4.2K and the intermediate solid curve above T_c.

Curve 750167-A

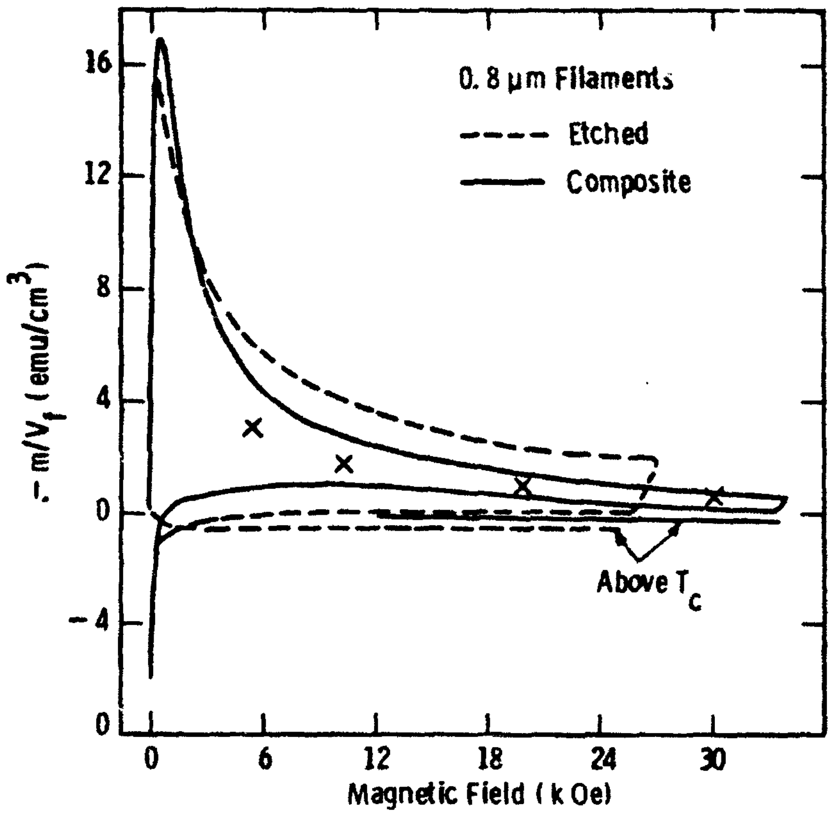

Figure 3. Same as Figure 2, but for the 0.8 μm samples. The lower solid and dashed curves were taken above T_c.

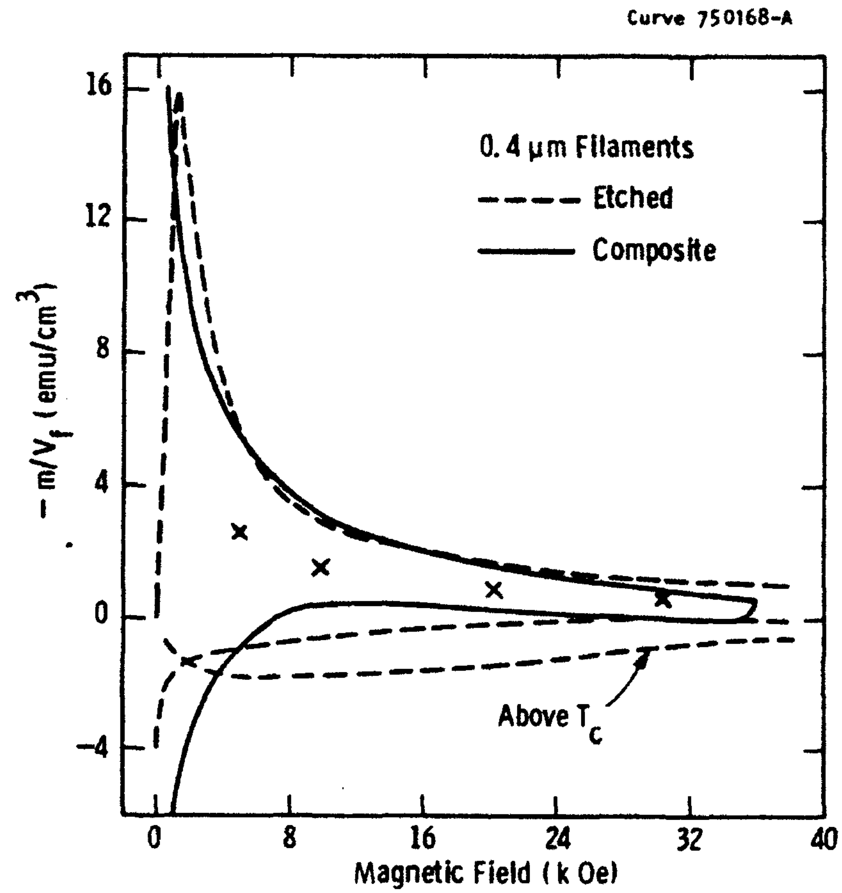

Figure 4. Same as Figure 2, but for the 0.4 μm samples. The lower dashed curve was taken above T_c.

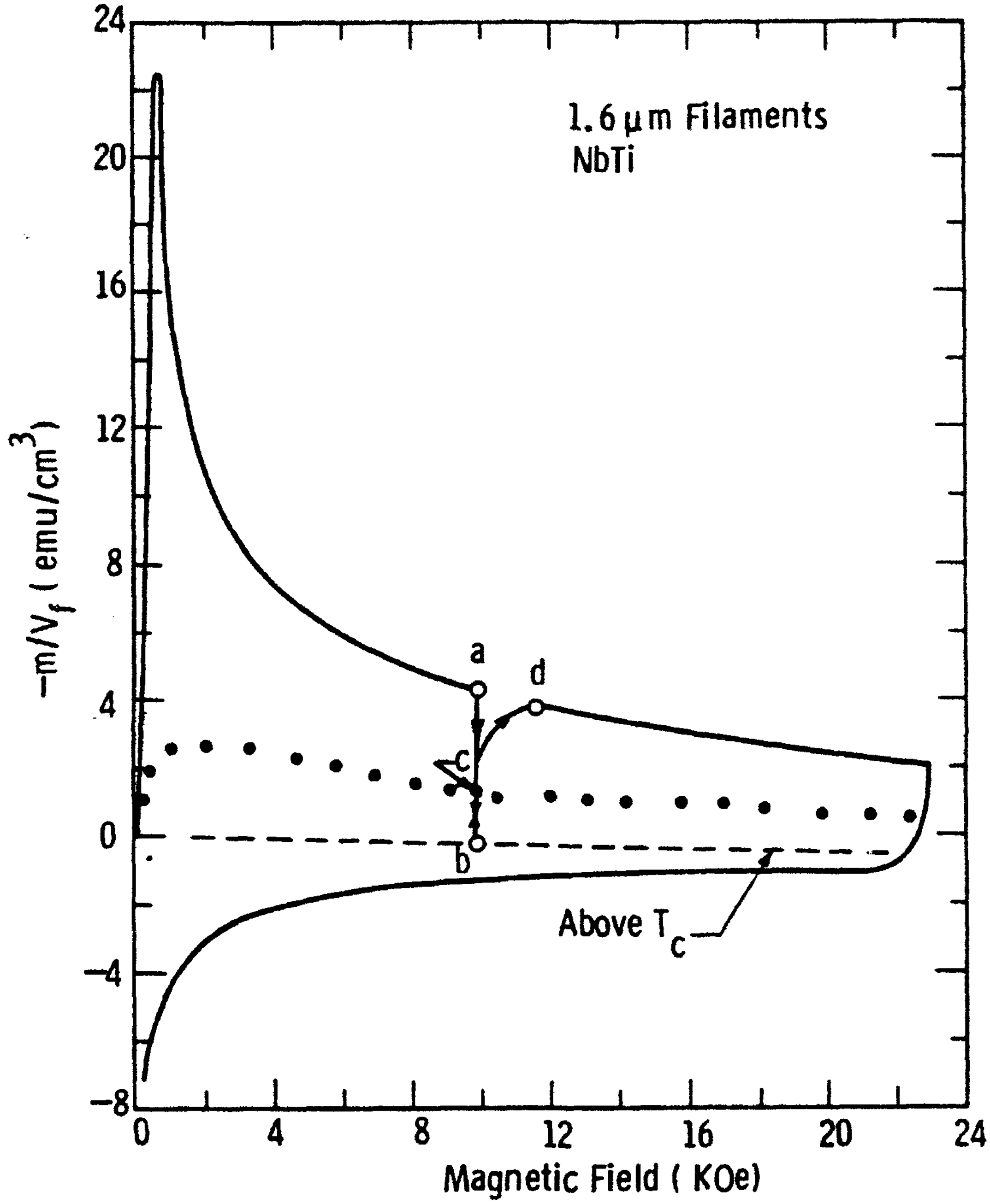

Figure 5. The magnetic moment per unit volume of the 1.6 μm sample vs. the applied transverse magnetic field. At point a the sample is heated in constant field above T_c and the moment goes to point b in the normal state. Upon cooling to 4.2 K at constant field, the moment goes to point c. Increasing the field at 4.2 K takes the moment to poind d. The solid points are the locus of points c obtained in this way along the hysteresis loop.

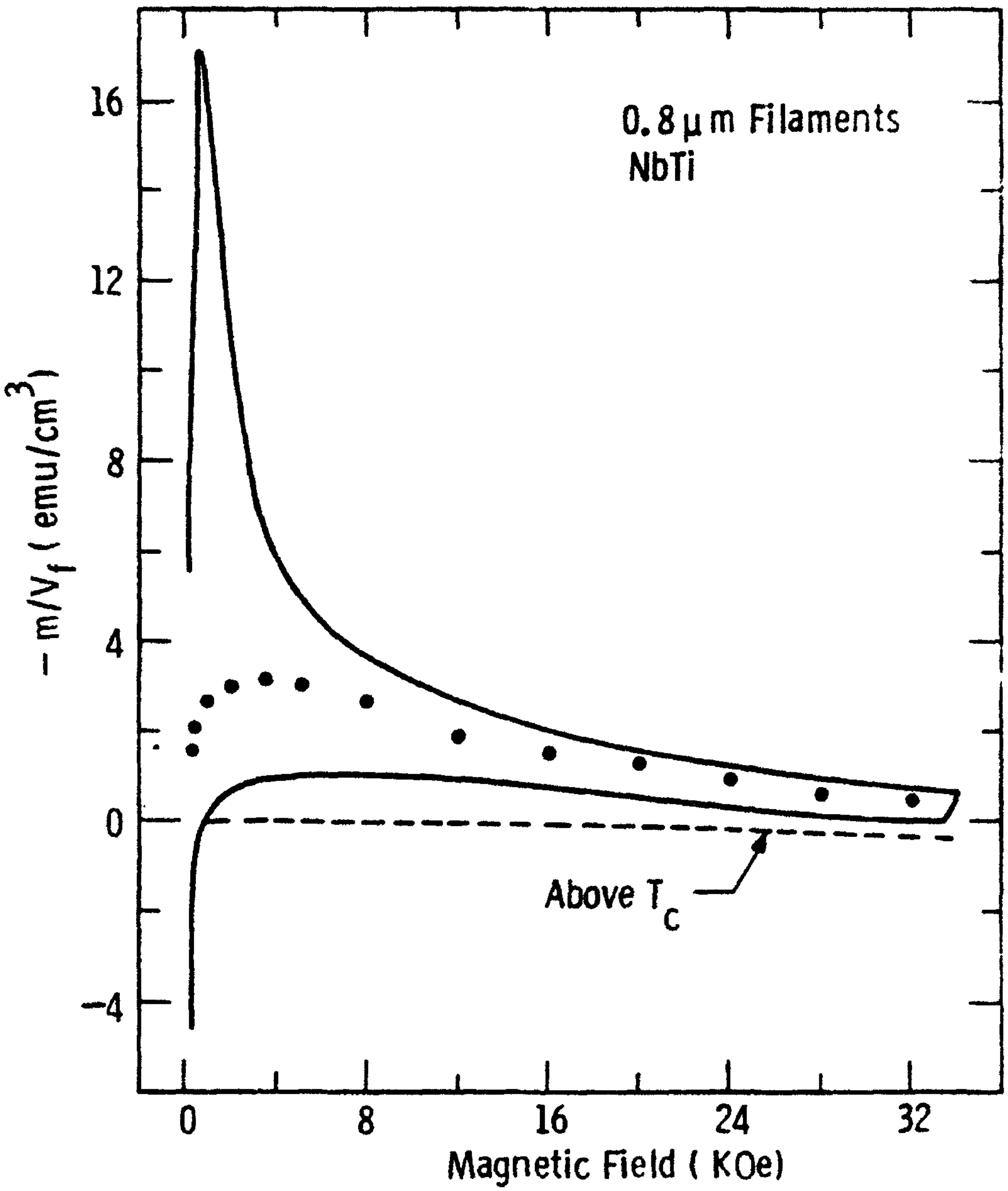

Figure 6. Same as Figure 5, but for the 0.8 μm filaments.

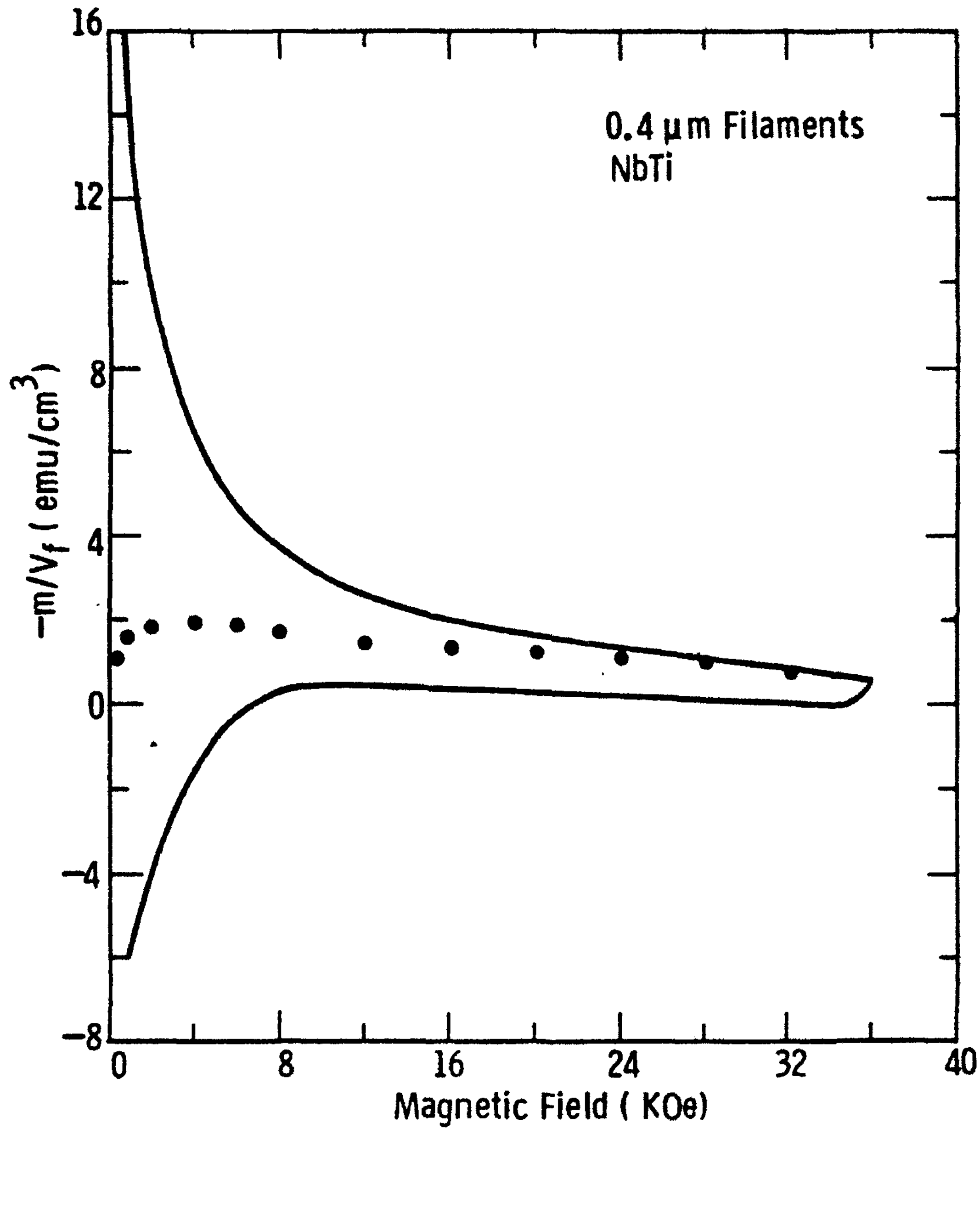

Figure 7. Same as Figure 5, but for the 0.4 μm filaments.